NON-LINEAR ANALYSIS

OF REINFORCED CONCRETE

THICK PLATES FOUNDAION

ON SOIL

A thesis
Submitted to the College
Of Engineering of the University of Babylon in
Partial Fulfillment of the Requirements for
The Degree of Master of Science (M.Sc.) in
Civil Engineering
(STRUCTURE)

By
IHSAN MOSLIM ABDUL-KAREEM
(B.Sc.)

October
٢٠٠٣

NOTATIONS

[A]	Matrix which contains the differential operators
As	Cross–sectional area of the bar
{a}	Displacement vector
$\{a\}^e$	Nodal displacements
B	Body forces
[B′]	Strain–displacement matrix of the bar element
[B]	Strain – displacement matrix
C_p	Plasticity coefficient
[D]	Constitutive matrix
$[D]^e$	Elastic constitutive matrix
$[D]^{ep}$	Elasto-plastic consitutive matrix
[D′]	Constitutive matrix of the bar element
D_{cr}	Cracked material stiffness in local axes
{f}	Element assemblage external nodal force vector
{f}	Internal force vector
f′c	Ultimate compressive strength of concrete (cylinder test)
f_t	Maximum tensile strength of concrete
G	Shear modulus of elasticity
$\bar{I}_1$	First strain invariant
I_1	First stress invariant
[J]	Jacobian matrix
$\bar{J}_2$	Second deviatoric strain
J_2	Second deviatoric stress invariant
[k]	Stiffness matrix
[k′]	Stiffness matrix of the bar element
$[k]_{tpf}$	Stiffness matrix of thick plate foundation
l, m, n	Directional cosines with the x, y, and z directions respectively
[N]	Matrix containing interpolation functions
N_i	Shape function at the ith node
{P}	Applied load vector
Q	Deviator stress
{r}	Out of balance load vector
S	Part of the surface of the body where external tractions are prescribed
T	Surface traction
$\{u\}^e$	Displacement vector at any point within the element
u, v, w	Displacement components in x, y and z – direction respectively

u_i, v_i, w_I	Nodal displacement
V	Volume
W_{ext}	External work
W_I	Weight of sample point
W_{int}	Internal work
x, y, z	Global coordinates
x_i, y_i, z_I	Global coordinates of ith node
E_1	Reduced modulus of elasticity
H'	Hardening parameter
α, β	Material parameters
α_1	The rate of stress release as the crack widens
α_2	Sudden loss of stress at instant of cracking
β_1	Reduction factor
$\{\varepsilon\}$	Strain vector
$\{\varepsilon'\}$	Strain vector of bar element
$\{\varepsilon_p\}$	Effective accumulated plastic strain vector
ε	Strain
ε'_o	Total strain corresponding to the parabolic part of the curve
ε_c	Total effective strain of concrete
ε_{cr}	Cracking strain
ε_{cu}	Ultimate concrete strain
ε_e	Elastic component of total effective strain of concrete
ε_n	Strain normal to the cracked plane
ε_p	Plastic component of total effective strain of concrete
γ_1	Rate of decay of shear stiffness as the crack widens
γ_2	Sudden loss in shear stiffness at the instant of cracking
γ_3	Residual shear stiffness due to the dowel action
λ	Compression reduction factor
$\bar{\sigma}$	Equivalent uniaxial stress
$\{\sigma\}$	Stress vector
σ	Stress
σ_o	Equivalent effective stress at the onset of plastic deformation
σ_{cr}	Cracking stress of concrete
σ_n	Stress normal to the cracked plane
ξ, η, ζ	Natural coordinate system

Certification

We certify that this thesis titled ***Nonlinear Analysis of Reinforced Concrete Thick Plate Foundation on Soil*** was prepared by Mr. Ihsan Moslim Abdul-Kareem under our supervision at the university of Babylon in fulfillment of partial requirements for the degree of ***Master of Science in Civil Engineering (Structural Engineering)*.**

Signature:

Name: ***Asst. Prof..Dr. Haitham Al-Daami***

(Supervisor)

Signature:

Name***: Asst. Prof. Dr. Ammar Yaser Ali***

(Supervisor)

Date: / / ٢٠٠٣ Date: / / ٢٠٠٣

Examining Committee Certificate

We certify that we have read this thesis titled ***Nonlinear Analysis of Reinforced Concrete Thick Plate on Cohesive Soil,*** and as an examining committee, examined the student ***Mr. Ihsan Moslim Abdul-Kareem*** in its contents and in what is connected with it, and that in our opinion it meets the standard of a thesis for the degree of ***Master of Science in Civil Engineering (Structural Engineering).***

Signature: Signature:

Name: ***Asst. Prof. Dr. Haitham Al-Daami*** Name***: Asst. Prof. Dr. Ammar Yaser Ali***

(Supervisor) (Supervisor)

Date: / / ٢٠٠٣ Date: / / ٢٠٠٣

Signature: Signature:

Name: ***Asst. Prof. Dr. Ali Al- Athary*** Name: ***Asst. Prof. Dr. Mustafa B. Dawood***

(Member) (Member)

Date: / / ٢٠٠٣ Date: / / ٢٠٠٣

Signature:

Name: ***Prof. Dr. Husain M. Husain***

(Chairman)

Date: / / ٢٠٠٣

Approval of the Civil Engineering Department
Head of Civil Engineering Department

Signature:
Name:

Date: / / ٢٠٠٣

Approval of the Deanery of the College of Engineering
Dean of the College of Engineering

Signature:
Name: ***Asst. Prof. Dr. Haroon A.K Shahad***
(The Dean)
Date: / / ٢٠٠٣

LIST OF CONTENTS

ABSTRACT

This research deals with the analysis of reinforced concrete thick plate foundation by finite elements. The material nonlinearity is taken into account for concrete. A twenty-node isoparametric brick element with sixty degrees of freedom is imployed to model the concrete foundation. The formulation of stiffness matrix is based on including all types of stress and strain. The reinforcement bars are modeled as axial members imbedded within the concrete brick element with perfect bond between them.

Soil is considered to have compressional and frictional restraints, the compressional component is represented by Winkler, Kondner, and Polynomial models, while the horizontal component is represented by Winkler and Coulomb models. The polynomial model shows good agreement with other available numerical studies.

The present finite element and the available experimental and numerical results for plates and plate foundations have shown good agreement, the maximum percentage of difference is not more than (٥.٨٨ %) for ultimate load and (٧.٧٨ %) for deflection for circular plate foundation.

Parametric studies have been carried out to examine the effect of some selected parameter (boundary condition, stiffness variation, reinforcement ratio, type of loading, type of soil, and elastic foundation modulus) on the behavior of the plate. It was found that the ultimate load for free-edges thick plate foundation is greater than for simply supported and fixed-edge thick plate, the ultimate load is increased with increasing the reinforcement ratio, the deflection for thick plate under distributed load is greater than that of thick plate under concentrated load at failure, the deflection increased with decreasing the density of soil, and the pressure under the thick plate increased with increasing the density of the soil.

ACKNOWLEDGMENT

*Firstly, all the thank and praise be to **God** in enabling me to achieve this research work.*

*I would like to express my deepest gratitude and gratefulness to **Dr. Haitham Al-Daami** and **Dr. Ammar Yaser Ali** the supervisors of this study for their valuable guidance, encouragement, and constructive suggestions.*

A word of thank to Mr. Ausama Hamied (M.Sc.) for his help and to my friends " Nabeel,Thair, Mohammed, Khalid, Tho-Alfiqar, Wathik, and Shaymaa"

Ihsan

٢٠٠٣

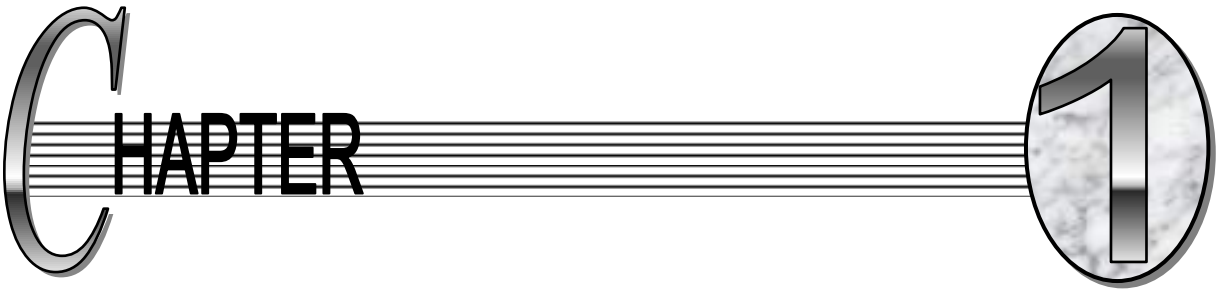

INTRODUCTION

١.١ General

Reinforced concrete is the most widely used material for construction throughout the world and reinforced concrete plates are the main parts of such constructions. Therefore, analytical and experimental studies for the response of reinforced concrete plates have focused the activity of many engineers for many years.

Elastic analysis of reinforced concrete always involves approximations so the design will be safed, but, it is uneconomic structural result. Therefore, non-linear analysis of such structures is essential in order to achieve improvements in design efficiency by accurately evaluating the deflection, stress and over-load carrying capacity. The prediction of deflection and lateral load carrying capacity (limit load) of thick plates has interest and importance in the design of some structures that are subjected to high pressures such as nuclear power plants and thick plates used as foundations for heavy structures like towers, vibrating machines, rocket launchers, nuclear reactors, …etc.

The formulations of classical plate and shell theories are based on certain simplified assumptions that were originally made for the formulation of Euler-Bernoulli theory for bending of beams [٥٥], these assumptions are:

١- Plane transverse sections before bending will remain plane after bending (linear strain distribution in a cross section)

٢- Normal line to the middle plane will remain normal to the deflected middle plane (no transverse shear deformation)

٣- Normal strain in the normal lines to the middle plane are neglected (no change in thickness)

٤- The deformations are small (linear theory of small deformations).

While Reissner [٤٧] showed that by including the transverse shear deformation in to the classical thin plate theory, straight line originally normal to the middle surface of plate will be remaining straight but not normal to the deformed middle surface. The Love-Kirchoff approximation involves neglecting the effect of both transverse strain and transverse stresses on deformation. Thus, the differential equation for thin plate theory and the boundary conditions have been derived by neglect the effect of normal stress (σ_z) and transverse shear stresses (τ_{xz}) and (τ_{yz}).

The main difference between thick and thin plate theories is that when the thickness of the plate increases with respect to other dimentions, the effect of transverse shear stresses and strains as well as transverse direct normal stress and strain on elasto-plastic behavior of the plate becomes very effective and shoud be considered in the analysis, unlike that for thin plates in which the effect of these stresses are negligible. Thus, the errors are not only in the stresses but also in strains and hence in deformation.

The post-elastic analysis of reinforced concrete plates has gained importance for the following two major reasons:

١- Reinforced concrete structures behave nonlinear even under working loads, since concrete is weak in tension and cracks form relatively at low tensile stress, therefore, cracking and the consequent nonlinearity are

considered approximately at a load equal to one quarter of the ultimate load capacity for intermediate steel ratios. This material nonlinearity in the early loading stages cannot be predicted by linear analysis.

٢- Cracks in concrete change stiffness and stress distribution in the plate and thus redistribution of stress under design loads must not be neglected; This is especially in the case of highly statically indeterminate structures, like plates. Therefore, in the case of extensive cracking for variable mesh reinforcement widely variable rigidities throughout the plate are produced which in turn give greater differences in moments and stresses from that of the elastic uncracked range. This may affect the amount of reinforcement required for ultimate load considerations.

Various equations have been proposed [٣٥] for the representation of the stress-strain curve for concrete. Most investigations have been directed to the formulation of the stress-strain relations of concrete under uniaxial loading. However, if refined methods are to be used in the analysis and design of structural concrete, then at least a biaxial stress-strain relationship for concrete must be developed, and eventually triaxial formulations must be followed.

Analytical procedures which may accurately determine stress and deformation states in reinforced concrete members are complicated due to many factors, among them are:

١. The nonlinear load deformation response of concrete and the difficulty in forming suitable constitutive relationship under combined stresses.
٢. Progressive cracking of concrete under increasing load and the complexity in formulation of the failure behavior for various stresses.
٣. Consideraion of steel reinforcement and the interaction between concrete and steel.
٤. Time dependant effects as creep and shrinkage of concrete.

Numerical techniques that solve this problem yield approximate results, which are acceptable for most practical purposes. One of most general numerical techniques used in the feild is the finite element method. This method has become increasly popular in recent years.

The development of numerical methods such, as the finite element and the finite difference methods, permit realistic evaluation of internal stresses, displacements and tracing the nonlinear response of the structure throughout its entire load range.

١.٢ *Non-Linear Behavior of Soil*

Most phenomena in the solid mechanics are non-linear. In many applications, however, it is practical and convenient to use linear formulations for problems to obtain engineering solutions. On the other hand, some problems definitely require non-linear analysis if realistic results are to be obtained.

The stress –strain relation of any type of soil depends on a number of different factors including density, water content, structure of the soil, drainage conditions, strain condition (i.e. plane strain, triaxial), duration of loading, stress history and confining pressures [٣].

It is commonly found [١٣] that the stress – strain curve for all soils is non-linear except in a very narrow region near the origin. **Kondner** [٤] proposed that the stress-strain curve, which is shown in Fig. (١.١), could be represented by a hyperbolic equation of the form: -

$$\sigma_1 - \sigma_3 = \frac{\in}{a + b \in} \qquad \ldots (١.١)$$

where

σ_1 and σ_3 are the major principal stresses.

$\in$: is the axial strain in the direction of σ_1 and

(***a***) and (***b***) are constants which can be determined experimentally.

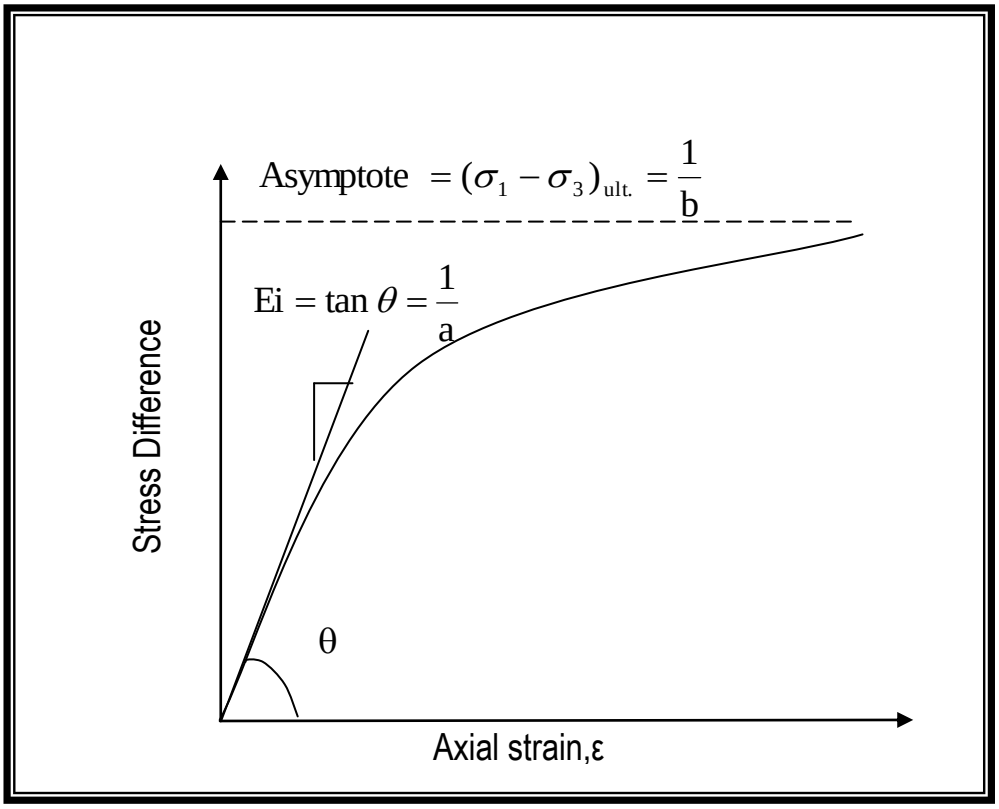

Figure (١.١): Proposed Hyperbolic Stress – Strain Curve of Soil.

١.٣ *Scope and Aims*

The thick plate foundation is a very important construction used for the condition of heavy loads to be transmitted to the soils. The main aim of this work is to include all types of stresses and strains to present a better understanding for thick plate foundation behavior and to predict the ultimate load that causes failure for the thick plate foundation. To achieve this aim a theoretical work using a non-linear finite element analysis is carried out. The behavior of reinforced concrete thick plate foundation is studied by using a brick element to represent the concrete while the foundation is represented by different models (Winkler, Kondner, Polynomial) for normal subgrade reaction but the horizontal subgrade reaction is represented by Winkler and Coulomb models.

١.٤ *Thesis Layout*

The thesis is organized in seven chapters. The present introductory chapter is being the first. Chapter two is devoted to the review of literature. Chapter three concerns with the constitutive relations for reinforced concrete material. Chapter four is specified for explaining various elastic foundation models.

Chapter five presents the numerical algorithm used for the solution of the non-linear reinforced concrete problem. In chapter six several numerical examples are presented and verified with available analytical and experimental studies. Chapter seven gives the conclusions and suggestions for further studies.

REVIEW OF LITERATURE

٢.١ Introduction

The review presented here aims at showing the most important developments and steps that has taken the path leading to knowledge of today in this subject. As mentioned in the introduction the problem concerns to include all types of stresses and strains to represent the behavior of thick plates have interested a large number of researchers.

In this chapter a literature survey is divided into three major scopes:

١. Thick plate.

٢. Reinforced concrete.

٣. Thick plate on elastic foundation.

٢.٢ Thick Plate

A large amount of literature exists on the development of thick plate theories, in certain cases, simple modification to the classical theory can be used when deflection is the prime concern. Such corrections are based upon including the deflections due to transverse shear strain to that of bending effect considered in the classical theories. Another approach for correction of the classical thin plate theory is by adopting the effects of transverse shear deformation, normal stress and normal strain. Others use high order deformation theory or the exact three-dimensional analysis.

Various improved theories for plate have been worked out in different forms and techniques and mostly by benefit from **Timoshenko's** [٥٥] **[١٩٢١]** development for bending of deep beams. The remarkable progress is due to the formulation that allows the normal line to the middle plane to rotate independently of the rotation of the middle plane. The transverse shearing deformations are thus considered.

The step by Timoshenko pushed many researchers to improve the classical plate theory. **Reissner** [٤٧] **[١٩٤٥]** developed a system of equations for the theory of bending of thick elastic plates, which takes into account the transverse shear deformations of the plate. This system of equations is of nature has three boundary conditions that must be prescribed along each edge of the plate. It is assumed that the bending stresses σ_x, σ_y and shear stress τ_{xy} are distributed linearly over the thickness of the plate. The remaining components of the stress tenser are obtained by using the equilibrium differential equations, when the faces of the plate are assumed to be free from shear stress. The resulting transverse normal stress σ_z is then a function of third order in (z). It has been assumed also that the displacement at the edge, u and v vary linearly though the thickness of the plate, while w is constant over the thickness. In view of that simplifing assumptions Reissner's theory is inconsistent; the deformations will cause a decline from the linearity of u and v, and the effect of σ_z will vary the deflection throgh the thickness. In order to obtain complete system of

differential equations, Reissner used Castigliano's theory least work to overcome the inconsistency in stress relations.

Salerno and **Goldbreg** [٤٨]**[١٩٦٠]** used the partial differential equations derived by Reissner [٤٧] and reduced them to a fourth-order partial differential equation of deflection and a second-order differential equation of stress function. The general solution of these two partial differential equations has been applied to a plate subjected to a uniform load and with either all edges simply supported or two opposite edges simply supported and the other free.

Pryor et al. [٤٣] **[١٩٧٠]** presented a finite element analysis including transverse shear deformation capable of applying to the bending of rectangular plates. The equations of Reissner theory were used with a value of (k) (a numerical factor representing the restraint of cross section against warping), commonly assumed to be (٦/٥), but the effect of the normal stress (σ_z) was neglected. Several examples of simply supported plates were used to test the validity of procedure. The first example of uniform distributed load showed excellent agreement with Reissner theory for various ratios of plate thicknesses to lateral dimension. The second example of the concentrated central load showed that the influence of transverse shear on maximum deflection is more dominant for concentrated load condition. The third example studied the distribution of shearing forces (Q_x) and (Q_y) and twisting moment (M_{xy}) along the edge. Results obtained showed good agreement with those of Reissner theory for maximum displacement and for distribution of stress resultants along the supports.

Speare and Kemp [٥٠] **[١٩٧٦]** made a comparison between a number of plate theories which includes the effect of shear deformations. The use of finite difference and finite element methods for their solutions were also discussed. They illustrated that the percentage of errors introduced by neglecting shear deformations was greater for concentrated load than for uniform loads and for clamped edges was greater than for simply supported edges.

Lee and Wong [٣٧] **[١٩٨٢]** developed two new finite element approaches for Mindlin theory of plate bending problem. The formulation was based on the modified Hellinger- Reissner principle with independent transverse shear strain. The numerical examples indicated that even with properly assumed transverse shear strains, these new elements do not exhibit locking effect and even for very thin plates.

After Reissner, a thick plate Mindlin theory has been presented, which is actually applicable to both thick and thin plates. **Mindlin** [٣٩] **[١٩٥١]** deduced a two dimensional theory of flexural motion of isotropic elastic plates from the three-dimensional equation of elasticity. The theory includes the effect of rotatory inertia and shear stress in the same manner as Timoshenko's one-dimensional theory of beams.

Mindlin and shear deformation theories have been considered by many authors. **Hinton et al.** [٢٧] **[١٩٧٥]** used a plate bending finite element with curved boundaries and variable thickness, allowing for transverse shearing deformation. The element is of parabolic isoparametric type. The given examples show applications involving thin, thick, cellular, sandwich plate and deck of bridge.

Reddy [٤٥] **[١٩٨٤]** presented a high order deformation theory of plates. The theory contains the same dependent unknown as that in Hencky-Mindlin first orders shear deformation theory and accounted for parabolic distribution of the transverse shear strains through the thickness of the plate. He obtained an exact solution for simply supported plates using the linear theory and the results were

compared with the exact solutions of the ٣-D elastic theory, the first order shear deformation theory, and the classical plate theory. More accurate results (deflection and stresses) were obtained when compared with first order and the classical plate theory.

Reddy [٤٦] **[١٩٨٦]** presented a refined third order theory and considered the transverse shear deformation. The Navier solutions were used with finite element method. Since the transverse shear stress was presented parabolically, the shear correction factor has not been required. He concluded that the high order shear deformation theory gives in general more accurate solution for the bending of laminated anisotropic plates than the classical plate theory. Also the first order shear deformation theory gives overestimation in the deflection, and underestimation in the natural frequencies and buckling loads for thick plates.

Three-dimensional problems of elasticity have been formulated to solve the problem of the bending of plate. This method of analysis gives an accurate and exact results , but it needs more time and computations than other theories.

Srinivas et al. [٥٢] **[١٩٦٩]** used a three dimensional, linear, small deformation theory of elasticity to solve by the direct method the flexure of simply supported homogeneous, isotropic, thick rectangular plates under arbitrary loading, the solution in terms of finite series. This analysis was readily extended for laminated plates of isotropic materials. They showed that the assumptions in Reissner theory are justifiable for plates of thickness to span ratios up to about ١٠٪. It has been also shown that the thin plate theory is quite accurate for plates of thickness to span ratio up to ٥٪, when subjected to uniformly distributed loads and the error increases with the non-uniformity of loading.

Srinivas and Rao [٥١] **[١٩٧٣]** used three-dimensional analysis for the flexure of thick rectangular plates. The transverse shear deformation and the direct stress (σ_z) were neglected. They studied deflection and stresses for the case of

uniform load with various thickness to span ratios and boundary conditions. They concluded that the thin plate theory gives underestimation of the maximum deflection and stress at the center of the plate, and the thin plate errors increased rapidly with the thickness, thus thin plate analysis could be used for plates up to ٥٪ thickness to span ratio.

Fan and Ye[٢٢] [١٩٩٠] obtained a set of equations for an orthotropic body by considering the three dimensional elasticity without any initial assumptions. They presented a series solution for a simply supported rectangular thick plate with arbitrary ratios of thickness to width and under any given load. They obtained numerical results for a simply supported orthotropic plate and compared with the results of Reissner's theory.

٢.٣ *Reinforced Concrete*

Reinforced concrete is the most commonly used construction material but concrete is relatively weak and brittle in tension. Concrete cracking as well as interaction between steel and cracked concrete may cause highly non-linear behavior in some reinforced concrete structures. Today with the help of computers, it is possible to carry out the finite element or finite difference analysis to simulate such non-linear behavior. However, the success of such analysis depends on the modeling of the composite material behavior.

Many investigators studied the non-linear (material or geometry or both together) behavior of the plate. Some of them used the finite element and assumed that the material to be elastic perfectly plastic and considered the concept of the full yield criterion (all material throughout the thickness of the plate will yield when the moment at that point reaches the yield envelope). Therefore, the rigidities of the plate will vary suddenly from elastic to elastic-plastic rigidities in accordance with the flow rule, which implies that the total strain increment can be divided into elastic and plastic increments and that the

increment of plastic strain is normal to the yield surface. This condition can be satisfied by a thin metallic plate, while the non-linearity of reinforced concrete is affected by the cracking of concrete. Also cracking propagates throughout the depth of plate continuously up to the ultimate load; so, the rigidity of the plate at each Gaussian point will decrease gradually.

Firstly, the non-linear representation adopted by many authors for the analysis of reinforced concrete plates has many shortcomings:

١- Cracking of concrete and yield of steel are not taken explicitly in the calculation of stiffness matrix but they are taken implicitly through the moment-curvature relationship

٢- The variation due to biaxial stresses, strain hardening in reinforced steel , aggregate interlock and tension stiffening in the post- cracking range cannot be taken explicitly into account

٣- Concrete and steel stresses cannot be determined exactly , and tracing the crack depth at various stages of loading is not possible. Therefore, a layer analysis has been used to overcome the above shortcomings.

٢.٣.١ Layer Model

Hand and Schnobrich [٢٥] **[١٩٧٣]** were the first who used the layer finite element procedure for determining the load-deflection history up to failure for reinforced concrete plates and shells. They assumed that the reinforcing steel behaved in elastic-plastic form and the concrete was assumed to be limited in tension and to yield in biaxial compression in accordance with the yield criterion propose by **Kupfer et al. (١٩٦٧).** The incremental variable elasticity technique is used to obtain the load deflection curve for many general plates or shells. The need for shear retention factor to improve the torsional and shear stiffness for cracked concrete and to account for the aggregate interlock and dowel action was demonstrated. It appeared that this analysis technique was capable to

determine the load-deflection history of reinforced concrete plates and shells accurately and economically.

Wanchoo and May[٥٧] [١٩٧٥] examined the behavior of reinforced concrete plate bending by apply the layer model. The normal discretization associated with finite element method allows for variation in material and geometry. The analysis was restricted to small deformation bending theory, and perfect shear bond is assumed between layers. The concrete is of elastic behavior in tension up to cracking, and elastic-plastic in compression. The steel is modeled by the two-dimensional layer obeying the Von Mises criterion and associated flow rule. This criterion is adopted also for concrete compressive yielding.

Gilbert and Waner[٢٤] [١٩٧٨] used a layered discrete element method to investigate the short term behavior of reinforced concrete slabs, and a comparison was made of various techniques to include the tension stiffening effect. A simple method based on a modified stress-strain diagram for the tensile steel was found to give accurate results with efficient computer time. They indicated that the stiffness of reinforced concrete slab in the post-cracking surface load range is significantly increased due to tension stiffening effect in the concrete between cracks. When this effect is ignored, the calculated slab deflections may be up to ١٠٠ % larger in the post-cracking range.

Crisfield[١٩] [١٩٨٢] used the finite element tangential method for material nonlinearly of beam and slabs. In plane degrees of freedom were taken into account for rectangular elements to include the effect of membrane action with plate bending. Reinforcement steel was modeled as elastic-perfectly plastic and concrete was assumed to be governed by Von Mises yield criterion in the biaxail compressive principal stress zones. He studied the effect of some parameters of the non-linear analysis, such as tension stiffening, load increment size, iterative

procedure, tolerance etc., which may lead to local instability or nonunique solution.

Damjanic and Owen [٢٠] **[١٩٨٤]** considered the numerical modeling of concrete behavior for the use in the finite element analysis of reinforced concrete structures. The consideration is restricted to the post-cracked concrete behavior. Simple tension stiffening and shear stiffening models for cracked concrete are imployed. They showed that an adequate combination of selected tension stiffening and shear retention parameters has a direct influence on the numerical results.

Hu and Schnobrich[٢٨] **[١٩٩٠]** developed a nonlinear material model for cracked reinforced concrete plate subjected to in-plane shear and normal stresses. Thus, they derived a set of constitutive equations suitable for incremental finite element analysis. The model includes the cracked representation, rotating crack approach, tension stiffening, stress degarding effect for concrete parallel to the crack direction, and shear retention of concrete on the crack surface.

Naser[٤١] **[١٩٩١]** dealt with linear and nonlinear analysis of reinforced concrete thick plates by using the finite difference method with layer approach. Transverse shear deformation and normal stress were considered. In concrete layer, the nonlinear behavior and crushing were considered in compression. In tension, cracking and tension stiffening were considered for cracked layers. He studied thick plates with different boundary conditions. The results obtained showed good agreement with the available experimental results.

Al-Imam[٤] **(١٩٩٢)** used layered Mindlin flat shell ٨-node isoparametric element for slab discretization. An element with ٢١-node was developed to model either concentric or eccentric edge beams. The steel reinforcement was treated as composite smeared layer. Perfect bond between concrete and steel was

assumed. The nonlinearities included were the cracking of concrete in tension, the nonlinear response of concrete in compression, concrete crushing, and yield of reinforcement.

Abdul-Razzak[1] (٢٠٠٢) studied the nonlinear behavior of reinforced concrete plates for different load conditions (concentrated and distributed loads), and for the effect of tension stiffening on material and geometric nonlinearities. A ٩-node element was employed in this analysis. The results obtained showed good agreement with the experimental result.

Layer approach for reinforced concrete structures has several disadvantages:

١- The quadrature rule used to integrate quantities such as the residual forces and the tangential stiffness through the thickness is not very accurate and many layers (٨-١٢) must be used to ensure reasonable accuracy.

٢- The large number of the sampling points used per element makes the evaluation of the tangential stiffness matrix and the internal force vector quite expensive.

٣- The plane stress assumption in the layered plate or shell implies that the normal stress perpendicular to the mid-surface is neglected. Furthermore, in most models, in-plane stresses are treated separately from transverse shear stresses, usually in an inconsistent way.

٤- Cracking are assumed to form due to in-plane stresses only, the effect of transverse shear stresses being disregarded when checking for cracking. As a result, cracks are perpendicular to the mid-surface, which is an unrealistic constraint on the model that make it unable to represent non flexural failures.

٥- The elements used are usually of Mindlin type. These results in a priori imposed uniform distribution of tranverse shear strains through the thickness.

٦- Concrete slabs are usually moderately thick, so consideration of transverse shear strains and stresses are not insignificant, especially near the supports.

All these considerations point to the necessity of developing fully ٣-D models which can be used to analyze reinforced concrete structures both efficiently and accurately.

٢.٣.٢ *Three-Dimensional Model*

Cervera(١٥) **[١٩٨٧]** used the three dimensional analysis to study plates, shells and thick beams. He adopted ٢٠-node isoparametric element, the effect of shear and normal stresses were included in this analysis. In concrete, the non-linear behavior and crushing were considered in compression. In tension, cracking and tension stiffening were considered. The aggregate interlock was considered by introducing the shear retention factor for cracked Guassians point. The results obtained from this study showed good agreement with the experimental results.

Al-Naimi(٧) **[١٩٩٦]** studied the three dimensional reinforced concrete structures subjected to static and dynamic loading. Nonlinear behavior and time dependent effects were included in the finite element analysis. Material nonlinearities as a result of tension cracking, strain softening after cracking, the nonlinear response of concrete in compression, crushing of concrete and yield of reinforcement were considered. Concrete was considered as a time dependent material. The three-dimensional computation model was adopted with eight and twenty node hexahedral isoparametric elements. In the idealization of the reinforced concrete structure, the steel reinforcement was incorporated in the concrete brick element by assuming prefect bond.

٢.٤ *Thick Plate on Elastic Foundation*

There are many researchers who studied thick plate foundation:

Fridrick (٢٣) **[١٩٥٦]** modified the basic equations of Reissner theory to include the elastic foundation. He presented the solution of axisymmtric and asymmetric isotropic thick circular plates on elastic foundation by using Bessel functions.

The results were given in a table for different plate thickness to radius ratios and the comparisons between an infinite and finite circular plate on elastic foundation were shown in graphical plots.

Cheung and Nag[١٧] [١٩٦٨] analyzed plates and beams on elastic foundation by using the finite element method. Elastic foundation was represented by linear and nonlinear behavior. The horizontal contact pressure at the interface between the structure and foundation soil has been incorporated in the analysis and the effect due to separation on contact surfaces due to uplift has also been investigated.

Svec [٥٣] [١٩٧٠] used Reissner equation with finite element solution to solve simply supported thick plate and slab foundation. Elastic foundation was formulated by an elastic half space. The contact between the plate and the soil was assumed to be frictionless. A parametric study was performed by varying stiffness parameter (Young's modulus for the plate to Young's modulus for the soil) as well as the plate thickness.

Voyiadjis and Kattan [٥٦] [١٩٨٦] included the effect of transverse normal strain in addition to the transverse shear and normal stress effects in thick plates on elastic foundation. The solution of the governing equations was by using Navier and Levy methods, and comparisons were made with the classical plate theory and Reissner theory. The results showed the increasing influence of tranverse normal strain on the plate behavior as the parameters characterizing the influence of plate thickness.

Al- Jubori[٥] [١٩٩٢] solved the problem of isotropic thick rectangular plates on elastic foundations with both normal and frictional resistance by finite difference and finite element methods. Elastic foundation was represented by Winkler and Coulomb models. Results showed good agreement with the solution by the finite difference especially for plate with large thickness and under distributed loads.

Al-Mahdi[٦] **[١٩٩٤]** extended the same work of **Al-Jubori**[٥] for orthotropic plates.

Al-Azzawi[٢] **[١٩٩٥]** extended Mindlins thick plate theory to include isotropic and orthorropic circular plates with axisymmetriy subjected to generalized loading (distributed moment and forces). He used the finite difference and the finite element methods for analysis of thick plates on elastic foundation with both normal and frictional resistance. Winkler and Coulomb models represented elastic foundation. He found that when thickness becomes small, the formulation was found to be unsuccessful due to both shear and membrane locking. In this study many examples were analyzed and good agreement was obtained between finite difference and finite element methods.

Husain et al. [٣٠] **[١٩٩٩]** extended Mindlin thick plate theory to include the effect of external distributed moments over the plate. Thick plate with elastic foundations with both compressional and frictional resistance were analyzed by using this extended theory, the frictional resistance was represented by Winkler model or by Coulomb model. Finite difference and finite element methods were used to solve the governing equations. The results from these methods were plotted together to check the accuracy of these methods, and good agreement were obtained.

٢.٥ Present Study

The present study deals with the case of reinforced concrete thick plate foundation by using the three dimensional nonlinear finite element analysis. A ٢٠-node brick element with ٦٠ degrees of freedom is imployed to model the concrete; the effect of shear deformation and normal stress are included. Steel reinforcement is represented by an embedded bar through the brick element with perfect bond between concrete and steel. Foundation is represented by four

models with both compresional and frictional resistance: Winkler, Coulomb, Kondner, and Polynomial models.

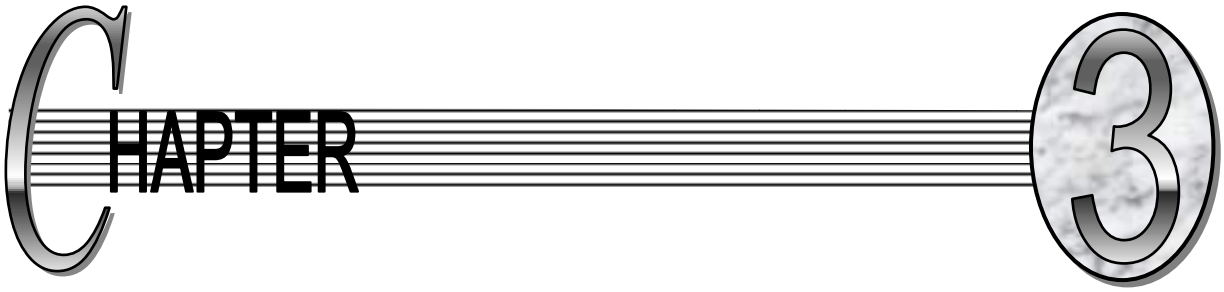

FINITE ELEMENT ANALYSIS

٣.١ Introduction

The limitations of the human mind are such that it cannot grasp the behavior of its complex surroundings and creations in one operation. Thus the process of subdividing all systems into their individual components or elements, whose behavior is readily understood, and then rebuilding the original system from such components to study its behavior is a natural way in which the engineer, the scientist, or even the economist proceeds (Zienkiewics ١٩٧٧).

The civil engineer follows a standard methodology developed over the years to analyze problems of a discrete nature dealing with structures. First, he calculates his force-displacement relationships for each element of the structure and then proceeds to assemble the whole, following a well-defined procedure of establishing local equilibrium at each node or connecting point of the structure. From such equations the solution of the unknown displacements becomes possible (Zienkiewics ١٩٧٧).

The method which has been developed since about ١٩٥٦ as a numerical method of stress analysis and which Clough (mentioned in Zienkiewics ١٩٧٧) called it finite elements, is still most widely used for this purpose. Also it has become useful in many other areas including heat conduction, seepage flow, fluid dynamics and electric and magnetic fields (Cook ١٩٧٤).

Nowadays, the method has been extensively used for the non-linear analysis of reinforced concrete members because it yields a wide range of information for a

single computer analysis. The information includes displacements, strains, distribution of normal and shear stresses in concrete, crack pattern at different stages of loading and forces in longitudinal steel bars and stirrups (Chen ١٩٨٢).

In the present study, the ٢٠-node isoparametric brick element is used for the idealization of concrete, while the steel reinforcement is formulated by using bar elements embedded inside the concrete with the assumption of perfect bond between the two types of elements. To study the interaction between the structural foundation elements and the supporting medium, the plate foundation is represented by the ٢٠-node isoparametric brick elements and the soil is represented by linear models (Winkler and Coloumb) and non-linear models (Kondner and Polynomial).

٣. ٢ Three – Dimensional Brick Element

In the finite element method, the construction of the stiffness matrix of the brick element has been facilitated by three advances in the finite element technology: natural coordinates, isoparametric definition and numerical integration (Al – Shaarbaf ١٩٩٠).

These advances revolutionized the finite element field in mid – ١٩٦٠'s, mainly, when the ٨ – node linear and the ٢٠ – node quadratic brick elements were used in representing the three dimensional solid bodies.

The quadratic ٢٠ - node brick element shown in Fig. (٣.١) is adopted to represent concrete. This type of element is popular due to its superior performance. A major advantage of the quadratic ٢٠ – node brick element over the ٨ – node brick element, when studying complex cases, is that less number of elements can be used, as well as it may have curved sides and therefore provides a better fit to curved sides of an actual structure [Cook (١٩٧٤), Moaveni (١٩٩٩)].

This element has been successfully used in three – dimensional non- linear analysis of reinforced concrete members by many researchers.

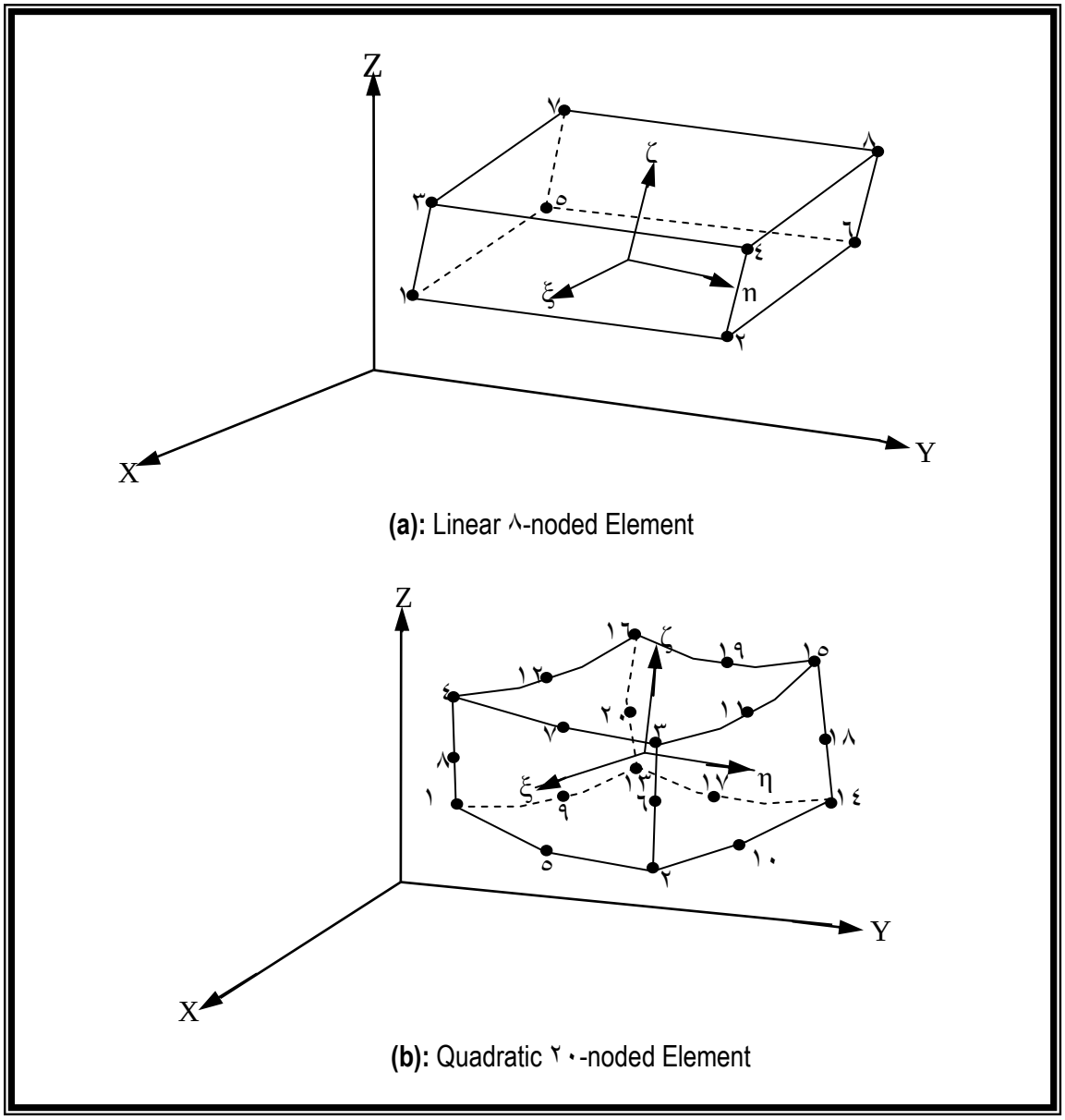

(a): Linear ٨-noded Element

(b): Quadratic ٢٠-noded Element

Figure (٣.١): Linear and Quadratic Isoparamatric Solid Element.

٣. ٢. ١ Shape Functions

The natural local coordinate system is used to describe the displacement components of a point p(ξ, η, ζ) within the element. These local coordinates (ξ,

η, ζ) are scattered in the center of the brick element where the origin point is located as shown in the Fig. (٣.٢)

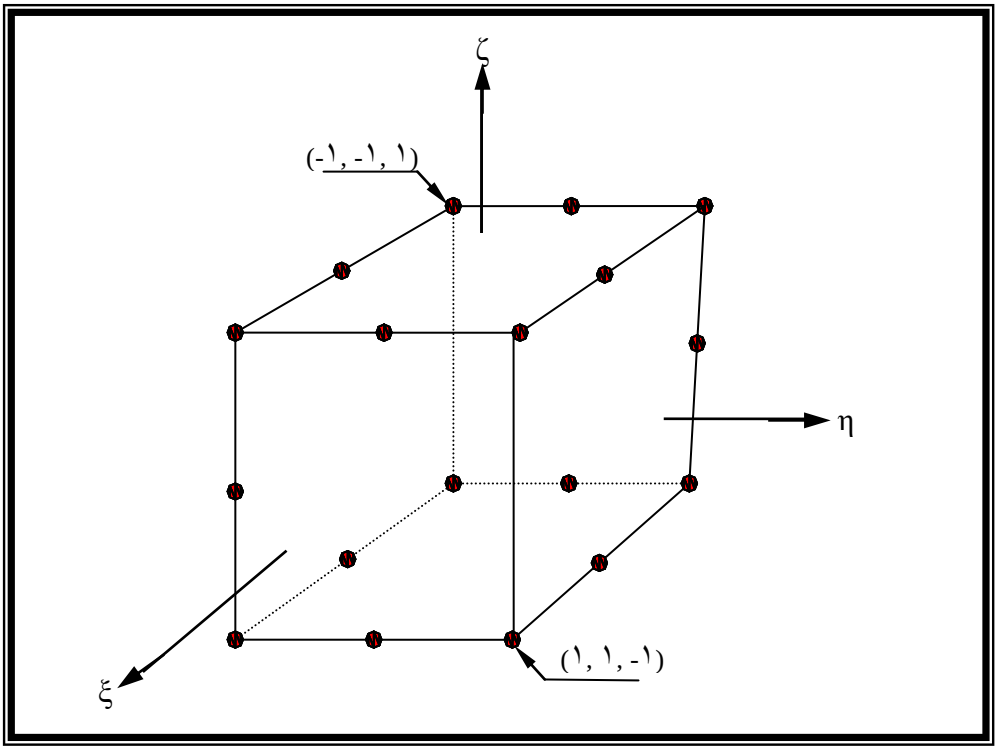

Figure (٣.٢): Local Coordinate System

The element has ٢٠ nodes and ٦٠ d.o.f and bounded by planes with ξ, η, and ζ = ± ١ in ξ, η, ζ space. The starting point for the stiffness matrix derivation is the element displacement field. The isoparametric definition of displacement components is:

$$\left.\begin{aligned} u(\xi,\eta,\zeta) &= \sum_{i=1}^{n} Ni\,(\xi,\eta,\zeta)\,ui \\ v(\xi,\eta,\zeta) &= \sum_{i=1}^{n} Ni\,(\xi,\eta,\zeta)\,vi \\ w(\xi,\eta,\zeta) &= \sum_{i=1}^{n} Ni(\xi,\eta,\zeta)\,wi \end{aligned}\right\} \qquad ...(٣.١)$$

where N_i (ξ, η, ζ) is the shape function at the i-th node and u_i, v_i and w_i are the corresponding nodal displacements. The shape functions of the quadratic ٢٠-node brick element are shown in Table (٣.١)

Table (٣.١): Shape Functions of the Quadratic ٢٠-Node Brick Element (Cook ١٩٧٤)

Location	ξ	η	ζ	Ni (ξ, η, ζ)
Corner nodes	±١	±١	±١	$(١+\xi\,\xi_i)(١+\eta\,\eta_i)(١+\zeta\zeta_i)\,(\xi\,\xi_i+\eta\,\eta_i+\zeta\,\zeta_i-٢)/٨$
mid – side nodes	٠	±١	±١	$(١-\xi^{٢})(١+\eta\,\eta_i)(١+\zeta\,\zeta_i)/٤$
mid – side nodes	±١	٠	±١	$(١-\eta^{٢})(١+\xi\,\xi_i)(١+\zeta\,\zeta_i)/٤$
mid – side nodes	±١	±١	٠	$(١-\zeta^{٢})(١+\xi\,\xi_i)(١+\eta\,\eta_i)/٤$

To check the above mathematical model, each of its ٢٠ shape functions has a value of unity at its specified node and a value of zero at any of the other ١٩ nodes.

In the isoparametric group of elements, the interpolation shape functions are also used to define the geometry of the element and the global coordinates of any point p(ξ, η, ζ) in the terms of the natural local coordinates by using the relations:

$$\left.\begin{aligned} x(\xi,\eta,\zeta) &= \sum_{i=1}^{20} Ni\,(\xi,\eta,\zeta)\,xi \\ y(\xi,\eta,\zeta) &= \sum_{i=1}^{20} Ni\,(\xi,\eta,\zeta)\,y_i \\ z(\xi,\eta,\zeta) &= \sum_{i=1}^{20} Ni\,(\xi,\eta,\zeta)\,zi \end{aligned}\right\} \qquad ...(٣.٢)$$

where x_i , y_i and z_i are the global coordinates of the node i .

٣. ٢. ٢ *Stress and Strain Fields*

Since geometrical nonlinerities are not considered in the present work, displacement gradients remain small throughout the loading process and hence the engineering components of strain can be expressed in terms of the first

partial derivatives of the displacement components. Therefore, the linearized strain – displacement relationships may be written as:

$$\{\varepsilon\} = \begin{Bmatrix} \varepsilon_x \\ \varepsilon_y \\ \varepsilon_z \\ \gamma_{xy} \\ \gamma_{yz} \\ \gamma_{zx} \end{Bmatrix} = \begin{Bmatrix} \frac{\partial u}{\partial x} \\ \frac{\partial v}{\partial y} \\ \frac{\partial w}{\partial z} \\ \frac{\partial u}{\partial y} + \frac{\partial v}{\partial x} \\ \frac{\partial v}{\partial z} + \frac{\partial w}{\partial y} \\ \frac{\partial w}{\partial x} + \frac{\partial u}{\partial z} \end{Bmatrix} = \sum_{i=1}^{20} \underbrace{\begin{bmatrix} \frac{\partial Ni}{\partial x} & 0 & 0 \\ 0 & \frac{\partial Ni}{\partial y} & 0 \\ 0 & 0 & \frac{\partial Ni}{\partial z} \\ \frac{\partial Ni}{\partial y} & \frac{\partial Ni}{\partial x} & 0 \\ 0 & \frac{\partial Ni}{\partial z} & \frac{\partial Ni}{\partial y} \\ \frac{\partial Ni}{\partial x} & 0 & \frac{\partial Ni}{\partial z} \end{bmatrix}}_{[B]} \cdot \underbrace{\begin{Bmatrix} u_i \\ v_i \\ w_i \end{Bmatrix}}_{\{a\}^e} \qquad \ldots(٣.٣)$$

Since the shape functions N_i are functions of the local coordinates rather than Cartesian coordinates, a relationship needs to be established between the derivatives in the two coordinates systems. By using the chain rule, the partial differential relation can be expressed in matrix form as:

$$\begin{bmatrix} \frac{\partial Ni}{\partial \xi} \\ \frac{\partial Ni}{\partial \eta} \\ \frac{\partial Ni}{\partial \zeta} \end{bmatrix} = \underbrace{\begin{bmatrix} \frac{\partial x}{\partial \xi} & \frac{\partial y}{\partial \xi} & \frac{\partial z}{\partial \xi} \\ \frac{\partial x}{\partial \eta} & \frac{\partial y}{\partial \eta} & \frac{\partial z}{\partial \eta} \\ \frac{\partial x}{\partial \zeta} & \frac{\partial y}{\partial \zeta} & \frac{\partial z}{\partial \zeta} \end{bmatrix}}_{[J]} \cdot \begin{bmatrix} \frac{\partial Ni}{\partial x} \\ \frac{\partial Ni}{\partial y} \\ \frac{\partial Ni}{\partial z} \end{bmatrix} \qquad \ldots. (٣.٤)$$

where [J] is the Jacobian matrix and the elements of this matrix can be obtained by differentiation of equation (٣.٢).

The Jacobian matrix can be expressed as:

$$[J] = \begin{bmatrix} \sum \frac{\partial Ni}{\partial \xi} x_i & \sum \frac{\partial Ni}{\partial \xi} y_i & \sum \frac{\partial Ni}{\partial \xi} z_i \\ \sum \frac{\partial Ni}{\partial \eta} x_i & \sum \frac{\partial Ni}{\partial \eta} y_i & \sum \frac{\partial Ni}{\partial \eta} z_i \\ \sum \frac{\partial Ni}{\partial \zeta} x_i & \sum \frac{\partial Ni}{\partial \zeta} y_i & \sum \frac{\partial Ni}{\partial \zeta} z_i \end{bmatrix} \quad \text{.... (٣.٥)}$$

Then, the derivatives of the shape function with respect to Cartesian coordinates can obtain as:

$$\begin{bmatrix} \frac{\partial Ni}{\partial x} \\ \frac{\partial Ni}{\partial y} \\ \frac{\partial Ni}{\partial z} \end{bmatrix} = [J]^{-1} \cdot \begin{bmatrix} \frac{\partial Ni}{\partial \xi} \\ \frac{\partial Ni}{\partial \eta} \\ \frac{\partial Ni}{\partial \zeta} \end{bmatrix} \quad \text{.... (٣.٦)}$$

Where $[J]^{-١}$ is the inverse of Jacobian matrix given by:

$$[J]^{-1} = \begin{bmatrix} \frac{\partial \xi}{\partial x} & \frac{\partial \eta}{\partial x} & \frac{\partial \zeta}{\partial x} \\ \frac{\partial \xi}{\partial y} & \frac{\partial \eta}{\partial y} & \frac{\partial \zeta}{\partial y} \\ \frac{\partial \xi}{\partial z} & \frac{\partial \eta}{\partial z} & \frac{\partial \zeta}{\partial z} \end{bmatrix} \quad \text{.... (٣.٧)}$$

As $[J].[J]^{-١} = [J]^{-١}.[J] = [I]$ (unit matrix)

The vector of stresses is given by:

$$\{\sigma\} = \begin{Bmatrix} \sigma_x \\ \sigma_y \\ \sigma_z \\ \tau_{xy} \\ \tau_{yz} \\ \tau_{zx} \end{Bmatrix} \quad \ldots.(٣.٨)$$

and the stress – strain relationship is represented as:

$$\{\sigma\} = [D].\{\varepsilon\} \quad \ldots.(٣.٩)$$

Where [D] is the constitutive matrix.

٣. ٢. ٣ Stiffness Matrix Calculation

In order to establish the governing equations of static equilibrium, which will lead to the derivation of the stiffness matrix, the principle of virtual displacements for a deformable body is used. It simply states that a deformable body is in equilibrium if the total work done by all the external forces plus the total work done by all the internal forces during any kinematically admissible virtual displacement is zero (Hussain ٢٠٠٢) or in other words, gain in strain energy is equal to loss of potential work by external forces:

$$\delta W_{int} - \delta W_{ext} = 0 \quad \ldots.(٣.١٠)$$

The external work can be expressed as the work done in moving the body forces ***b*** and surface traction ***t*** through the virtual displacement $\{\partial U\}$, as:

$$\delta W_{ext} = \int_v \{\partial u\}^T \{b\}\, dv + \int_s \{\partial U\}^T \{t_s\} ds \quad \ldots.(٣.١١)$$

where v is the volume of the body and s is that part of the surface of the body where external tractions are prescribed.

The change in the strain energy. or internal work, due to a set of virtual strains, $\{\partial\varepsilon\}$, corresponding to the virtual displacement $\{\partial u\}$ is:

$$\delta W_{int} = \int_v \{\partial\varepsilon\}^T \{\sigma\} dv \quad \text{..... (٣.١٢)}$$

By substituting equations (٣.٩) into equation (٣.١٢) then

$$\delta W_{int} = \int_v \{\partial\varepsilon\}^T [D]\{\varepsilon\} dv \quad \text{..... (٣.١٣)}$$

By substituting equations (٣.١١) and (٣.١٣) into equation (٣.١٠), then:

$$\int_v \{\partial\varepsilon\}^T [D]\{\varepsilon\} dv - \int_v \{\partial u\}^T \{b\} dv - \int_S \{\partial u\}^T \{t_S\} ds = 0 \quad \text{..... (٣.١٤)}$$

This expression represents the equation of static equilibrium for a general body.

The basic concept of finite element analysis is to discretize the continuum into arbitrary numbers of small elements connected together at their common nodes. For a finite element, e, of the discrete model, the displacement vector at any point is:

$$\{U\}^e = [N]\ \{a\}^e \quad \text{.....(٣.١٥)}$$

Where [N] is a matrix containing the interpolation functions which relate the displacement $\{U\}^e$ to the nodal displacements $\{a\}^e$ of the element.

By differentiation of the displacements, the corresponding strains, $\{\varepsilon\}^e$, are obtained such that:

$$\{\varepsilon\}^e = [A]\{U\}^e \quad \text{....(٣.١٦)}$$

where [A] is the matrix, which contains the differential operators. Substituting of equation (٣.١٥) into equation (٣.١٦) yields:

$$\{\varepsilon\}^e=[A][N]\{a\}^e \qquad \text{....(٣.١٧)}$$

or

$$\{\varepsilon\}^e=[B]\{a\}^e \qquad \text{.....(٣.١٨)}$$

where [B] is the strain-displacement matrix, which represents the values of the strain at any point within the element, due to unit values of nodal displacements. In the discrete model, the equations of equilibrium of the continuum may be written as the sum of integration over the volume and surface area for all the finite elements. Therefore, by making use of equation (٣.١٥) and (٣.١٨), equation (٣.١٤) becomes:

$$\partial\{a\}^T\left\{\sum_{n}\int_{V}[B]^T[D][B]dv^e\{a\}^e-\sum_{n}\int_{V}[N]^T\{R\}^e dv^e-\sum_{n}\int_{S}[N]^T\{T_S\}^e ds^e\right\}=0 \qquad \text{.....(٣.١٩)}$$

Since the relationship must be valid for any set of virtual displacements, and since $\partial\{a_e\}^T$ is arbitrary or $\partial\{a_e\}^T$ not equal ٠, then equation (٣.١٩) is written in brief for one element ***e*** as:

$$\{f\}^e=[k]^e.\{a\}^e \qquad \text{....(٣.٢٠)}$$

where [k] is the structural stiffness matrix of the assmblage of the elements and given by:

$$[k]=\sum_{n}[k]^e \qquad \text{....(٣.٢١)}$$

and {a} is the corresponding element assemblage nodal displacement vector, and {f} is the element assemblage of external nodal force vector given by:

$$\{f\} = \sum_{n} \int_{v^e} [N]^T \{b\}^e \, dv^e + \sum_{n} \int_{s^e} [N]^T \{T_s\}^e \, ds^e \qquad \ldots.(٣.٢٢)$$

For an element of volume ***v***, the stiffness matrix is presented implicitly in equation (٣.٢١) as:

$$[K]^e = \int_{v^e} [B]^T . [D] . [B] \, dv^e \qquad \ldots.(٣.٢٣)$$

For three – dimension elements, the differential volume dv^e, may be written as:

$$dv^e = dxdydz \qquad \ldots.(٣.٢٤)$$

Equation (٣.٢٤) can be transformed into the natural coordinates as:

$$dv^e = |J| d\xi d\eta d\zeta \qquad \ldots.(٣.٢٥)$$

where $|J|$ is the determinant of the Jacobian matrix. The limits of integration in the natural coordinates become -١ an $+١$ and the element stiffness matrix can therefore be written as:

$$[K]^e = \int_{-1}^{+1} \int_{-1}^{+1} \int_{-1}^{+1} [B]^T [D][B] |J| d\xi d\eta d\zeta \qquad \ldots.(٣.٢٦)$$

In general it is not possible to evaluate the element stiffness matrix explicitly. Thus, numerical integration has to be used.

٣.٣ Reinforcement Idealization

In developing a finite element model for reinforced concrete members, at least three alternative representations of reinforcement have been used:

a) Distributed Representation

In this representation, Fig. (٣.٣a), the steel is assumed to be distributed within the concrete element with a particular orientation angle θ. In the composite concrete reinforcement constitutive relation is used in this case [ASCE (١٩٨١), Chen (١٩٨٢)]. To derive such a relation, a perfect bond is usually assumed between the concrete and the steel.

b) Discrete Representation

A discrete representation of the reinforcement by using independent one – dimensional elements has been widely used, Fig. (٣.٣b). Axial force members, or bar links, may be used and they are assumed to be pin connected with two – degrees of freedom at the nodal points. Beam elements may also be used, and assumed to be capable of resisting axial force, shear, and bending, with three degrees of freedom assigned at each node. In either case, the one – dimensional reinforcement elements are easily superimposed on the multi – dimensional finite element mesh representing the concrete. A significant advantage of the discrete representation in addition to its simplicity is that it can account for possible displacement of the reinforcement with respect to the surrounding concrete (bond slip). [Cook (١٩٨١), Chen (١٩٨٢)].

c) Embedded Representation

An embedded representation, Fig. (٣.٣c), may be used in connection with higher order isoparametric concrete elements [ASCE (١٩٨١)]. The reinforcement bar is considered to be an axial member built into the isoparametric concrete element such that its displacements are consistent with those of the element. Perfect bond between the steel and the concrete has been assumed in this case. A major advantage of this approach is that the steel bars

can be placed in their correct positions without imposing any restrictions on mesh choice and hence the finite element analysis can be carried out with a smaller number of brick elements compared to the discrete representation of reinforcement. Therefore, the embedded representation is adopted in the present work.

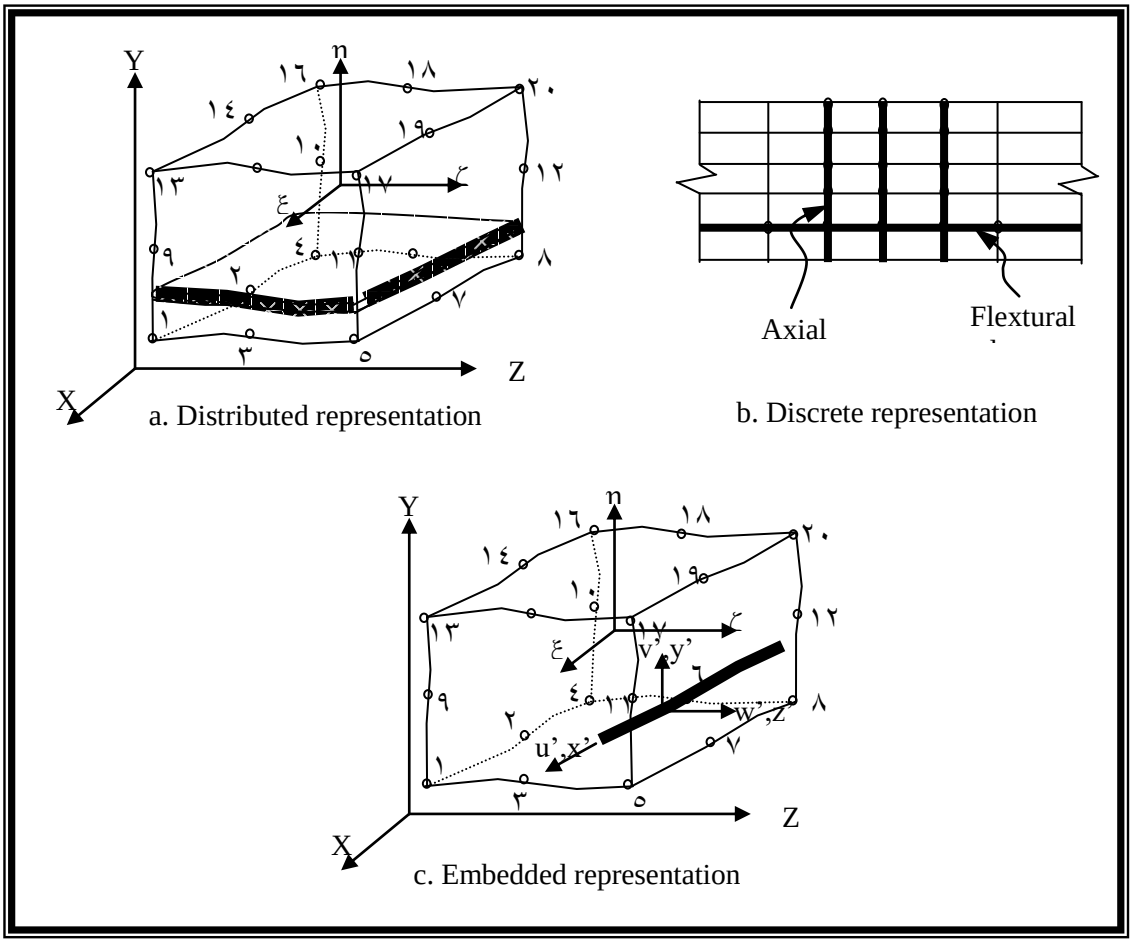

Figure (٣.٣): Alternative Representations of Steel Reinforcement

For particular types of problems, a combination of representations may be used. As an example, discrete beam elements may be used for main reinforcement in beams while axial bar elements for stirrups. Or a distributed model can be used for the steel throughout the surface of the curved shell and discrete bar or beam elements for special reinforcement along the edge.

A derivation is presented in this section for a bar parallel to the local coordinate axis ξ. A similar derivation can be used for bars paralleled to η and ζ axes [Phillips and Zienkiewicz (١٩٧٦)].

For a bar lying inside a hexahedral brick element and parallel to the local coordinate axis ξ, with $\eta = \eta_c$ and $\zeta = \zeta_c$, the displacement representations are:

$$\left.\begin{aligned} u &= \sum_{i=1}^{n} N_i(\xi) u_i \\ v &= \sum_{i=1}^{n} N_i(\xi) v_i \\ w &= \sum_{i=1}^{n} N_i(\xi) w_i \end{aligned}\right\} \qquad \text{....(٣. ٢٧)}$$

The strain-displacement relationship can be expressed in the local coordinate system as:

$$\varepsilon' = \sum_{i=1}^{n} \left[\frac{1}{h^2} \begin{bmatrix} c_1 & c_2 & c_3 \\ c_2 & c_4 & c_5 \\ c_3 & c_5 & c_6 \end{bmatrix} \begin{bmatrix} \frac{\partial N_i}{\partial x} \\ \frac{\partial N_i}{\partial y} \\ \frac{\partial N_i}{\partial z} \end{bmatrix} \right] . \begin{bmatrix} u_i \\ v_i \\ w_i \end{bmatrix} \qquad \text{....(٣. ٢٨)}$$

where:

$$c_1 = (\partial x/\partial \xi)^2,$$
$$c_2 = (\partial x/\partial \xi)(\partial y/\partial \xi),$$
$$c_3 = (\partial x/\partial \xi)(\partial z/\partial \xi)$$
$$c_4 = (\partial y/\partial \xi)^2,$$
$$c_5 = (\partial y/\partial \xi)(\partial z/\partial \xi),$$
$$c_6 = (\partial z/\partial \xi)^2$$

and

$$h = \sqrt{c_1^2 + c_4^2 + c_6^2} \qquad \ldots.(٣.٢٩)$$

Eq. (٣.٢٨) is expressed in a compact form as:

$$\{\varepsilon'\}=[B']\{a\}^e \qquad \ldots.(٣.٣٠)$$

where [B′] is the strain-displacement matrix of the bar element. Then the stiffness matrix of an axially loaded bar element may be expressed as:

$$[K']^e=[B']^T\,[D']\,[B']dv^e \qquad \ldots.(٣.٣١)$$

The constitutive matrix [D′] represents the modulus of elasticity of the steel bar for the case of one-dimensional bar element lying in the direction parallel to the natural coordinate lineξ, and the volume differential dv^e can be written as:

$$dv^e=As.dx'=Ashd\xi \qquad \ldots.(٣.٣٢)$$

where ***As*** is the cross-sectional area of the bar. By substitution of Eq. (٣.٣٢) into Eq.(٣.٣١), the stiffness matrix of the embedded bar can be expressed as:

$$[K']^e = As\int_{-1}^{+1} [B]^T [D'] [B']hd\xi \qquad ....(٣.٣٣)$$

٣.٤ Elastic foundation

For foundation represented by compressional and frictional resistance the stiffness matrix is:

$$[K]_f = \begin{bmatrix} [R_w] & 0 & 0 & 0 & 0 & 0 & 0 & 0 & 0 & . & 0 \\ 0 & [R_w] & 0 & 0 & 0 & 0 & 0 & 0 & 0 & . & 0 \\ 0 & 0 & [R_w] & 0 & 0 & 0 & 0 & 0 & 0 & . & 0 \\ 0 & 0 & 0 & [R_w] & 0 & 0 & 0 & 0 & 0 & . & 0 \\ 0 & 0 & 0 & 0 & [R_w] & 0 & 0 & 0 & 0 & . & 0 \\ 0 & 0 & 0 & 0 & 0 & [R_w] & 0 & 0 & 0 & . & 0 \\ 0 & 0 & 0 & 0 & 0 & 0 & [R_w] & 0 & 0 & . & 0 \\ 0 & 0 & 0 & 0 & 0 & 0 & 0 & [R_w] & 0 & . & 0 \\ 0 & 0 & 0 & 0 & 0 & 0 & 0 & 0 & 0 & . & 0 \\ . & . & . & . & . & . & . & . & . & . & . \\ 0 & 0 & 0 & 0 & 0 & 0 & 0 & 0 & 0 & 0 & 0 \end{bmatrix}_{n*n} \qquad ....(٣.٣٤)$$

where n is the total number of node per element,

$$[R_w] = \begin{bmatrix} K_{f1} & 0 & 0 \\ 0 & K_{f2} & 0 \\ 0 & 0 & K_{f3} \end{bmatrix} \qquad ....(٣.٣٥)$$

The stiffness of foundation distributed on the node of element like the distribution of pressure load on the bottom surface of the element (ζ=-١), thus at node k

$$K_{f1} = \int_{-1}^{+1}\int_{-1}^{+1} k_x.N(\xi,\eta).|J(\xi,\eta,\zeta)|.d\xi.d\eta \qquad ....(٣.٣٦)$$

$$K_{f2} = \int_{-1}^{+1}\int_{-1}^{+1} k_y.N(\xi,\eta).|J(\xi,\eta,\zeta)|.d\xi.d\eta \qquad ....(٣.٣٧)$$

$$K_{f2} = \int_{-1}^{+1}\int_{-1}^{+1} k_z.N(\xi,\eta).|J(\xi,\eta,\zeta)|.d\xi.d\eta \qquad ....(٣.٣٨)$$

were k_x, k_y, and k_z are the subgrade coefficients in the local coordinate x,y, and z, $N^k(\xi,\eta)$ is the shap function at node k and $|J(\xi,\eta,\zeta)|$ is the determinant of the Jacobian matrix.

The total stiffness of the thick plate foundation system will be:

$$[K]_{tpf} = [K]^e + [K]_f \qquad ....(٣.٣٩)$$

٣.٥ Numerical Integration

To perform the integration required to set up the element stiffness matrix, suitable scheme of numerical integration has to be made. In finite element work, the Gauss-Legendre quadrature scheme has been found to be accurate and efficient. The finite integral of the element stiffness matrix given in Eq. (٣.٢٦), can be expressed in the form [Irons (١٩٧١)]:

$$I = \int_{-1}^{1}\int_{-1}^{1}\int_{-1}^{1} F(\xi,\eta,\zeta)\,d\xi\,d\eta\,d\zeta \qquad ....(٣.٤٠)$$

which may be rewritten numerically as:

$$I = \sum_{i=1}^{ni} \sum_{j=1}^{nj} \sum_{k=1}^{nk} Wi.Wj.Wk\, F(\xi_i, \eta_j, \zeta_k) \qquad \ldots.(٣.٤١)$$

where ***ni, nj, nk*** are the number of Gaussian points ξ_i, η_j, ζ_k. The function $F(\xi_i, \eta_j, \zeta_k)$ represents the matrix multiplication ($[B]^T.[D].[B].det[J]$) at sampling points ξ_i, η_j, ζ_k.

In a similar manner, the integral of the stiffness matrix of the embedded reinforcement can be written as:

$$I = \sum_{i=1}^{ni} Wi\, F(\xi_i) \qquad \ldots.(٣.٤٢)$$

The application of the three-dimensional finite element analysis in connection with the non-linear behavior of reinforced concrete structures needs a large amount of computation time, due to the frequent evaluation of the stiffness matrix. Therefore, it is necessary to choose a suitable integration rule that minimizes the computation time with sufficient accuracy. Several types of integration rules can be used such as the eight (٢ x ٢ x ٢), and the twenty-seven (٣ x ٣ x ٣) Gaussian rules are used to integrate the stiffness matrix of eight-node linear and twenty node quadratic brick element. Also, there is the fifteen -node Gauss-type integration rule that evaluates the integration for the twenty-node quadratic brick element [Irons (١٩٧١)].

The integration rules, which exist in this program, are the ٢٧ (٣ x ٣ x ٣) Gauss quadrature and the ١٥ points type integration rule. The weights and

abscissa of the sampling points are listed in Appendix (A) .The relative distribution of the Gaussian points over the element is given in Fig. (٣.٤).

In the present study, ١٥ Gauss points are used for the numerical integration, because the reduced integration rules were found to be accurate and computationally efficient than other types of integration rules. This is due to the fact that the reduced integration rule can significantly reduce the effect of shear locking which may occur in plate analysis when the full integration rule has been used. (Al- Shaarbaf and Mohammed (١٩٩٩))

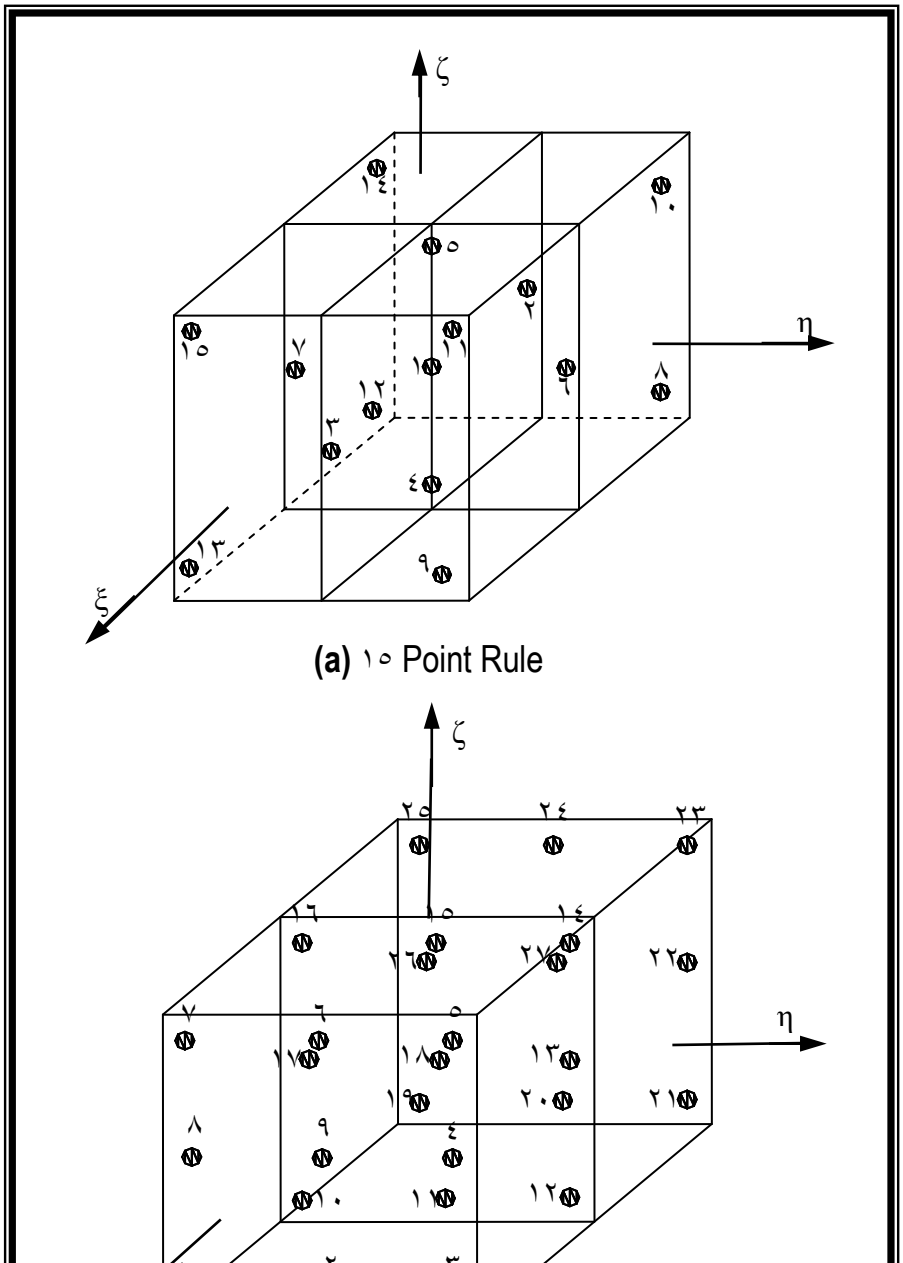

(a) ١٥ Point Rule

٣ . ٦ *Uniaxial and Multi-Axial Behavior of Concrete*

A typical stress-strain relationship for concrete in compression is shown in Fig. (٣.٥). It can be seen that the stress-strain curve has a nearly elastic behavior up to about ٣٠ percent of its maximum compressive strength ***(f′c)***.For the stress above this point, the curve shows a gradual increase in curvature up to about ***(٠.٧٥ f′c - ٠.٩٠ f′c)***, beyond which it bends more sharply and approaches the peak point at ***(f′c)***. Beyond this point, the stress-strain curve has a descending part until crushing failure occurs at some ultimate strain ε_u (Chen ١٩٨٢).

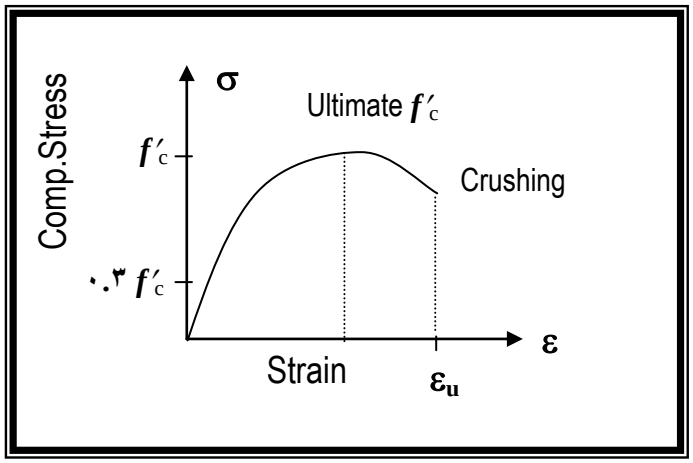

Figure (٣.٥): Typical Uniaxial Stress –Strain Curve for Concrete in Compression

Poisson ratio ***(ν)***, which is defined as the ratio of lateral strain to the principal compressive strain has been observed in the experiments to be constant up to a stress level of ***(٨٠٪)*** of f'_c and ranges between ٠.١٥ and ٠.٢٢ (Chen ١٩٨٢).

Under tensile stresses, the shape of the stress-strain curve of concrete shows many similarities to the uniaxial compression curve. There are, however, some differences, that the uniaxial tension state of stress tends to arrest the crack much less frequently than the compressive state of stress. Therefore, it can be expected that the interval of stable crack propagation is relatively short. It has been found that the ratio between the uniaxial tensile and compressive strength (f_t and f'_c) may vary considerably but usually ranges from ٠.٠٥ to ٠.١. The modulus of elasticity under uniaxial tension is somewhat higher and Poisson ratio some what lower than in compression (Mehta ١٩٨٦).

The behavior of concrete under multi-axial stress condition is very complex if it is compared with that under uniaxial stress condition and has not yet been assessed experimentally in a complete manner. Various material models with considerable simplifying assumptions have been proposed in literature. A typical biaxial strength envelope is shown in Fig. (٣.٦) (Kupfer et. al. ١٩٦٩). It is seen that the maximum compressive strength increases for biaxial compression state. A maximum strength increase of approximately ٢٥ percent is achieved at a stress ratio of $(\sigma_2 / \sigma_1 = 0.5)$, and this is reduced to about ١٦ percent at an equal biaxial compressive state $(\sigma_2 / \sigma_1 = 1)$. Under biaxial compression – tension state of stress, the compressive strength decreases almost linearly as the applied tensile stress is increased [Chen (١٩٨٢)].

Under biaxial tension, the strength is almost the same as that of uni-axial tensile strength. When subjected to triaxial compressive stresses, concrete exhibits strength which increases with increasing the confining pressure [Mehta (١٩٨٦)].

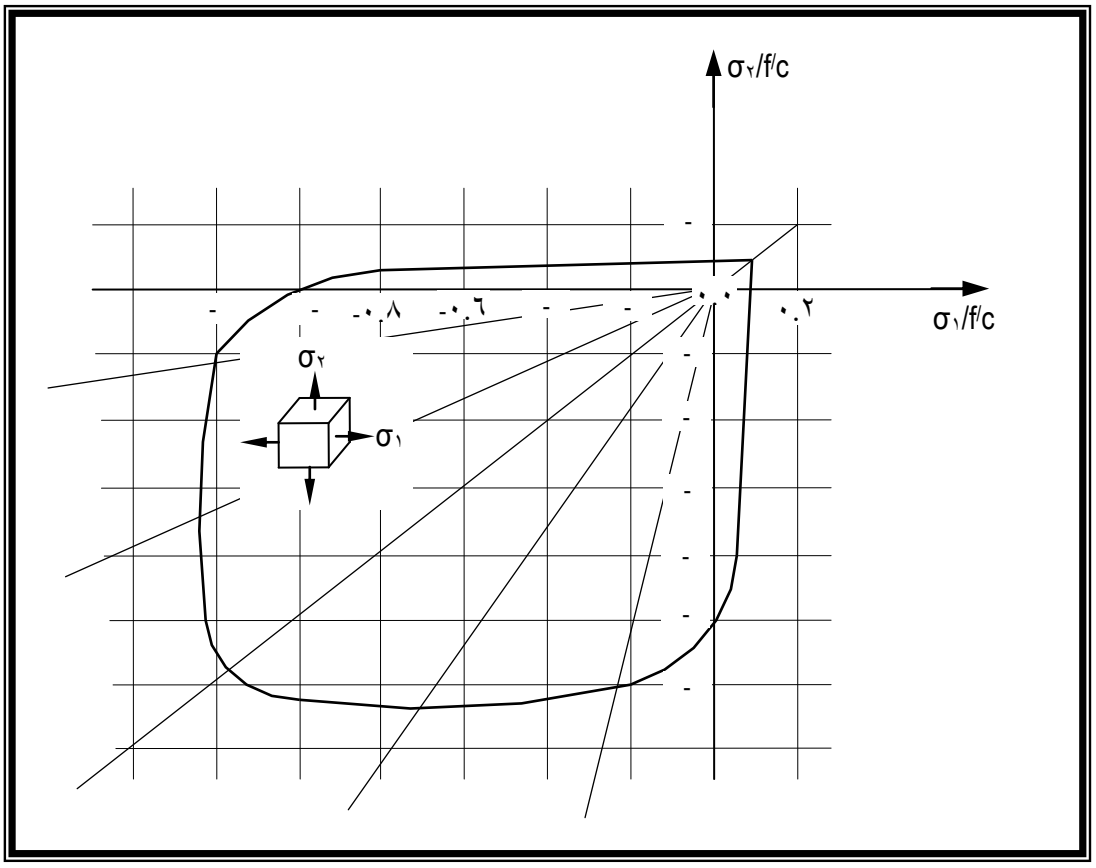

Figure (٣.٦): Biaxial Strength of Concrete (Kupfer et. al. ١٩٦٩)

Experiments indicate that concrete in triaxial stresses has a fairly consistent failure surface which is a function of the three principal stresses, Fig. (٣.٧). This failure surface can be represented by threestress invariants. These invariants are the first invariant of the stress tensor (I_1), and the second and the third invariant of the deviatoric stress tensor (J_2) and (J_3) (Chen ١٩٨٢).

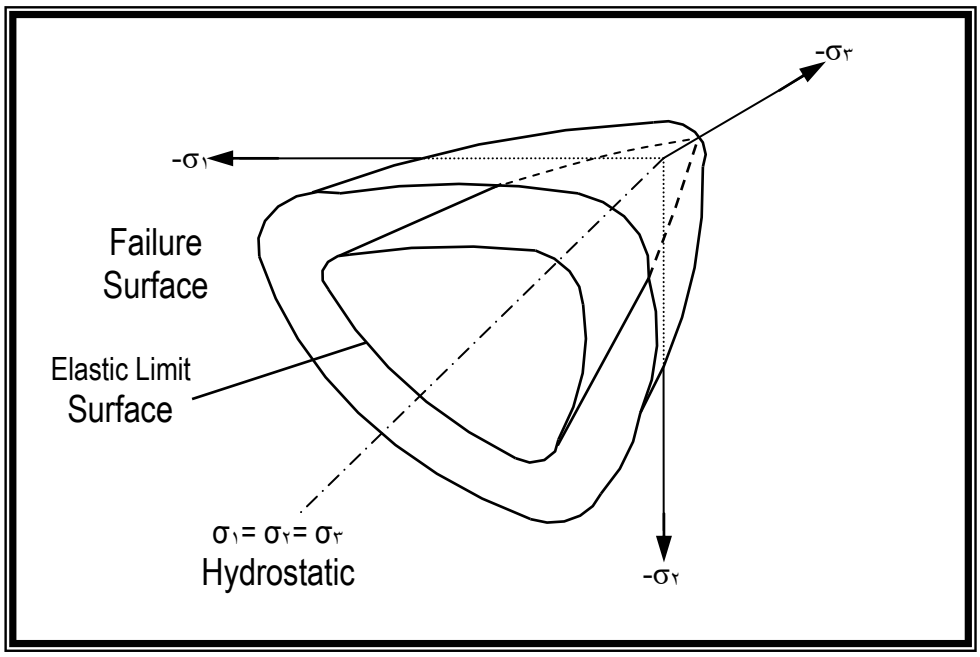

Figure(٣.٧): Triaxial Strength Envelope of Concrete (Chen, ١٩٨٢)

٣.٧ Numerical Modeling of Concrete Properties

Concrete is a heterogeneous material. So, it has a non- linear behavior under loading. This non- linearity in reinforced concrete structures may be due to inelastic response of concrete in compression, cracking of concrete in tension and interactive effects between concrete and reinforcement. Despite the complex behavior, it is required to model these properties to include the different sources of non-linearity in the finite element analysis. Therefore, the following aspects of behavior must be included in the numerical modeling of concrete: [AL-Shaarbaf (١٩٩٠), Bathe and Ramaswamy (١٩٧٩)]

- Stress-strain model to represent the behavior of concrete prior to failure.
- A failure criterion to simulate the cracking and crushing of concrete.
- A model for crack representation.
- Modeling of the post-cracking stress-strain relationship.
- Modeling of the reduction in compressive strength due to orthogonal cracking.

٣.٧.١ Stress-Strain Models

Several approaches for describing the complicated stress-strain relationship of concrete under various combined stress-strain states have been usually used. These approaches can be divided generally into:

-Elasticity based models.
-Plasticity based models.

Elasticity based models may be linear or non-linear elastic models. In the former, the stress-strain relation for uncracked and cracked concrete is developed depending on the theory of linear elasticity. These models are

adequate when the failure condition is the tensile cracking of concrete. However, these models fail to identify the inelastic deformation. This disadvantage becomes obvious when the material experiences unloading. This can be improved by introducing non- linear elastic models.

Non – linear elastic models are based on two approaches, the total and the incremental stress-strain formulation. With the total stress-strain model, the current state of stress is assumed to be uniquely expressed as a function of the current state of strain. This type of model is reversible and path independent, which is generally not true for concrete. Also, it suffers from inability to predict the inelastic deformation. For the incremental formulation, the state of stress is dependent on the current state of strain and on the stress path followed to reach such a state (this type of formulation is incrementally reversible and path dependent). This formulation gives a good representation for concrete behavior as compared with the total stress formulation.

Plasticity based models have been used extensively in recent years for modeling ofconcrete in compression. It is known that under triaxial compression, concrete can flow as a ductile material on the yield surface before reaching the crushing strain.

To account for this property, various plasticity models have been introduced. In these models, concrete may be defined as an elastic – perfectly plastic material or as a strain hardening material. The prediction of the overall behavior by using the plasticity based models gives good agreement with experimental results. So, this type of modeling is adopted in the present work.

3.8 Modeling of Concrete Fracture

Generally, concrete fracture may be either a compression fracture (i.e. crushing of concrete) or a tension fracture (i.e. cracking of concrete).

The crushing failure occurs when the material can resist no further compressive loading while the tension failure of concrete is characterized by a gradual growth of cracks that join together and eventually disconnect larger parts of the structure. It is a usual assumption that formation of cracks is a brittle process and that the strength in the tension-loading direction abruptly goes to zero after such cracks have formed, Fig. (٣.٨a). But when reinforcement bars bridge the concrete cracks, the strength mechanism becomes more complex and the carrying strength of concrete between cracks can be safely exploited [Chen (١٩٨٢)].

3.8.1 *Cracking Models*

In general, the models, which have been developed to represent cracking in connection with the finite element analysis of reinforced concrete members, are composed of three basic components, a criterion for crack initiation, a method of crack representation and a method for cracking propagation.

Two fracture criteria are commonly used, the maximum principal stress criterion and the maximum principal strain criterion. When a principal stress or strain exceeds its limiting value a crack is assumed to occur in a plane normal to the direction of the offending principal stress or strain, Figure (٣.٨b).

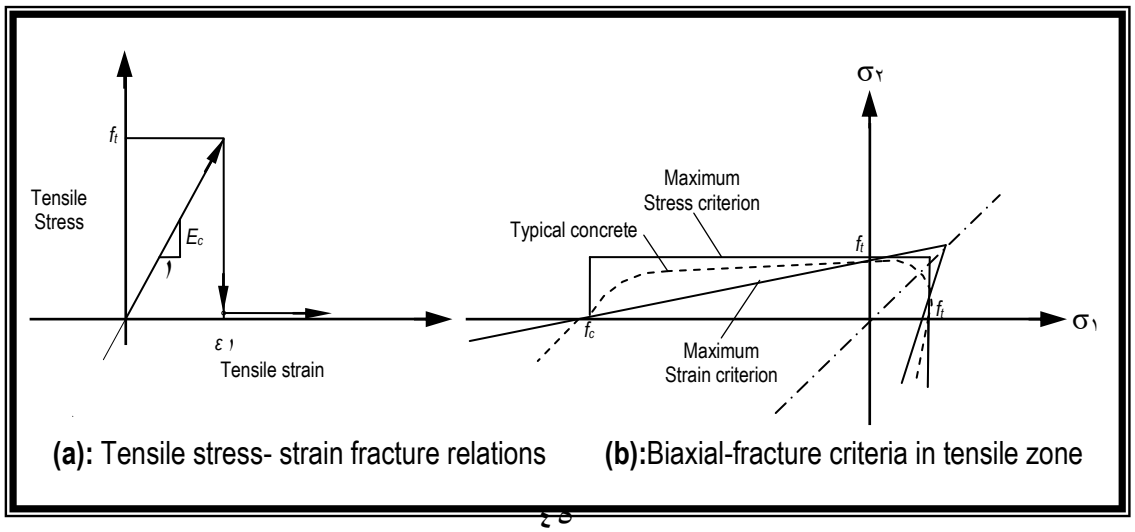

Figure (٣.٨): Cracking of Concrete (Chen, ١٩٨٢)

In finite element analysis of concrete structures, two approaches have been employed for crack modeling, these are the smeared cracking and the discrete cracking models. The particular cracking model to be selected depends upon the purpose of the analysis. If overall load-deflection behavior is desired, without regard to completely realistic crack patterns and local stresses, the smeared crack model is probably the best choice, while if detailed local behavior is of interest, adoption of the discrete cracking model is useful. The two approaches will be discussed in the following sections.

3.8.1.1 *Smeared cracking model*

In this approach, the cracked concrete is assumed to remain a continuum, i.e., the cracks are smeared out in a continuos fashion. It is assumed that concrete becomes orthotropic or transversely isotropic after the first cracking has occurred, one of the material axis being oriented along the direction of cracking. In the smeared cracking model, a crack is not discrete but implies an infinite number of parallel fissures across that part of the finite element, Figure (٣.٩) [Bathe and Ramaswamy (١٩٧٩), Chen (١٩٨٢)].

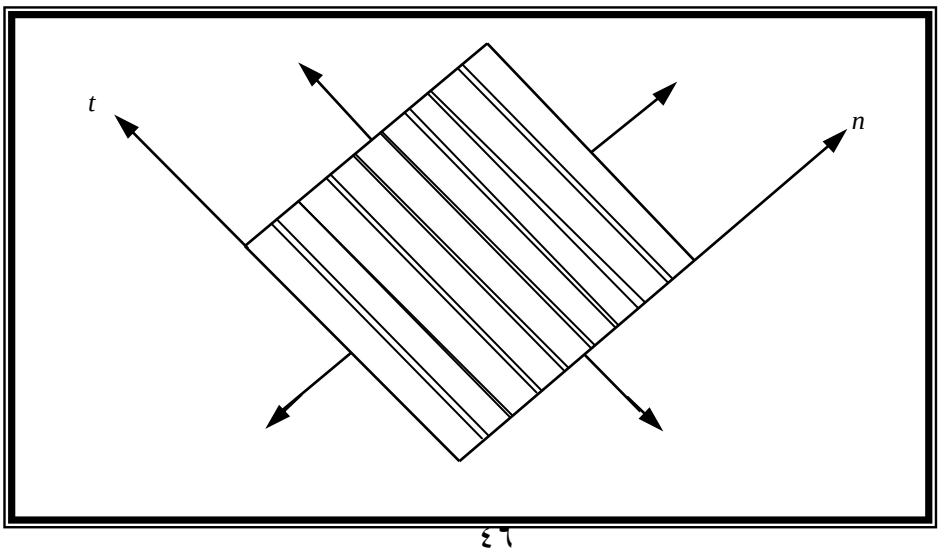

Figure (٣-٩): Smeared Cracked Model

Two different models are used for defining the crack direction. The first is the fixed orthogonal crack. In this approach, the direction of the crack is fixed normal to the direction of the first principal tensile stress that exceeds the cracking stress. By fixing the direction of the cracks, the subsequent rotation of the principal stress is ignored. The second model is the rotating or swinging crack model. In this approach, the crack direction is assumed to be normal to the principal tensile strain direction when the tensile strains reaches a specified limiting value. With further loading and changing of the principal strain direction, the crack is assumed to rotate and the orthotropic material axes are set in the new crack direction.

3.8.1.2 *Discrete cracking model*

An alternative to the continuous smeared cracking model is the introduction of discrete crack model. This is normally done by disconnecting the displacements at nodal points for adjoining elements as shown in Fig. (٣.١٠). One obvious difficulty in such an approach is that the location and orientation of the cracks are not known in advance. Thus, geometrical restriction imposed by the preselected finite element mesh can hardly be avoided. This can be rectified to some extent by redefinition of element nodes. Such techniques are unfortunately extremely complex and time consuming [Al-Shaarbaf (١٩٩٠)]. In the present study, the smeared fixed – crack model has been adopted.

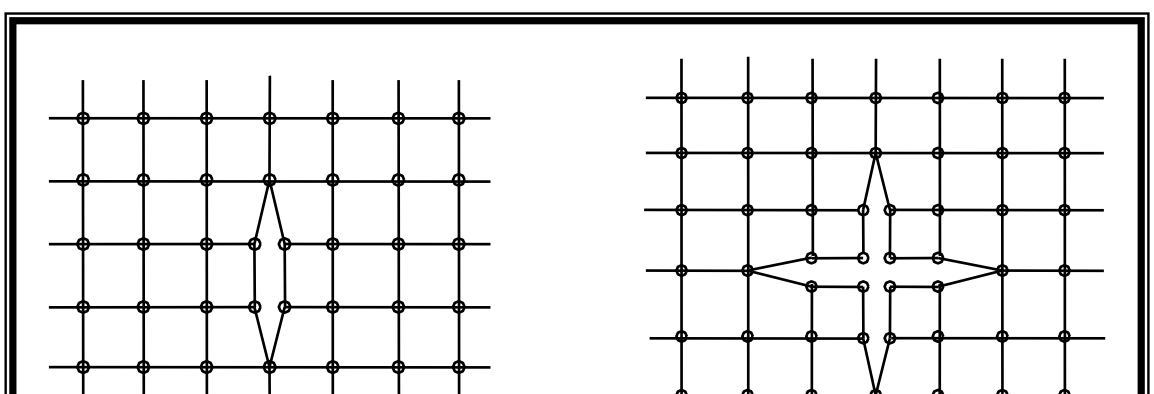

3.8.2 *Post Cracking Models*

In plain and reinforced concrete structures, cracking is not a perfectly brittle phenomenon and experimental evidence shows that the tensile stresses normal to a cracking plane are gradually released as the crack width increases. This type of response is usually modeled in the finite element analysis by using either the tension stiffening or the strain softening concepts. For reinforced concrete structures where the behavior is characterized by the formation of closely spaced cracks, the first concept seems to be more suitable than the latter. The latter is found to be useful for analyzing plain concrete structures where the behavior is governed by the formation of a single macro-crack or a few dominant cracks (Chen ١٩٨٢).

In the case where reinforcement exists, the nature of the stress release is further complicated by the restraining effect of the reinforcing steel. After cracking, the concrete stresses drop to zero and the steel carries the full load. The concrete between cracks, however, still carries some tensile stresses. This tensile stress drops as the load increases and the drop is associated primarily with bond deterioration between steel and concrete. This ability of concrete to share the tensile load with the reinforcement is termed as ***tension stiffening*** phenomenon (Chen ١٩٨٢).

The tension stiffening effect of concrete has been studied in finite element analysis by using two procedures. First, the tension portion of the concrete stress-strain curve has been given a descending branch. Descending branches of many different shapes have been employed, Linear, bilinear and curved shapes. The second is to increase the steel stiffness. The additional stress in the steel represents the total tensile force carried by both the steel and the concrete between the cracks (Chen ١٩٨٢).

3.8.3 *Shear Transfer across the Cracks*

Several mechanisms exist by which shear is transferred across reinforced concrete sections. Among these mechanisms are the shear stiffness of uncracked portion of concrete, aggregate interlock in the crack surface (or interface shear transfer), dowel action in the reinforcement bars and the combined effect of tension in reinforcement and arching action.

For the shear transfer across the cracked concrete planes crossed by reinforcement, the two major mechanisms are the dowel action and the aggregate interlock. Shear transfer by these two mechanisms is accompanied by slippage or relative movement of crack faces. In the dowel action, shear forces are partially resisted by the stiffness of reinforcing bars because slippage imposes bearing forces of opposite direction on the bars. The aggregate interlock mechanism is of frictional nature. Slippage causes the irregular faces of the crack to separate slightly. Tensile stresses created in the steel bars by the separation of crack faces in turn develop some shear resistance (Al-Shaarbaf ١٩٩٠).

3.9 *Concrete Model Adopted in the Analysis*

In this study, a plasticity-based present model is adopted for the non-linear analysis of three-dimensional reinforced concrete structures under static loads. In compression, the behavior of concrete is simulated by an elastic-plastic work hardening model followed by a perfectly plastic response, which is terminated at the onset of crushing. The plasticity model in compression state of stress has the following characteristics: (Al-Shaarbaf ١٩٩٠).

١. yield criterion
٢. hardening rule
٣. flow rule
٤. crushing condition

In tension, linear elastic behavior prior to cracking is assumed. A smeared crack model with fixed orthogonal cracks is adopted to represent the fractured concrete. The model will be described in terms of the following:

١. cracking criterion
٢. post-cracking formulation
٣. shear retention model

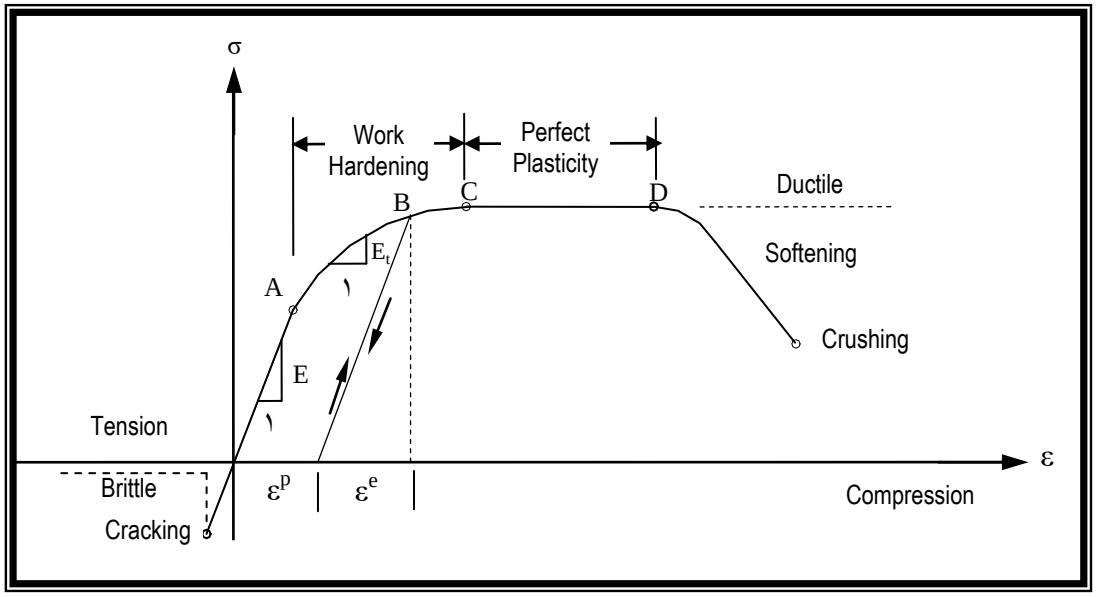

Figure (٣.١٠): Uniaxial Stress-Strain Curve, Pre-and Post-Failure Regime(Chen, ١٩٨٢)

3.9.1 Modeling of Concrete in Compression

3.9.1.1 The yield criterion

Under a triaxial state of stress, the yield criterion for concrete is generally assumed to be dependent on three stress invariants. However, a yield criterion dependent on two stress invariants only has been proved to be adequate for most practical situations. The yield criterion incorporated in the present model is of such type and it has been successfully used in research. It can be expressed as (Al-Shaarbaf ١٩٩٠)

$$f(\sigma) = f(I_1, J_2) = (\alpha I_1 + 3\beta J_2)^{1/2} = \sigma_o \qquad \ldots(٣.٤٣)$$

where (α) and (β) are material parameters, (I_1) is the first stress invariant given by:

$$I_1 = \sigma_x + \sigma_y + \sigma_z \qquad \ldots(٣.٤٤)$$

J_2 is the second deviatoric stress invariant given by:

$$J_2 = \frac{1}{3}\{(\sigma_x^2 + \sigma_y^2 + \sigma_z^2) - (\sigma_x\sigma_y + \sigma_y\sigma_z + \sigma_z\sigma_x)\} + \tau_{xy}^2 + \tau_{yz}^2 + \tau_{xz}^2 \ldots(٣.٤٥)$$

and $\sigma o \geq 0$ is the equivalent effective stress at the onset of plastic deformation, this σ_o can be determined from the uniaxial compression test as:

$$\sigma_o = Cp \cdot f'_c \qquad \ldots(٣.٤٦)$$

where $0 \le Cp \le 1.0$ is the plasticity coefficient, which is used to mark the initiation of the plastic deformation.

The parameters (α) and (β) are determined by using the uniaxial and biaxial compression tests. Then for a uniaxial compression state, the yield stress is given by:

$$\sigma_x = -\sigma_o \qquad \ldots(٣.٤٧)$$

and for the equal biaxial compression state, the yield stress is given by:

$$\sigma_x = \sigma_y = -\gamma\sigma o \qquad \ldots(٣.٤٨)$$

If the results obtained by **Kupfer et al. (١٩٦٧)** for the a failure envelope is employed for initial yield, the value of the constant (γ) is equal to (١.١٦). From Eq. (٣.٤٣) through Eq. (٣.٤٨), the material constants can be found to be:

$$\alpha = 0.35468\sigma o \quad \text{and} \quad \beta = 1.35468 \qquad \ldots(٣.٤٩)$$

Writing $C = \dfrac{\alpha}{(2\sigma o)} = 0.17734$

Therefore Eq. (٣.٤٣) can be written as:

$$f(\sigma) = (2C\sigma_o I_1 + 3\beta J_2)^{1/2} = \sigma_o \qquad \ldots(٣.٥٠)$$

this can be solved for σ_o as:

$$f(\sigma) = C.I_1 + \{(C.I_1)^2 + 3\beta J_2\}^{1/2} = \sigma_o \qquad \ldots(٣.٥١)$$

3.9.1.2 Hardening rule

The concept of plastic flow in work hardening materials extends to the notion of perfectly plastic solids for which the yield or failure surface remains fixed in stress space. The hardening rule defines the motion of the subsequent loading surfaces during plastic loading. A number of hardening rules has been proposed to describe the growth of subsequent loading surface for work-hardening materials. Some of these rules are; isotropic hardening, kinematic hardening and mixed hardening. The isotropic model applies mainly to proportional loading. For cyclic and reversed types of loading, kinematic hardening rule is more appropriate. Combinations of isotropic and kinematic hardening are called mixed hardening rules (Chen ١٩٨٢).

An isotropic hardening rule is used in the present study. Therefore, from Eq. (٣.٥١), the subsequent loading surface may be expressed as (Al-Shaarbaf ١٩٩٠).

$$f(\sigma) = C.I_1 + \{(C.I_1)^2 + 3\beta J_2\}^{1/2} = \bar{\sigma} \qquad \ldots(٣.٥٢)$$

where $\bar{\sigma}$ represents the stress level at which further plastic deformation will occur and this is termed as the effective stress or equivalent uniaxial stress.

The incremental theory of plasticity implies a relationship between the effective stress and the effective plastic strain. The effective plastic strain increment $\delta\varepsilon_p$ that results from an incremental plastic work dw_p, may be determined by using the work-hardening hypothesis as:

$$d\varepsilon_p = \frac{dw_p}{\bar{\sigma}} = \frac{\{\sigma\}^T d\{\varepsilon_p\}}{\bar{\sigma}} \qquad \ldots(٣.٥٣)$$

where $d\varepsilon_p$ represents the effective accumulated plastic strain increment along the strain path.

The effective plastic strain can be written as:

$$\varepsilon_p = \int d\varepsilon_p \qquad \ldots(٣.٥٤)$$

In the present model, a parabolic stress-strain curve is used for the equivalent uniaxial stress-strain relationship beyond the limit of elasticity, $(C_p\, f'_c)$. This relationship represents the work-hardening stage of behavior. When the peak compressive stress is reached, a perfectly plastic response is assumed to occur. Figure (٣.١١) shows the equivalent uniaxial stress-strain curve in the various stages of behavior. These are given by:

(a) During the elastic stage, when $\bar{\sigma} \le C_p . f'_c$

$$\bar{\sigma} = E . \varepsilon_c \qquad \ldots(٣.٥٥)$$

(b) After the initial yielding and up to the ultimate concrete compressive strength, when:- $C_p\ f'_c \le \bar{\sigma} \le f'_c$

$$\bar{\sigma} = C_p\ f'_c + E[\varepsilon_c - \frac{C_p . f'_c}{E}] - [\frac{E}{2\varepsilon_o}][\varepsilon_c - \frac{C_p f'_c}{E}]^2 \qquad \ldots(٣.٥٦)$$

c) for $\varepsilon_c \ge \left(2 - C_p\right) f'_c / E$

$$\bar{\sigma} = f'_c \qquad \ldots(٣.٥٧)$$

Where ε_o^- represents the total strain corresponding to the parabolic part of the curve that can be calculated from:

$$\bar{\varepsilon}_o = \frac{2(1 - C_p)}{E} f'_c \qquad \ldots(٣.٥٨)$$

A value of ٠.٣ is assumed for the plasticity coefficient ***(Cp)*** in the present study and hence plastic yielding begins at a stress level equals to ***(٠.٣ f′c).***

The total effective strain ε_c is composed of two parts, elastic and plastic components:

$$\varepsilon_c = \varepsilon_e + \varepsilon_p \qquad \ldots(٣.٥٩)$$

The elastic strain ε_p is given by:

$$\varepsilon_e = \frac{\bar{\sigma}}{E} \qquad \ldots(٣.٦٠)$$

By substituting Eq. (٣.٥٩) and Eq. (٣.٦٠) into Eq. (٣.٥٦), the effective stress-plastic strain relation can be expressed as:

$$\bar{\sigma} = C_p f'_c - E\,\varepsilon_p + (2E^2.\varepsilon_o \varepsilon_p)^{1/2} \qquad \ldots(٣.٦١)$$

Differentiation of Eq. (٣.٦١) with respect to the plastic strain leads to the slope of the tangent of the effective stress-plastic strain curve, which represents the hardening coefficient, H, that is needed in the formulation of the incremental stress-strain relation:

$$\bar{H} = \frac{d\,\bar{\sigma}}{d\varepsilon_p} = E\left(\sqrt{\frac{\varepsilon_0}{2\varepsilon_p}} - 1\right) \qquad \ldots(٣.٦٢)$$

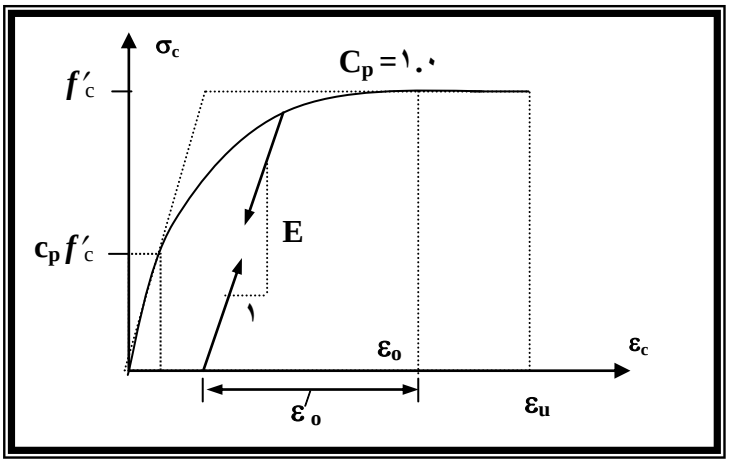

Figure (٣.١١): Uniaxial Stress-Strain Curve for Concrete (AL-Shaarbaf ١٩٩٠)

3.9.1.3 *Flow rule*

In plasticity theory, a flow rule must be defined so that the plastic strain increment can be determined for a given stress increment. The associated flow rule has been widely used for concrete models mainly because of its simplicity. This approach, is adopted in the current model. The plastic strain increment is expressed as:

$$d(\varepsilon_p) = d\lambda \ \frac{\partial f(\sigma)}{\partial \sigma} \qquad \ldots(٣.٦٣)$$

The normal to the current loading surface $\frac{\partial f(\sigma)}{\partial \sigma}$ is termed as the flow vector, The yield function derivatives with respect the stress components define the flow vector **{a}** as:

$$\{a\} = \left[\frac{\partial f}{\partial \sigma_x}, \frac{\partial f}{\partial \sigma_y}, \frac{\partial f}{\partial \sigma_z}, \frac{\partial f}{\partial \tau_{xy}}, \frac{\partial f}{\partial \tau_{yz}}, \frac{\partial f}{\partial \tau_{zx}} \right]^T \qquad \ldots(٣.٦٤)$$

These derivatives are given in Appendix (B):

3.9.1.4 *The incremental stress-strain relationship*

During the plastic loading, both of the initial yield and the subsequent stress states must satisfy the yield condition. $\boldsymbol{F(\sigma, K) = 0}$. The yield function defined in Eq. (٣.٥٦), can be rewritten as,

$$F(\sigma, K) = f(\sigma) + f(k) = 0 \qquad \ldots(٣.٦٥)$$

where k, is the hardening parameter, which governs the expansion of the yield-surface. By differentiating Eq. (٣.٦٥), then

$$dF = \frac{\partial F}{\partial \sigma} d\sigma + \frac{\partial F}{\partial K} dK = 0 \qquad \ldots(٣.٦٦)$$

or

$$a^T d\sigma - A\, d\lambda = 0 \qquad \ldots(٣.٦٧)$$

where

$$A = -\frac{1}{d\lambda} \frac{\partial F}{\partial k} dk \qquad \ldots(٣.٦٨)$$

The total incremental strain vector can be rewritten as:

$$d\{\varepsilon)\} = d\{\varepsilon^e\} + d\,\lambda \frac{\partial F}{\partial \sigma} \qquad \ldots(٣.٦٩)$$

The elastic strain increment is related to the stress increment by the elastic constitutive relation which is given in:

$$d\{\sigma\} = [D] d\{\varepsilon_e\} \qquad \ldots(٣.٧٠)$$

where [D] is the elastic constitutive matrix given by

$$[D] = \frac{E}{(1+\nu)(1-2\nu)} \begin{bmatrix} 1-\nu & \nu & \nu & 0 & 0 & 0 \\ \nu & 1-\nu & \nu & 0 & 0 & 0 \\ \nu & \nu & 1-\nu & 0 & 0 & 0 \\ 0 & 0 & 0 & (1-2\nu)/2 & 0 & 0 \\ 0 & 0 & 0 & 0 & (1-2\nu)/2 & 0 \\ 0 & 0 & 0 & 0 & 0 & (1-2\nu)/2 \end{bmatrix} \qquad \ldots(٣.٧١)$$

Substitution of Eq. (٣.٧٠) into Eq. (٣.٦٩) yields

$$d\varepsilon = [D]^{-1} d\sigma + d\lambda\{a\} \qquad \ldots(٣.٧٢)$$

Pre-multiplying both sides of Eq. (٣.٧٢) by $\{a\}^T [D]$ and eliminating $a^T . d\sigma$ by making use of Eq. (٣.٦٧), the following expression for the plastic multiplier $d\lambda$ is obtained,

$$d\lambda = \left[\frac{\{a\}^T [D]}{\bar{H} + \{a\}^T [D]\{a\}} \right] d\{\varepsilon\} \qquad \ldots(٣.٧٣)$$

By substituting Eq. (٣.٧٣) into Eq. (٣.٦٩) and pre-multiplying both sides by [D], the complete elastic incremental stress-strain relationship can be expressed as:

$$d\{\sigma\} = \left[[D] - \frac{[D]\{a\}\{a\}^T [D]}{\bar{H} + \{a\}^T [D]\{a\}} \right] d\{\varepsilon\} \qquad \ldots(٣.٧٤)$$

where the second term in the brackets represent the stiffness degradation due to the plastic deformation.

3.9.1.5 *Crushing condition*

Crushing indicates the complete rupture and disintegration of the material under compressive stress state. After crushing, the current stresses drop rapidly to zero and the concrete is assumed to lose its resistance completely against further deformation. In the adopted model, concrete is considered to crush when the strain reaches a specified ultimate value. Hence, rewriting the yield condition from Eq. (٣.٥١) in terms of the peak strain, the following crushing criterion is obtained:

$$C\ \bar{I}_1 + \sqrt{\left(C\bar{I}_1\right)^2 + \beta\bar{J}_2} = \varepsilon_{cu} \qquad \ldots(٣.٧٥)$$

where $\bar{I}_1$: is the first strain invariant

$\bar{J}2$: is the second deviatoric strain

ε_{cu}: is the ultimate concrete strain that can be extrapolated from the uniaxial compression test.

3.9.2 Modeling of Concrete in Tension

3.9.2.1 Cracking criterion

The maximum tensile stress criterion is used in this research work to monitor cracking. For a previously uncracked sampling point, if the principal stress σ_i exceeds the limiting value of tensile stress f_t, a crack is assumed to form. The limiting tensile stress required to define the onset of cracking can be calculated for states of triaxial tensile stress and for combination of tension and compression principal stresses as follows: (Bathe and Ramaswamy ١٩٧٩).

a) For triaxial tension zone $(\sigma_1 \geq \sigma_2 \geq \sigma_3 \geq 0)$

$$\sigma_i = \sigma_{cr} = f_t \qquad i = 1,2,3 \qquad \ldots(٣.٧٦)$$

b) For the tension-tension-compression zone $(\sigma_1 \geq \sigma_2 \geq 0, \sigma_3 \leq 0)$

$$\sigma_i = \sigma_{cr} = f_t\left[1 + \frac{0.75\,\sigma_3}{f'_c}\right] \qquad i = 1,2 \qquad \ldots(٣.٧٧)$$

c) For the tension-compression-compression zone $(\sigma_1 \rangle 0, \sigma_3 \leq \sigma_2 \leq 0)$

$$\sigma_1 = \sigma_{cr} = f_t\left[1+\frac{0.75\sigma_2}{f'_c}\right]\left[1+\frac{0.75\sigma_3}{f'_c}\right] \qquad \ldots(٣.٧٨)$$

where σ_{cr} is the cracking stress and both f_t and f'_c are given positive values, Eq. (٣.٧٧), incorporates the fact that compression in one direction favors cracking in the others and thus reduces the tensile capacity of the material.

When the major principal stress σ_1 violates the cracking criterion, planes of failure develop perpendicular to its direction. Concrete behavior is no longer isotropic, it becomes orthotropic with the direction of orthotropy coinciding with the direction of σ_1. Therefore, the normal and shear stresses across the plane of failure and the corresponding normal and shear stiffness are reduced, and the concrete is assumed to be transversely isotropic with axes of isotropy being perpendicular to the direction of σ_1 . Thus, the incremental stress-strain relationship in the local axes can be expressed as:

$$\begin{Bmatrix} \Delta\sigma_1 \\ \Delta\sigma_2 \\ \Delta\sigma_3 \\ \Delta\tau_{12} \\ \Delta\tau_{23} \\ \Delta\tau_{31} \end{Bmatrix} = \begin{bmatrix} E_1 & 0 & 0 & 0 & 0 & 0 \\ 0 & E/\left(1-\nu^2\right) & \nu E/\left(1-\nu^2\right) & 0 & 0 & 0 \\ 0 & \nu E/\left(1-\nu^2\right) & E/\left(1-\nu^2\right) & 0 & 0 & 0 \\ 0 & 0 & 0 & \beta_1 G & 0 & 0 \\ 0 & 0 & 0 & 0 & G & 0 \\ 0 & 0 & 0 & 0 & 0 & \beta_1 G \end{bmatrix} \begin{Bmatrix} \Delta\varepsilon_1 \\ \Delta\varepsilon_2 \\ \Delta\varepsilon_3 \\ \Delta\gamma_{12} \\ \Delta\gamma_{23} \\ \Delta\gamma_{31} \end{Bmatrix} \qquad \ldots(٣.٧٩)$$

or in a condensed from:

$$\{\Delta\sigma\} = [D_{cr}]\{\Delta\varepsilon\} \qquad \ldots(٣.٨٠)$$

where E_1 is the reduced modulus of elasticity in the direction of σ_1, and $\beta_1 G$ is the reduced shear modulus across the failure plane.

$[D_{cr}]$ is the matrix of material stress-strain coefficiants (orconstitive coeffecients) in the local axes. The stress increments in the global axes (x, y, z)

may be obtained by using the coordinate transformation matrix such that:

$$\{\Delta\sigma\} = [T]^T [D_{cr}][T]\{\Delta\varepsilon\} \quad \ldots (٣.٨١)$$

where ***[T]*** is the transformation matrix expressed in terms of the direction cosines of local to global axes as:

$$[T] = \begin{bmatrix} l_1^2 & m_1^2 & n_1^2 & l_1 m_1 & m_1 n_1 & n_1 l_1 \\ l_2^2 & m_2^2 & n_2^2 & l_2 m_2 & m_1 n_1 & n_1 l_1 \\ l_3^2 & m_3^2 & n_3^2 & l_3 m_3 & m_1 n_1 & n_1 l_1 \\ 2l_1 l_2 & 2m_1 m_2 & 2n_1 n_2 & l_1 m_2 + l_2 m_1 & n_2 m_1 + n_1 m_2 & l_2 n_1 + l_1 n_2 \\ 2l_2 l_3 & 2m_2 m_3 & 2n_2 n_3 & l_2 m_3 + l_3 m_2 & n_3 m_2 + n_2 m_3 & l_3 n_2 + l_2 n_3 \\ 2l_3 l_1 & 2m_3 m_1 & 2n_3 n_1 & l_3 m_1 + l_1 m_3 & n_1 m_3 + n_3 m_1 & l_1 n_3 + l_3 n_1 \end{bmatrix} \quad \ldots (٣.٨٢)$$

where l_i, m_i and n_i represent the direction cosines of the local coordinate axes (x, y, z) with the global axes respectively.

For the tension – tension – compression and the triaxial tension states of stress, the cracking criterion may be violated by the major principal stress σ_1, and the second principal stress σ_2, simultaneously. Thus, two sets of orthogonal cracked planes may develop and the constitutive matrix in the local material axes becomes diagonal:

$$[D]_{cr} = \begin{bmatrix} E_1 & 0 & 0 & 0 & 0 & 0 \\ 0 & E_2 & 0 & 0 & 0 & 0 \\ 0 & 0 & E_3 & 0 & 0 & 0 \\ 0 & 0 & 0 & \beta_1 G & 0 & 0 \\ 0 & 0 & 0 & 0 & \beta_2 G & 0 \\ 0 & 0 & 0 & 0 & 0 & \beta_1 G \end{bmatrix} \quad \ldots (٣.٨٣)$$

In the current model, a maximum of three sets of cracking is allowed to form at each sampling point.

3.9.2.2 Post-cracking models

3.9.2.2.1 Tension- Stiffening Model

The tensile stresses normal to the cracked planes are gradually released, and

represented by an average stress-strain curve. In the present study such a relationship may be obtained by using the tension-stiffening model. This is specified by a linear descending stress-strain curve similar to that shown in Fig. (٣.١٢) and this is given by: [Bathe and Ramsawamy (١٩٧٩)]

a) for $\varepsilon_{cr} \leq \varepsilon_n \leq \alpha_1 \varepsilon_{cr}$

$$\sigma_n = \alpha_2 \sigma_{cr} \left[\frac{\alpha_1 - \frac{\varepsilon_n}{\varepsilon_{cr}}}{\alpha_1 - 1.0} \right] \qquad \ldots(٣.٨٤)$$

b) for $\varepsilon_n \rangle \alpha_1 \varepsilon_{cr}$

$$\sigma_n = 0.0 \qquad \ldots(٣.٨٥)$$

where σ_n and ε_n are the stress and strain normal to the cracked plane, ε_{cr} is the cracking strain associated with the cracking stress σ_{cr} , and α_1 and α_2 are the tension-stiffening parameters. α_1 represents the rate of stress release as the crack widens, while α_2 represents the sudden loss of stress at instant of cracking.

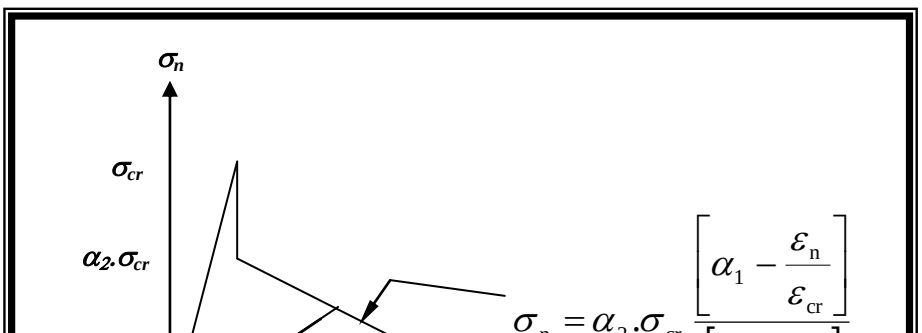

3.9.2.2.2 Shear Retention Model

At a cracked sampling point, the shear stiffness across the cracked plane becomes progressively smaller as the crack widens. A reduced shear modulus βG, has been used across the cracked plane. The value of β depends on the stage of loading and it is given by:

a) For $\varepsilon_n \leq \varepsilon_{cr}$

$$\beta = 1 \qquad \ldots(٣.٨٦)$$

b) For $\varepsilon_{cr} \leq \varepsilon_n \leq \gamma_1 \varepsilon_{cr}$

$$\beta = \frac{\gamma_2 - \gamma_3}{\gamma_1 - 1}\left[\gamma_1 - \frac{\varepsilon_n}{\varepsilon_{cr}}\right] + \gamma_3 \qquad \ldots(٣.٨٧)$$

c) For $\varepsilon_n \rangle \gamma_1 \varepsilon_{cr}$

$$\beta = \gamma_3 \qquad \ldots(٣.٨٨)$$

Figure (٣.١٣) shows schematically the value of (β) for different stages. γ_1, γ_2, and γ_3 are shear retention parameters. γ_1 represents the rate of decay of shear stiffness as the crack widens, γ_2 is the sudden loss in shear stiffness at the instant of cracking , and γ_3 is the residual shear stiffness due to the dowel

action.

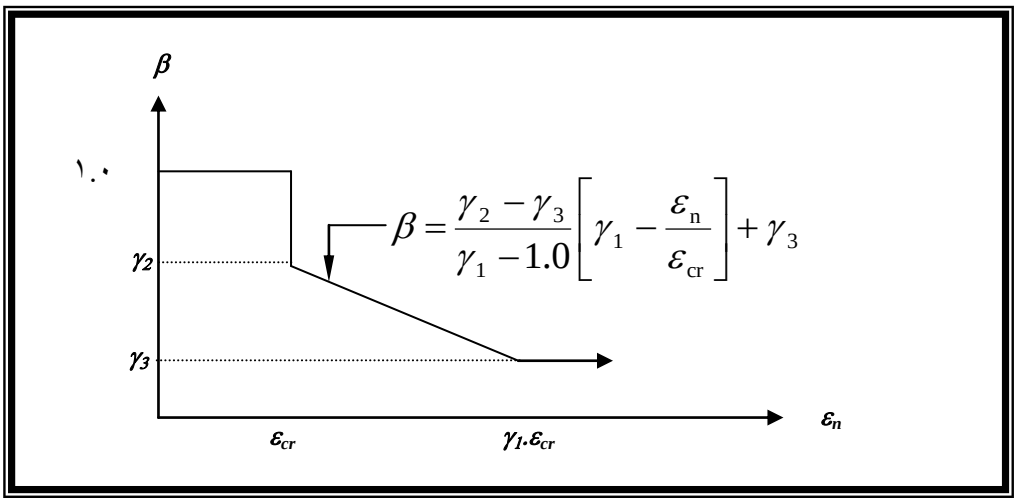

Figure (٣.١٣): Shear Retention for Concrete

3.9.2.3 *Modeling the compressive strength reduction due to orthogonal cracks:*

In a reinforced concrete member, a significant degradation in compressive strength can result due to presence of transverse tensile strain after cracking (Cervenka ١٩٨٥). In plasticity based model, the effect of these tensile strains on the yield criterion and the evolution of the subsequent loading surface can be simulated by scaling the equivalent uniaxial stress-strain relationships given by Eqs. (٣.٥٥) and (٣.٥٧), according to the current value of the compressive strength reduction factor.

The model used here is due to Cervenka and this depends on the reduction factor $(\lambda)$to reduce both the peak stress and the corresponding strain, Fig. (٣.١٤), from, Eqs. (٣.٥٥ and ٣.٥٧), the modified stress-strain relationship may be written: (Cervenka ١٩٨٥).

a) for $\bar{\sigma} \le Cp \,.\, f_c'$

$$\bar{\sigma} = \lambda E\, \varepsilon_C \qquad \ldots(٣.٨٩)$$

b) for $\lambda \ \mathrm{Cp}\, f'c \le \bar{\sigma} \le \lambda\, f'c$

$$\bar{\sigma} = \lambda\, \mathrm{Cp}\, f'c + E\left[\varepsilon_c - \frac{\lambda\, \mathrm{Cp}\ f'c}{E}\right] - \frac{E}{2\varepsilon_0}\left[\varepsilon_c - \frac{\lambda\ \mathrm{Cp}\ f'c}{E}\right] \qquad \ldots(٣.٩٠)$$

c) for $\varepsilon_c \ge (2 - \mathrm{Cp})\lambda\, f'c / E$

$$\bar{\sigma} \le \lambda\ f'c \qquad \ldots(٣.٩١)$$

where

$$\varepsilon'o = 2(1-\mathrm{Cp})\lambda\,.\,f_c'/E \qquad \ldots(٣.٩٢)$$

The effective stress-plastic strain relation can be modified as:

$$\bar{\sigma} = \lambda\, c_p\ f_c'\, E.\varepsilon_p + \left(2\,E^2\,\lambda.\varepsilon_o\ \ \varepsilon_p\right)^{1/2} \qquad \ldots(٣.٩٣)$$

and the hardening parameter can be expressed as:

$$\bar{H} = \frac{d\,\bar{\sigma}}{d\,\varepsilon_p} = E\left\{\left[\frac{\lambda\,\varepsilon_o}{2\,\varepsilon_p}\right]^{1/2} - 1.0\right\} \qquad \ldots(٣.٩٤)$$

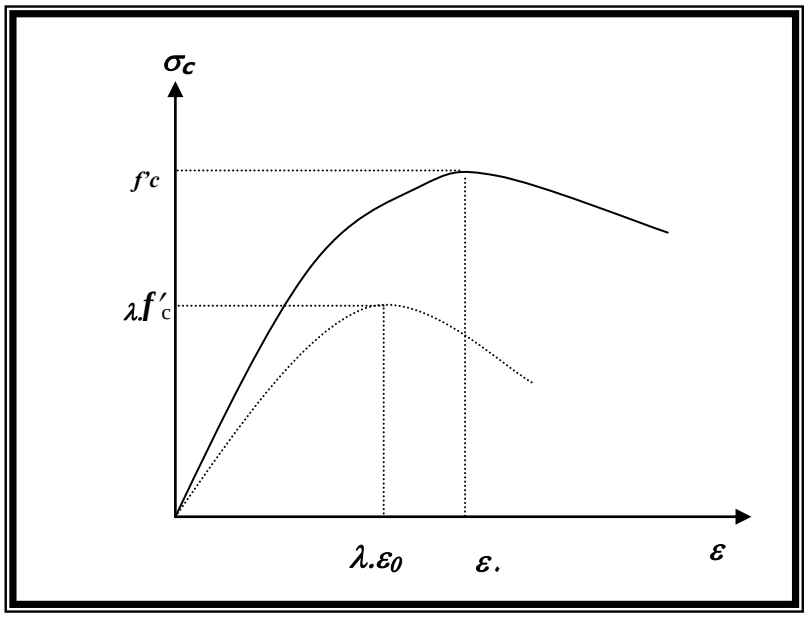

Figure (٣.١٤): Uniaxial Compressive Stress-Strain Relationship for Cracked Concrete

For a singly cracked sampling point, the compression reduction factor is given by:

$$\lambda = 1.0 - K_1 \frac{\varepsilon_1}{0.005} \le 1.0 - K_1 \qquad \ldots(٣.٩٥)$$

where ε_1 is the transverse tensile strain in principal direction (١), the strain normal to the cracked plane and K١ equal to (٠.٥٢) . Also for doubly cracked sampling point, the reduction factor may be taken as:

$$\lambda = 1.0 - K_1 \frac{\left(\varepsilon_1^2 + \varepsilon_2^2\right)}{0.005} \le 1.0 - K_1 \qquad \ldots(٣.٩٦)$$

where ε_2 is the tensile strain normal to the second crack.

3.10 Modeling of Reinforcement

Compared to concrete, steel is a much simpler material to represent. Its stress-strain behavior can be assumed to be identical in tension and compression. In reinforced concrete members, reinforcing bars are normally long and relatively slender and therefore they can be assumed to be capable of transmitting axial forces only. In the current study, the uniaxial stress-strain behavior of reinforcement is simulated by an elastic- linear work hardening model, as shown in Fig. (٣. ١٥).

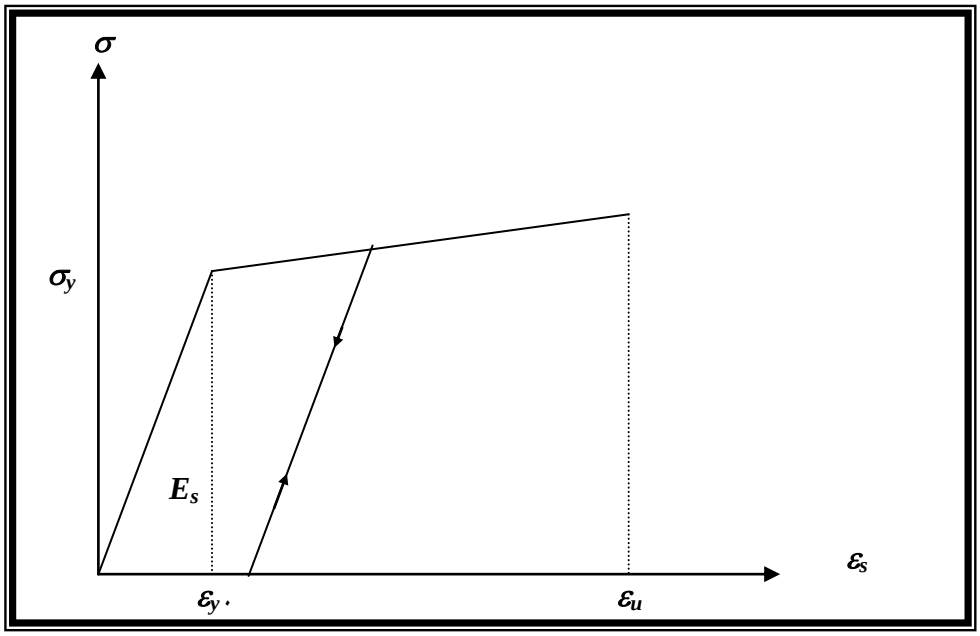

Figure (٣.١٥): Stress-Strain Relationship of Steel Bars Used in the Analysis

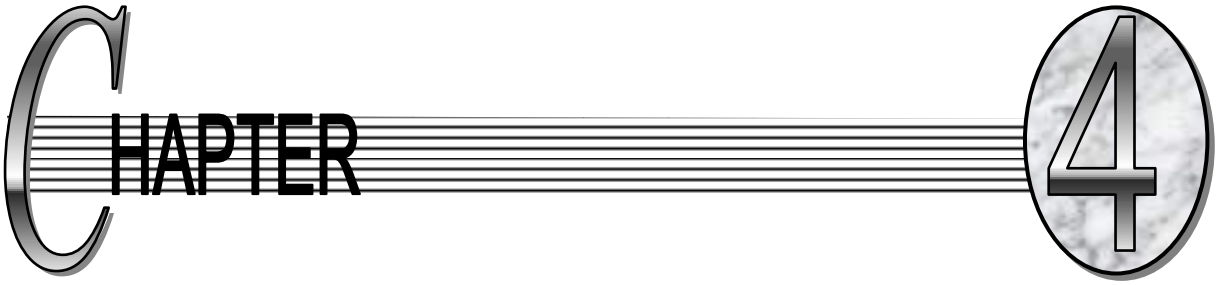

SOIL RESPONSE TO PLATE FOUNDATION

٤.١ Introduction

Evaluation of the response of soil media to the applied external loads can be made from knowledge of the complete stress-strain characteristics of the soil. The stress-strain relations are the mathematical distribution of the mechanical properties of the soil (the soil constitutive equation) [٢٦]. A complete stress-strain relationship for the soil will furnish, at the least in theory, the stresses and strains in a soil medium at any particular time under any given load conditions. It seems unlikely that generalized stress-strain relations can be developed to fulfill the requirements of every type of soil behavior, especially in the relation to the analysis of interaction between the soil and the foundation. There are many empirical, semi empirical, graphical, and theoretical approaches depending on many unrealistic assumptions for the soil behavior, while other approaches depend mainly on representation of practical problems by oversimplified models from which the required solutions may be obtained.

There are several parameters that go in the definition of soil structure interaction. some of these parameters are the importance only in especial problems, while other basic parameters are important in all soil-structure interaction problems. These basic parameters are [٤٩]:

١- The stiffness of both soil and structure.

٢- The non-linear stress dependency of the modulus of elasticity and Poisson's ratio of both soil and structure.

٣- The non-linear behavior of soil-structure interface.

٤- Time.

The effect of time can safely be neglected problems dealing with sand and problems of short loading duration, while the other three parameters must be included in the analysis of problems when incorporating correctly the actual behavior of soil and soil-structure interface in the analysis.

The inherent complexity in the behavior of real soils has led to the development of many idealized models of soil. The idealized foundation models are not the exact descriptions of even the gross physical properties of real soil media. The choice of an idealized behavior of the soil is dependent on type of soil and the soil condition, type of foundation and nature of external loading.

The constant of proportionality between the applied normal or shearing stress at a point on the surface of soil and the corresponding surface displacement is the modulus of subgrade reaction for the soil mass, or soil configuration at that point. The modulus of subgrade reaction gives the relationship between the soil pressure and the resulting deflection.

Soil configuration can be presented by using two kinds of subgrade reaction moduli on the area of foundation, the normal and the tangential. The normal subgrade reaction modulus (K_n) is defined as the load required to act normally on a unit area of the elastic foundation to produce a unit normal displacement. The tangential subgrade reaction modulus (K_t) is defined as the load required to act tangentially on a unit area to produced a unit horizontal displacement.

The normal subgrade reaction is modeled by Winkler, for linear and non-linear models while the tangential subgrade reaction is given by Winkler and Coulomb models.

٤.٢ Normal Subgrade Reaction (Kn)

A compressional resistance is the transverse reaction of the medium to overlying foundation. The following models are represented [٣٣] :

٤.٢.١ Winkler Model

This model assumes that the base is consisting of closely spaced, independent linear springs. Consequently, the contact pressure at any point on the soil structure contact is proportional to deflection at that point and it is independent of deflections at other points. The pressure beneath the foundation is given by:

$$P_{(x,y)}=K_z \cdot w \qquad \ldots (٤.١)$$

where K_z the modulus of subgrade reaction with a unit of stress per unit deflection.

٤.٢.٢ Non-Linear Behavior of Soil

Before the development of electronic computers, it was not feasible to perform analysis of loads on soil masses for other than the assumed linear elastic soil behavior.

Now, due to availability of high – speed computer and powerful numerical and analytical techniques, it is possible to approximate non-linear, inelastic soil behavior in analysis. In order to perform non- linear analysis of soil, however, it is necessary to be able to describe the load- deflection behavior of the soil in quantitative terms and to develop techniques for incorporating this behavior in the analysis.

٤.٢.٢.١ Soil characterization

The stress-strain relation of any type of soil depends on a number of different factors including density, water content, structure, drainage condition, strain

conditions (i.e. plane strain, triaxial), duration of loading ,stress history and confining pressure [٣٦].

In many cases it may be possible to take account of these factors by selecting soil specimens and testing condition which simulates the corresponding field conditions. When this can be done accurately, it would be expected that the strains resulting from given stress changes in laboratory would be representative for the same stress changes.

Among many theories established for studying different materials properties, the following theories are widely used in studying soil characteristics especially stress – strain relation under different stress changes:

١- Classical linear elastic theory.
٢- Plasticity theory.
٣- Elasto - plastic theory.
٤- Visco – elastic theory.
٥- Non – linear elasticity theory.

It is commonly found that the soil behavior over a wide range of stress is non-linear, inelastic, and dependent upon the magnitude of the confining pressure employed in the tests.

٤. ٢. ٢. ٢ Modeling of stress – strain curve of soils

The stress – strain curve for all soils is non-linear except in a very narrow region near the origin **[Bowels[١٣]]**. In this section, two models can be used to model the stress – strain response of soils: -

I-Hyperbolic stress-strain model.
II-Polynomial model.

I- Hyperbolic stress – strain model

In this model, the stress -strain curve could be represented by a hyperbolic curve. **Kondner** [٣٤] proposed a hyperbolic equation of the form:

$$\sigma_1 - \sigma_3 = \frac{\in}{a + b \in} \qquad \ldots (٤.٢)$$

Where,

σ_1 and σ_3 are the major (axial) and the minor (confining) principal stresses.

$\in$:Is the axial strain .

(***a***) and (***b***) are constants whose values may be determined experimentally.

The ultimate value of principal stresses difference $(\sigma_1 - \sigma_3)_{ult.}$ can be obtained by taking the limit of Eq. (٤.٢) as ($\in$) becomes very large , or

$$(\sigma_1 - \sigma_3)_{ult.} = \lim_{\in \to \infty} (\sigma_1 - \sigma_3) = \frac{1}{b} \qquad \ldots (٤.٣)$$

Differentiating Eq. (٤.٢) with respect to the strain and evaluating the derivative at ($\in$) equal to zero yields- :

$$\left(\frac{d(\sigma_1 - \sigma_3)}{d \in} \right)_{\in = 0} = \frac{1}{a} \qquad \ldots (٤.٤)$$

Thus, both of these constant ***a*** and ***b*** have a visualized physical meaning, referring to Fig. (٤.١), (***a***) is the reciprocal of the initial tangent modulus, ***Ei*** ,and **(*b*)** is the reciprocal of the asymptotic value of stress difference which the stress-strain curve approaches at infinite strain $(\sigma_1 - \sigma_3)_{ult.}$

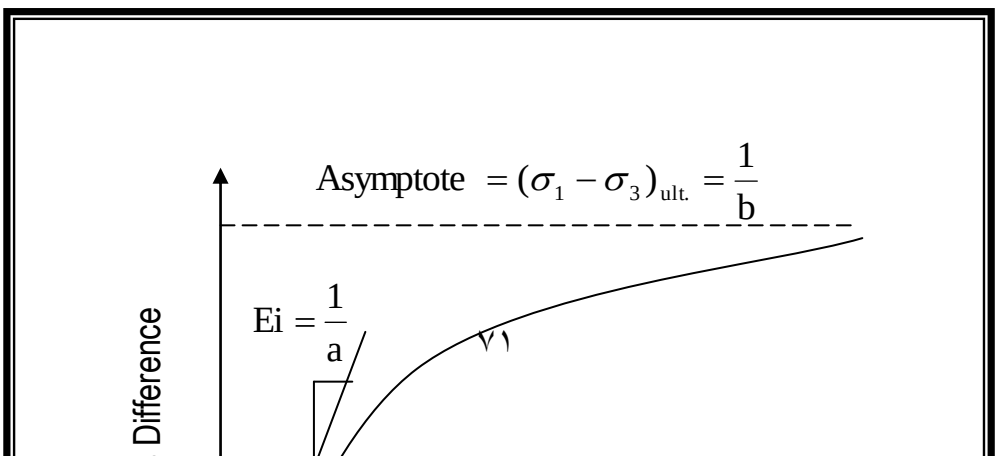

In order to develop a realistic model in soil mechanics, such a model must use a combination of:

١. Observations of the material behavior, and

٢. Laboratory experiments that will measure the physical parameters that are needed to transfer the model into usable mathematical equations.

Since the behavior of the soil under compressive loading is non-linear as verified by the results of plate – load test or considering the load – settlement curve a plate – load test in the field, the plate element resting on the soil has response which can approximately be modeled by using the two – constant hyperbolic stress – strain equation which now takes the following form:

$$\mathbf{P} = \frac{\delta}{\mathbf{a} + \mathbf{b}\delta} \qquad \ldots(٤.٥)$$

Eq.(٤٥.) was used firstly by **AL-Rubai** [٨]**,** to represent the non-linear behavior of the soil.

Fig. (٤.٢a) shows the hyperbolic load – settlement curve of plate – load test.

Differentiating Eq. (٤.٥) with respect to the settlement ,(δ) yields:

$$K_n = \frac{a}{(a + b\delta)^2} \qquad \ldots (٤٦.)$$

where,

P: is the lateral load on plate element that is concentrated at the control node.

δ : is the lateral displacement of the node .

$\mathbf{K_n}$: is the normal subgrade reaction of soil.

(***a***) and **(*b***) are the physical parameters required for the hyperbolic equation and these can be obtained from the load – settlement curve of the plate – load test.

The value of the coefficients (***a***) and (***b***) may be determined most readily if the load – settlement data are plotted on transformed axes as shown in Fig. (٤.٢b) when Eq. (٤٥.) is written in the following form:-

$$\frac{\delta}{p} = a + b\delta \qquad \ldots (٤.٧)$$

where , (a) and (b) are the intercept and the slope of the resulting straight line shown in Fig.(٤.٢ b),respectively.

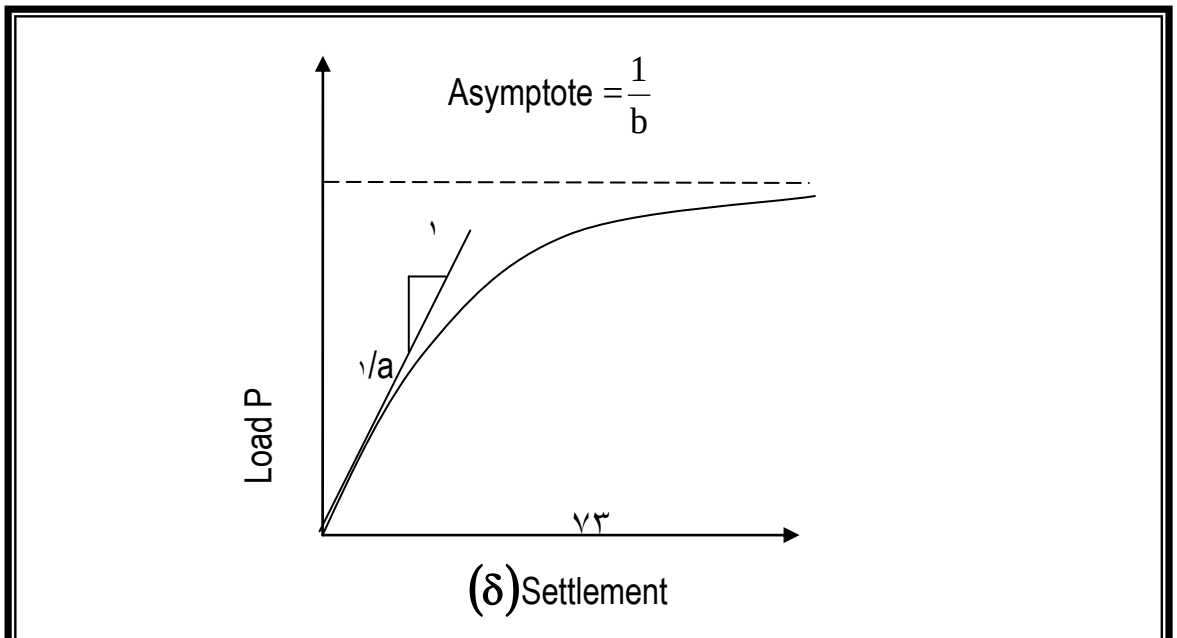

II- Polynomial model

In this model, the non linear behavior of the soil can be represented by a polynomial equation which takes the following form:

$$P = a_0 + a_1\delta + a_2\delta^2 + a_3\delta^3 + a_4\delta^4 + ... \quad ... (٤.٨)$$

where

$\mathbf{a_0, a_1, a_2, a_3}$ and $\mathbf{a_4}$ are the coefficients required for the polynomial Equation.

The values of the coefficients $\mathbf{a_1, a_2, a_3 .....}$ may be determined by making a curve fitting for the experimental load – settlement data.

Differentiating Eq. (٤.٨) with respect to settlement (δ) yields:

$$K_n = a_1 + 2a_2\delta + 3a_3\delta^2 + 4a_4\delta^3 + ... \quad ...(٤٩.)$$

Where:

δ :is the lateral displacement of the node.

K_n: is the normal subgrade reaction of soil.

٤.٣ Tangential Subgrade Reaction (Kt)

The application of loads on a plate resting on elastic foundations produce deformations (movement) in the contact face of the plates, these movement cause shearing or friction force which is dependent on the soil, the plate, and the applied loads.

There are several assumptions for the interface condition between a foundation and underlying soil medium. These ranges of completely smooth to completely adhering interfaces with either Winkler or Coulomb friction.

٤.٣.١ Winkler Model

According to the definition of compressional Winker model in section (٤.٢.١), the frictional resistace could be modeled on the same manner.

$$F_x=K_x.u \quad \text{... (٤.١٠)}$$

$$F_y=K_y.v \quad \text{...(٤.١١)}$$

where F_x and F_y are the friction force per unit area in x and y-direction, K_x and K_y are the frictional modulus of subgrade reaction in x and y-direction, with a unit of stress per unit displacement, and u or v is the horizontal displacement (in x or y direction)

٤.٣.٢ Coulomb Friction Model

Coulomb friction (or sliding friction between two surfaces in contact) is independent on the value of horizontal displacement (or sliding) but it is directly

proportional to the normal reaction. Accordingly, the friction forces F_x or F_y could be related to transverse displacement w as follows:

$$F_x=K_z.w.\tan(\delta_x) \quad \ldots(٤.١٢)$$

$$F_y=K_z.w.\tan(\delta_y) \quad \ldots(٤.١٣)$$

where (K_z.w) is the normal reaction of Winkler model, and δ_x or δ_y is the angle of friction between the soil and the foundation in x or y-direction.

CHAPTER 5

SOLUTION ALGORITHM OF THE NONLINEAR PROBLEM AND COMPUTER PROGRAM

5.1 Introduction

The nonlinear behavior of any reinforced concrete structure may be generally attributed to either material or geometric nonlinearity or a combination of both types. In reinforced concrete members, the geometric nonlinearity is usually neglected as a result of early onset of the material nonlinearity, with large deflections occurring only close to structural collapse. So, only material nonlinearity is considered in the present study.

The major sources of material nonlinearity are the presence of micro – cracks in concrete, formation and propagation of structural cracks, yielding of reinforcement and plastic deformations and crushing of concrete.

The techniques used in solving the nonlinear equations are (Cook ١٩٧٤):

١. Linear incremental technique.

٢. Iterative technique.

٣. Incremental – iterative technique.

5.2 Linear – Incremental Technique

In this method, Fig. (٥.١), the nonlinear behavior is determined by solving a

sequence of linear problems. The load is applied as a sequence of sufficiently small increments, so that during each load increment, the structure is assumed to respond linearly. The basic disadvantage of this method is that a real estimate of the solution accuracy is not possible, since equilibrium is not satisfied at any given load level. So, for stability requirements, it is necessary to use small load increments, which in turns will increase the computation cost if compared with the other techniques.

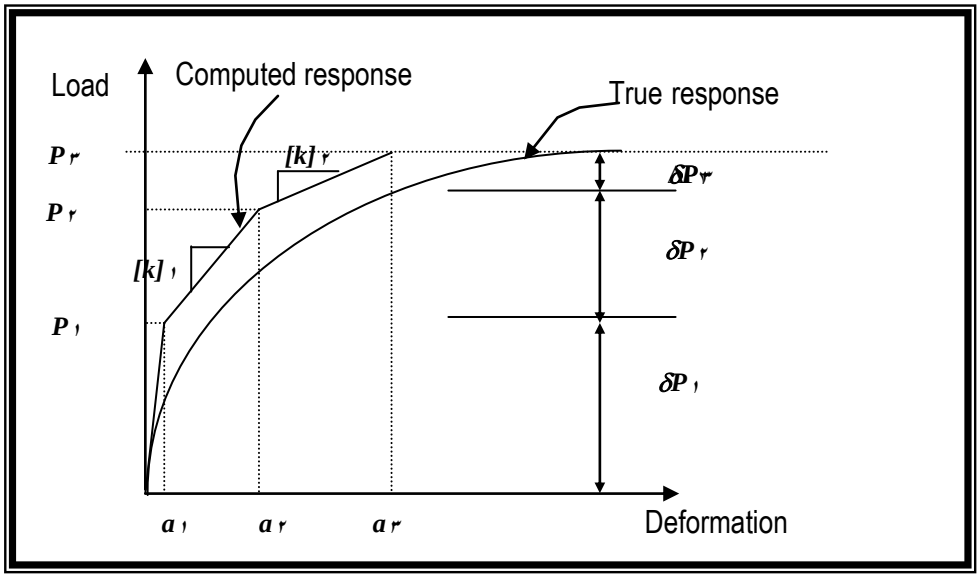

Figure (٥.١): Linear Incremental Method

5.3 Iterative Technique

The iterative procedure is a sequence of calculations in which the structure is fully loaded in one step to get an initial approximate solution. Then, this solution is improved step – by – step by using an iteration process until equilibrium is satisfied within a prescribed tolerance.

After each iteration, the portion of the total loading that is not balanced is calculated and used in the iterative process as an additional load to compute an approximate additional increment of the total displacements. This process is repeated until equilibrium is approximated to some acceptable degree. These

techniques fail to reach the required convergence for structures with high nonlinearity. There are several types of iteration procedures, some of them are:

- Conventional Newton – Raphson method.
- Modified Newton – Raphson method.
- Combined (conventional and modified) Newton – Raphson method.

5.4 Incremental – Iterative Technique

In this type of technique, Fig. (٥.٢), the load is applied as a series of increments, and at each increment, iterative solution is carried out to find the truest response of the structure. The conventional, modified and combined Newton – Raphson methods may also be used in the iteration process within each step. These methods are briefly discussed in the following sections.

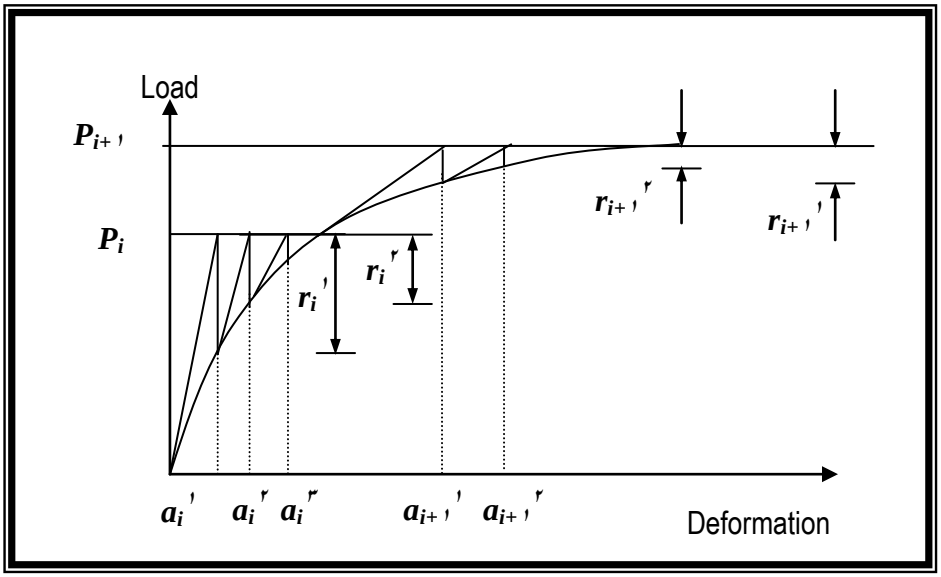

Figure (٥.٢): Incremental - Iterative Technique

5.4.1 Conventional Newton – Raphson Method

The conventional Newton – Raphson method, Fig. (٥.٣), is one of the earliest

known methods used in solving nonlinear problems. For simplicity, a single degree of freedom system is considered with a load level **{*P*}**., with the assumption that the corresponding deformed configuration of the system which may be denoted symbolically by **{*a*}**. is known. A new configuration, **{*a*}**١, corresponding to a load level **{*p*}**١ is determined where:

$$\{\mathrm{P}\}_1 = \{\mathrm{P}\}_0 + \{\delta \mathrm{P}\}_1 \qquad \ldots(٥.١)$$

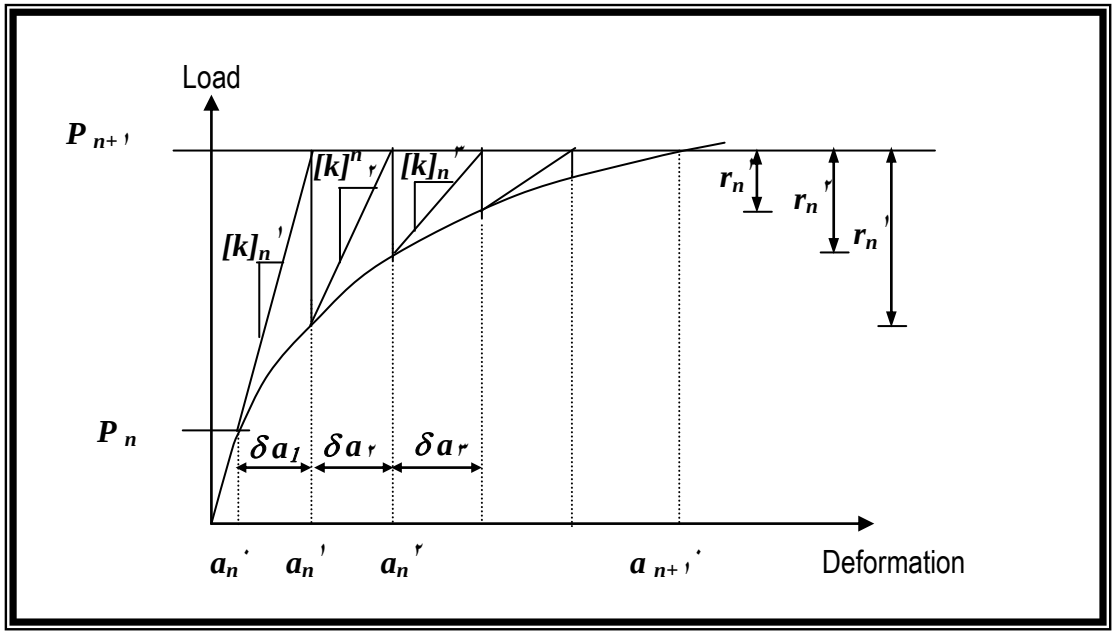

Figure (٥.٣): Conventional Newton – Raphson Method

Here $\{\delta P\}$١ is the additional applied load obtained by using a linearized analysis, and the change in configuration $\{\delta a\}$١ is first computed from:

$$\{\delta \mathrm{P}\}_1 = [\mathrm{k}]_0 \{\delta a\}_1 \qquad \ldots(٥.٢)$$

in which the tangent stiffness matrix [***k***]. is evaluated at the beginning of the load interval, i.e. the load level {***P***}.. The term {***a***}١ = {***a***}. + {δ***a***}١ represents an approximate configuration which is then corrected by updating a new tangent

stiffness matrix from the approximate configuration $\{a\}_1$. The internal forces $\{f\}_1$ corresponding to this configuration can be determined as:

$$\{f\}_1 = [k]_1 \{a\}_1 \qquad \ldots(٥.٣)$$

Generally for any level of iteration (j):

$$\{a\}_j = \{a\}_{j-1} + \sum_{m=1}^{n} \{\delta a\}_m \qquad \ldots(٥.٤)$$

where:

$\{a\}_j$ is the vector of displacement after the iteration. Then, the out of balance force vector $\{r\}_j$ can be obtained from:

$$\{r\}_j = \{P\}_f - \{f\}_j \qquad \ldots(٥.٥)$$

The unbalanced joint forces are then treated as load increments and the correction vector $\{\delta a\}_{j+1}$ is then obtained from the incremental relationship:

$$[k]_j \{\delta a\}_{j+1} = \{r\}_j \qquad \ldots(٥.٦)$$

A new approximate configuration is then computed by making use of Eq. (٥.٦). The process continues until the latest correction vector is sufficiently small.

The conventional Newton – Raphson method requires that the tangent stiffness matrix is to be updated and a new system of equations is solved for each iteration. This is expensive if the problem to be solved is too large. Accordingly various modifications have been proposed.

5.4.2 *Modified Newton – Raphson Method*

In this method, Figure (٥.٤), the stiffness matrix is updated only once for each increment of loading. As compared with the conventional Newton – Raphson method, the modified Newton – Raphson method is more economical. However, this method requires more steps for convergence, but each step is done quickly by avoiding time consuming repetitions of forming the tangent stiffness matrix.

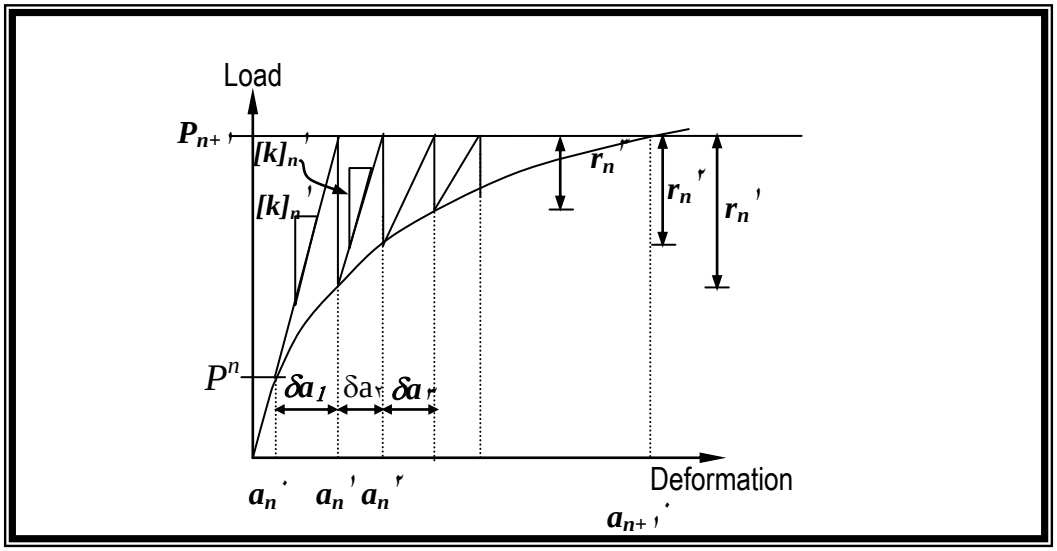

Figure (٥.٤): Modified Newton – Raphson Method

5.4.3 *Combined Newton - Raphson Method*

This method, Fig. (٥.٥), is a modification of the conventional Newton – Raphson method. It involves updating the stiffness matrix after remaining constant for certain number of iterations. The stiffness matrix can be recalculated at:

- The beginning of first iteration of each increment.
- Beginning of second iteration.

- First, eleventh, twenty first, … stiffness matrices over each load increment.
- Second, twelfth, twenty second, … stiffness matrices over each load increment.

The disadvantage of this method is represented in the fact that the convergence is slower than the modified Newton – Raphson method and requires a great number of iterations to achieve the solution within each load increment.

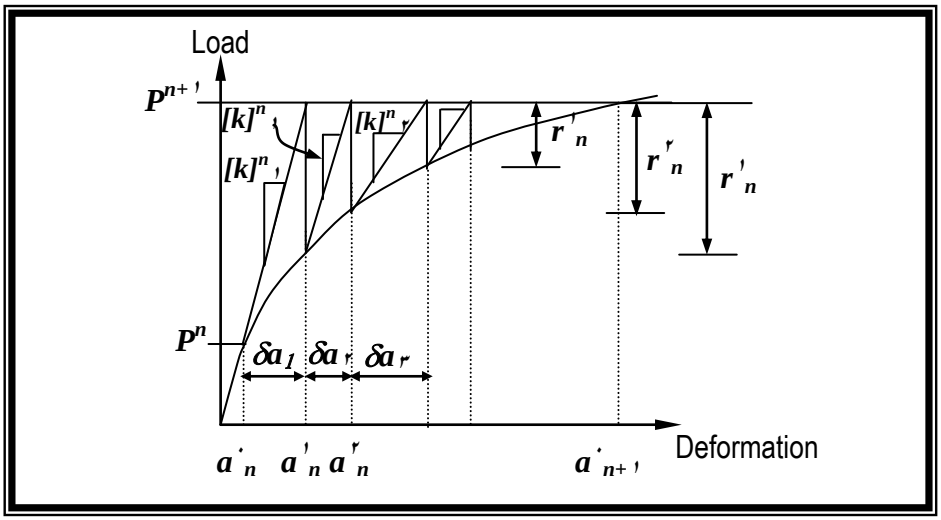

Figure (٥.٥): Combined Newton – Raphson Method

5.5 *Convergence Criterion*

A termination criterion for the iterative process should be used to stop iteration when a sufficient accuracy is achieved, i.e, when no further iterations are necessary. The different useful criteria are the displacement, the force and the work done criteria. Only the force criterion is adopted in the present study. This criterion depends on comparing the internal force vector $\{f\}$ and the applied load vector $\{P\}$. In other words, seeking a vector called "unbalanced force vector" to be small within a prescribed tolerance. The convergence is assumed

to occur when the inequality:

$$\left[\frac{\sum_{i=1}^{n}\left(\{P\}_i-\{f\}_i\right)^2}{\sum\left(\{P\}i\right)^2}\right]^{0.5} \le tol. \qquad \ldots(٥.١٧)$$

is satisfied.

5.6 Analysis Termination Criterion

The non-linear finite element analysis must be provided with a criterion to detect failure of the solution. In the physical test under load control, the collapse of a structure takes place when no further loading can be sustained. This is usually indicated in the numerical tests by successively increasing iterative displacements and continuous growth in the dissipated energy. Hence, convergence of the iterative procedure cannot be achieved and therefore, it is necessary to specify a suitable criterion to terminate the analysis and save wasting computation efforts.

In the present study, the non-linear analysis is terminated when the stiffness matrix is no longer positive definite, a steel bar has fractured, or excessive concrete crushing at sampling points has taken place.

٥.٧ Outline of Computer Program

The computer program ***٣DTPFA*** (three – dimensional thick plate foundation analysis) has been used in the present study. This program is a development version to the program ***P٣DNFEA*** (three – dimensional nonlinear finite element

analysis). This latter program was developed by Al – Shaarbaf (Al – Shaarbaf ١٩٩٠). The program is coded in ***FORTRAN ٧٧*** language. The main objective of the present program ***٣DTPFA*** is to analyze reinforced concrete thick plates resting on soil and subjected to transverse static load up to failure.

In the present study, the ***Fortran PowerStation ٤.٠*** compiler produced by Microsoft incorporation was used to operate the program under Pentium III with Intel MMX ٦٣٣ MHz processor and ١٢٨ MB RAM.

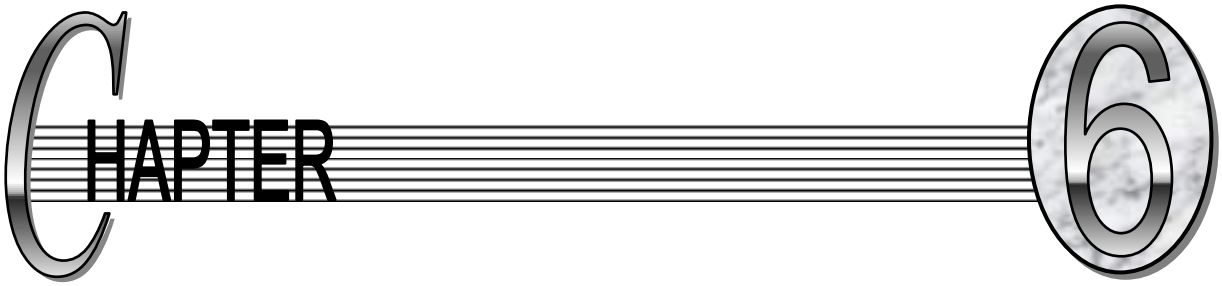

APPLICATION AND RESULTS

٦.١ *General*

In this chapter, some numerical examples are worked out to compare the results obtained by the finite element analysis to those obtain from available experimental and numerical solutions. A number of numerical examples has been analyzed with the computer program (٣DTPFA).

The examples also serve as means to check the validity of the material models used and to demonstrate the applicability and capability of the analysis method adopted in this study to a variety of three-dimensional reinforced concrete thick plate structures. It is important to mention that this theoretical study is approximate in nature due to various factors mainly;

١- Approximations in the material modeling of concrete, steel and soil.

٢- Approximation inherent in the finite element modeling technique.

٣- Approximation in the integration functions used in this numerical analysis.

٤- Approximation introduce due to the type of procedure used in solving the nonlinear system of equations.

Some of the numerical examples considered in this chapter were previously tested experimentally or numerically by other researchers, and the other example were used for parametric study.

٦.٢ *Simply Support Reinforced Concrete Deep Beam*

A simply support reinforced concrete beam is analyzed using the computer program (٣DTPFA). Such a beam was tested experimentally by Ramakrishan and Abathanaroyana (١٩٦٨), one beam is ٧٦٢ mm and the other ٥٠٨ mm. The first is subjected to two point loads located at the third portion of the beam, while the other is loaded with a uniform pressure, as shown in Fig. (٦.١.a). Due to symmetry of loading and geometry, only one half of the beam is analyzed using sixteen ٢٠-node brick elements for the first beam and twelve ٢٠-node brick elements for the second beam as shown in Fig. (٦.١.b).

The steel reinforcement is represented by embedded bar along the span length. Numbers of load increment are (٣١) for the first beam and (٢٧) for the second beam. Material properties of concrete and steel are given in Table (٦.١).

The load-deflection response at midspan of the beams is shown in Fig. (٦.٢). The computed deflection shows a good agreement with the experimental result for most loading levels. Fig. (٦.٣) shows a comparison of the calculate deflection with the previous study [Cervera et al (١٩٨٦)].

The crack patterns of beams at the load that causes crack and at failure load are shown in Fig. (٦.٤). The first cracking initiates at load (٢١.٧٪) of the ultimate load for the first beam and about (٢٢.٩٪) of the ultimate load for the second of ultimate load at bottom surface of the middle zone of the beam, where pure bending moment exists. The cracks spread in all three directions of the beams, throughout the increase of the loading levels.

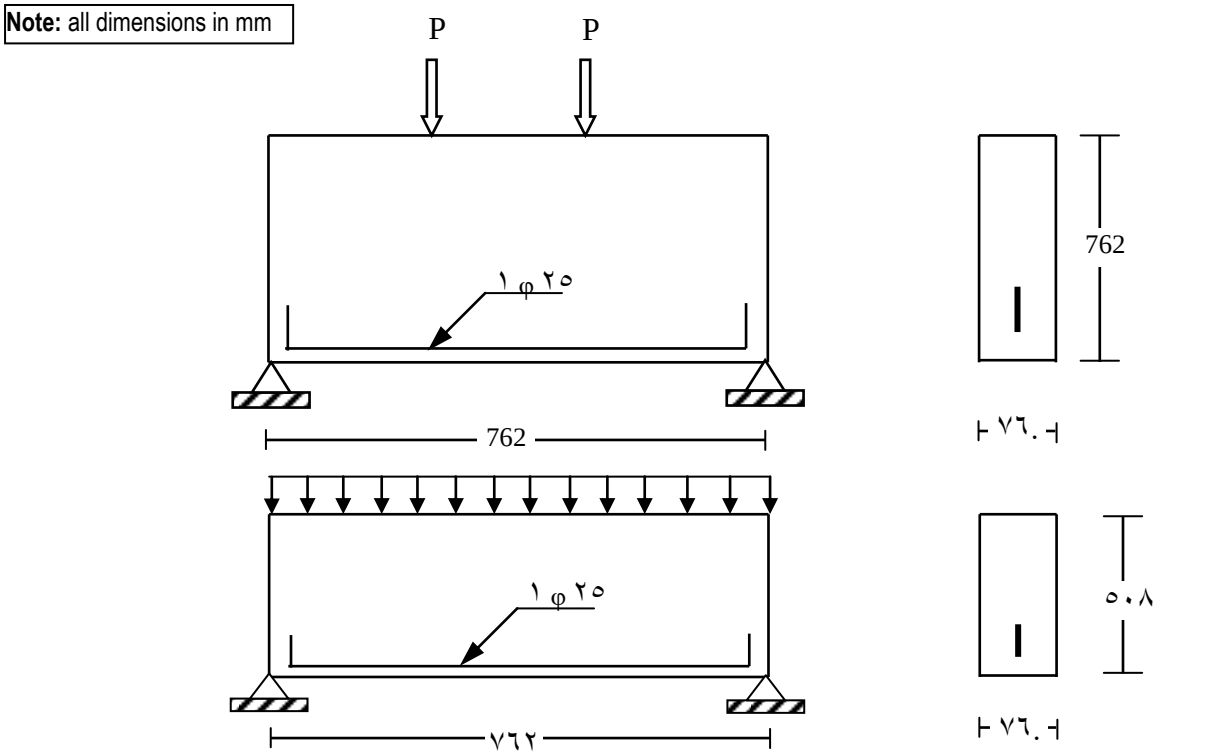

(a) Beams geometry and loading arrangement and reinforcement details

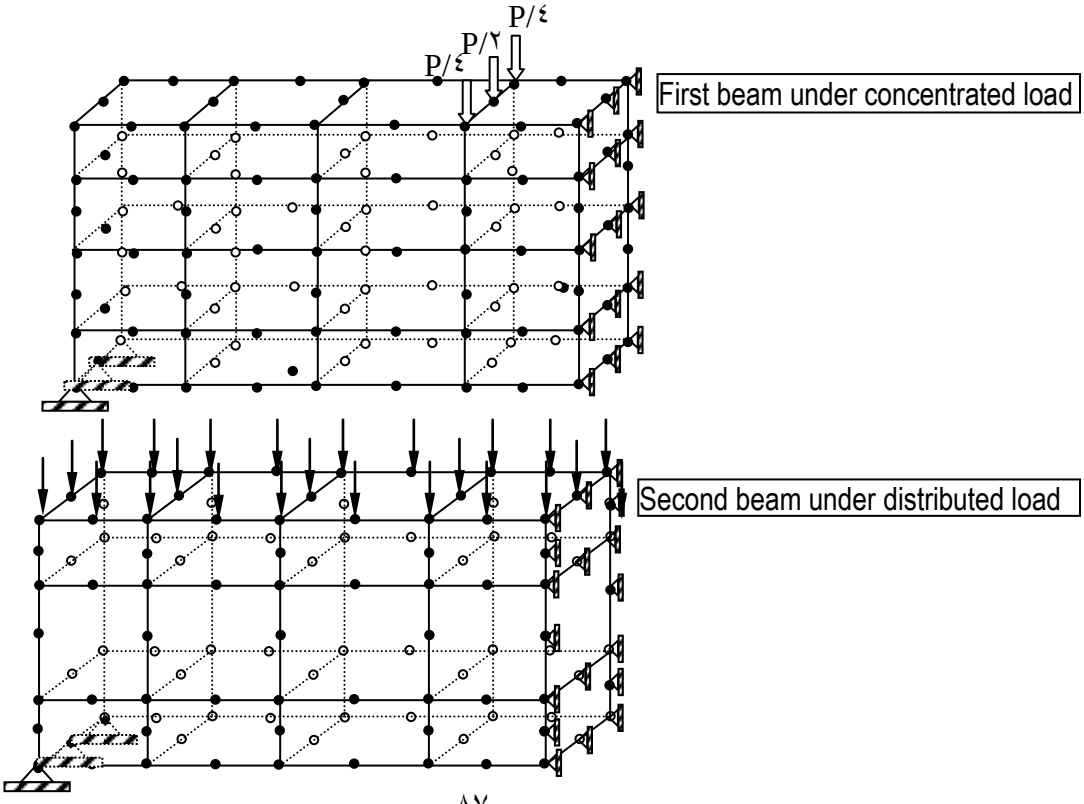

(b): Finite Element Idealization of Half of the Beams

Figure (٦.١): Simply Supported Reinforced Concrete Deep Beams

Table (٦.١): Material Properties and Additional Parameter of Simply Supported Deep Beams.

	Material properties and material parameters	Symbol	value
concrete	Young's modulus	$E_c(N/mm^2)$	٢٣٤٦٠
	Compressive strength	$Fc(N/mm^2)$	٢٣.٧٩٦
	Tensile strength	$F_t(N/mm^2)$	٣.٠
	Poisson's ratio	ν	٠.١٥
	Uniaxial crashing strain	ε_{cu}	٠.٠٠٣
Steel	Young's modulus	$E_s(N/mm^2)$	٢٠٠١٠٠
	Yield stress	$F_y(N/mm^2)$	٣٤٥
	Hardening parameter	H'	٠.٠
Tension stiffening parameter	Rate of stress release	α_1	٢٠.٠
	Sudden loss of tension stiffness at the instant of cracking	α_2	٠.٥
Shear retention parameters	Rate of decay of shear stiffness	γ_1	١٠.٠
	Sudden loss of shear stiffness at the instant of cracking	γ_2	٠.٥
	Residual shear stiffness due to the dowel action	γ_3	٠.١

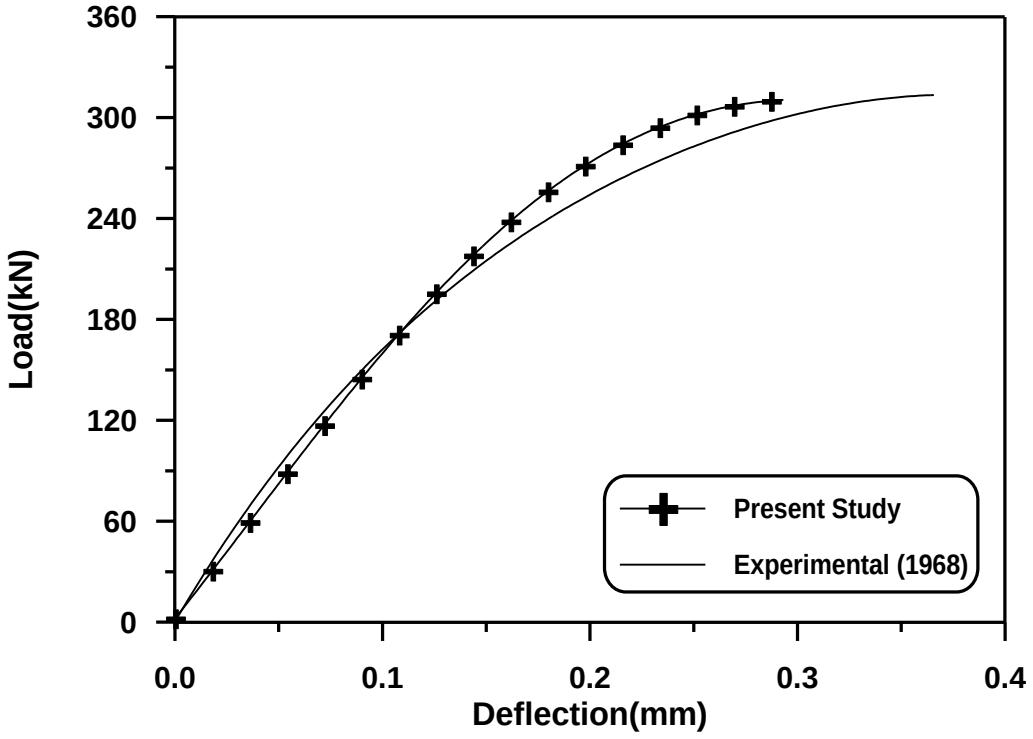

(a): Load-Deflection Curve for ٧٦٢ mm Deep Beam

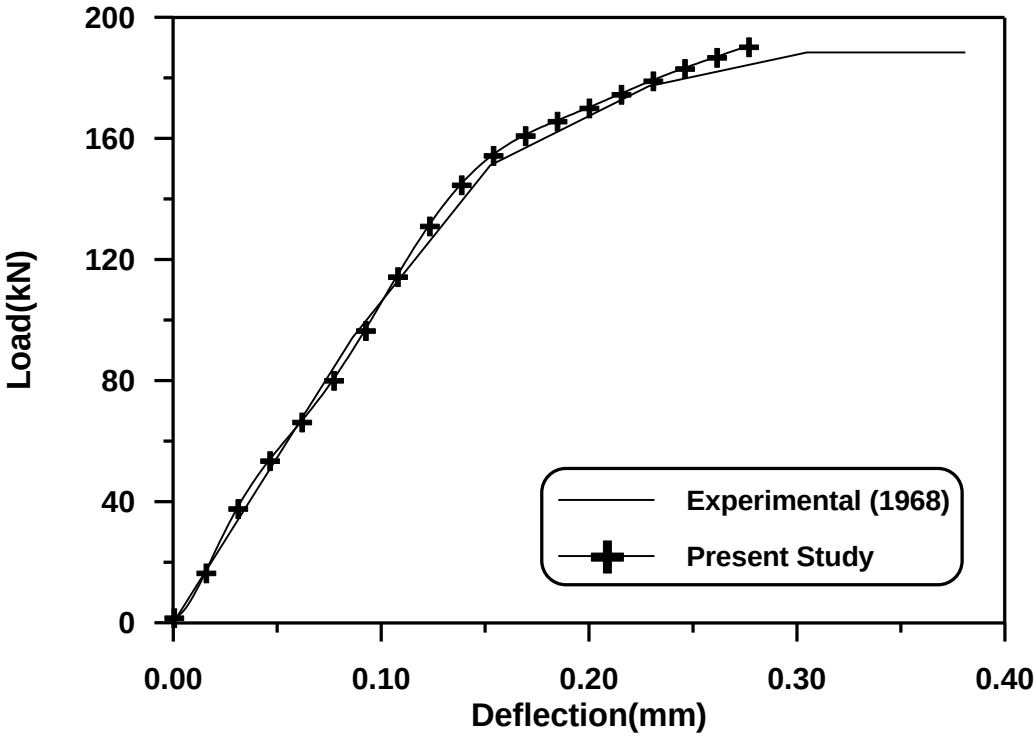

(b): Load-Deflection Curve for ٥٠٨ mm Deep Beam

Figure (٦.٢): Load Deflection Curve for Deep Beams

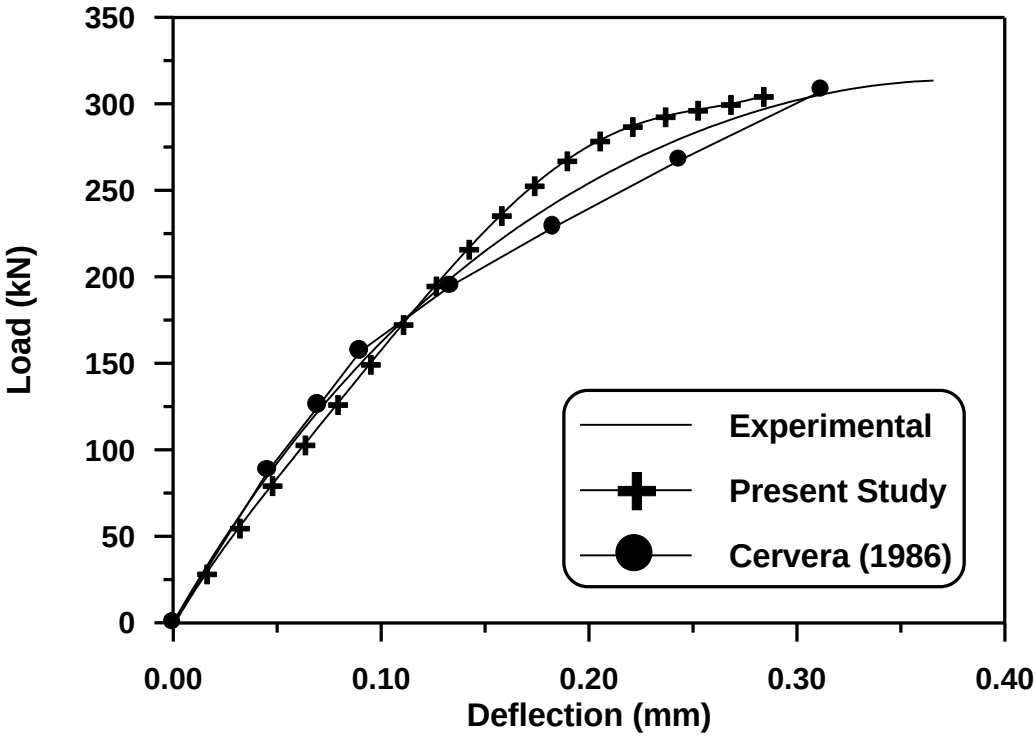

(a): Load-Deflection for ٧٦٢ mm Deep Beam
(Comparison with Previous Studies)

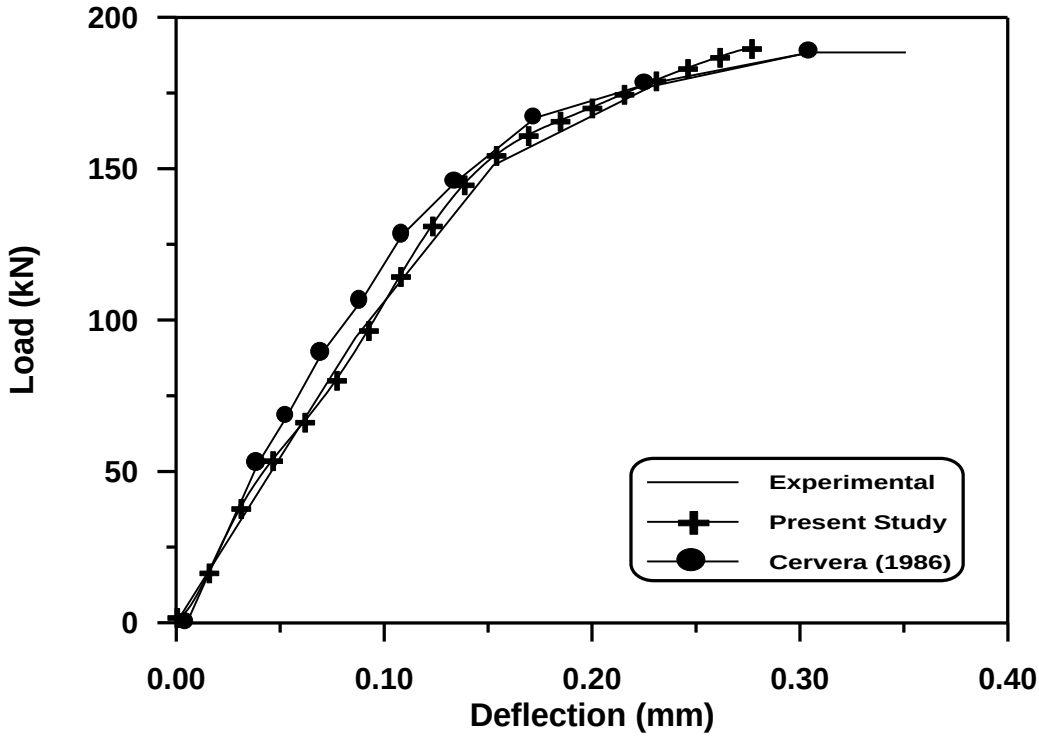

(b): Load-Deflection for ٥٠٨ mm Deep Beam (Comparison with Previous Studies)

Figure (٦.٣): Load-Deflection Curve for Deep Beams (Comparison with Previous Studies)

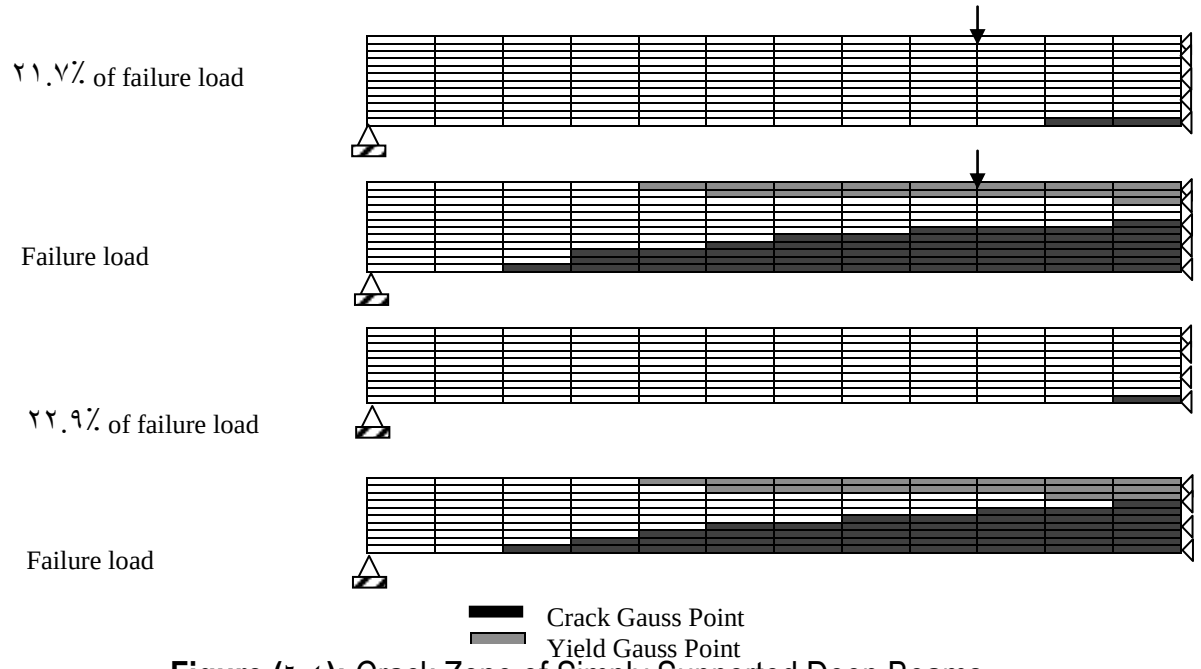

Figure (٦.٤): Crack Zone of Simply Supported Deep Beams

٦.٣ *One-Way Reinforced Concrete Slab*

A one-way slab, simply supported at two opposite edges was tested by **McNiece et al**. **(١٩٧١)**. The geometric details, reinforcement layout, loading and finite element meshes are all shown in Fig. (٦.٥). Taking the symmetry of loading and geometry, only one quarter of the slab is modeled by finite element method. A mesh of ٢٠-node brick elements was used for this quarter structure [see Fig.(٦.٥.c)]. The steel reinforcement is represented by embedded bar through the element with perfect bond between steel and concrete. The number of load increments adopted in the solution is (١٩). Material properties of the concrete and the steel are given in Table (٦.٢).

The load-deflection curve at mid-span of the slab is shown in Fig. (٦.٦). Fig.(٦.٧) shows the comparison with the previous studies. Good agreement with experimental results is obtained through most loading levels.

Crack first appeared at (٢٢.١٪) of failure load, in a region at midspan and under the concentrated point load at bottom surface. Spreading cracks are not only in horizontal direction but also through the thickness of the slab, resulting the neutral axis to shift upwards with increasing load. The crack patterns in the slab at different loading levels are drawn in Fig. (٦.٨).

Crushed Gauss points initiated at load of (٩٤.٧٪) of ultimate load. The presence of these crushed points at the top surface began when the compressive strain of the Gauss points exceeded the ultimate crushed strain, when the Gauss point was considered crushed. Zero stress and stiffness were assigned to them. Failure initiated due to excessive crushing at load (P=٣٩٨٠ N).

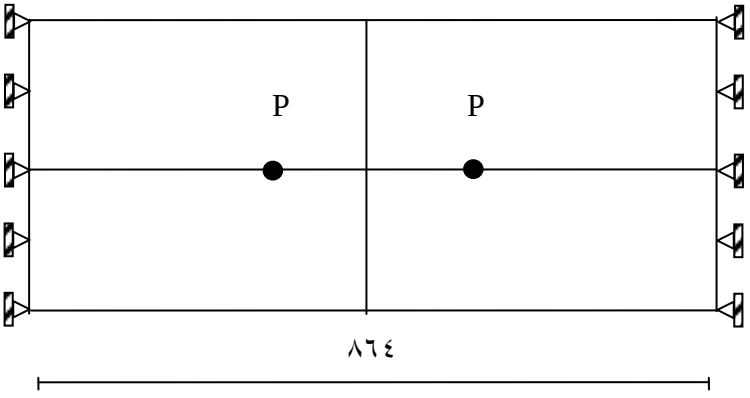

(a): Geometrical and Loading Details

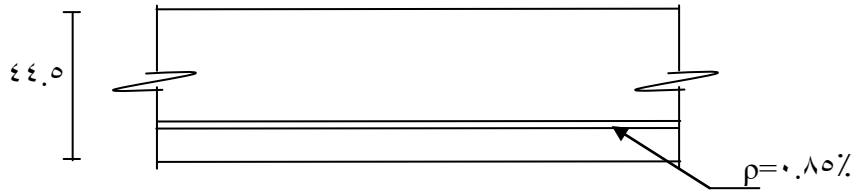

(b): Reinforcement Details

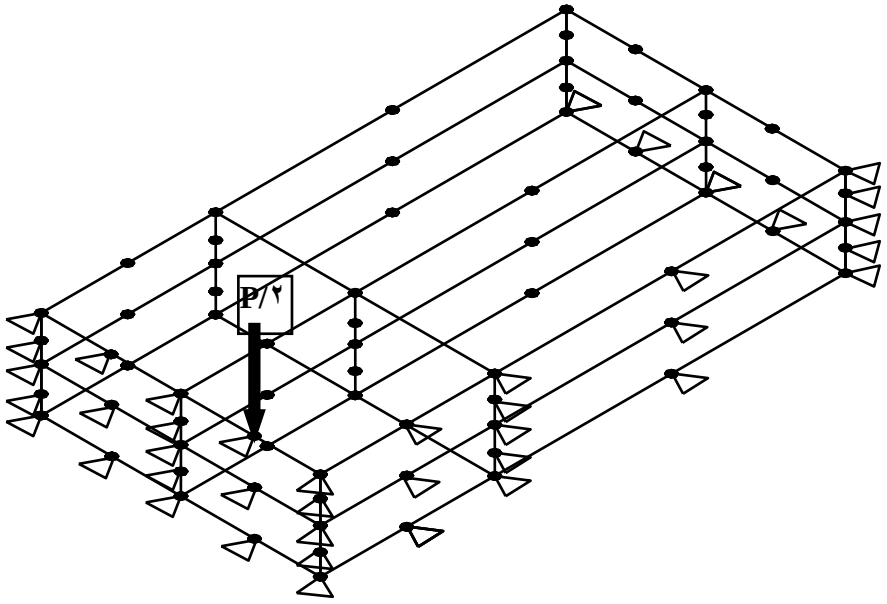

(c): Finite Element Mesh

Figure (٦.٥): One-Way Reinforced Concrete Slab

Table (٦.٢): Material Properties and Additional Parameter of One Way Slab

	Material properties and material parameters	Symbol	Value
Concrete	Young's modulus	$E_c(N/mm^2)$	٢٨٦٣٥
	Compressive strength (cylinder test)	$F_c(N/mm^2)$	٣٩.٦٤
	Tensile strength	$F_t(N/mm^2)$	٣.٠
	Poisson's ratio	ν	٠.١٥
	Uniaxial crushing strain	ε_{cu}	٠.٠٠٣
steel	Young's modulus	$E_s(N/mm^2)$	٢٠٠٠٠٠
	Yield stress	$F_y(N/mm^2)$	٣٤٥
	Hardening parameter	H'	٠.٠
Tension - stiffening parameter	Rate of decay of tension stiffness	α_1	٢٠.٠
	Sudden loss of tension stiffness at the instant of cracking	α_2	٠.٥
Shear retention parameter	Rate of decay of shear stiffness	γ_1	١٠.٠
	Sudden loss of shear stiffness at the instant of cracking	γ_2	٠.٥
	Residual shear stiffness due to the dowel action	γ_3	٠.١

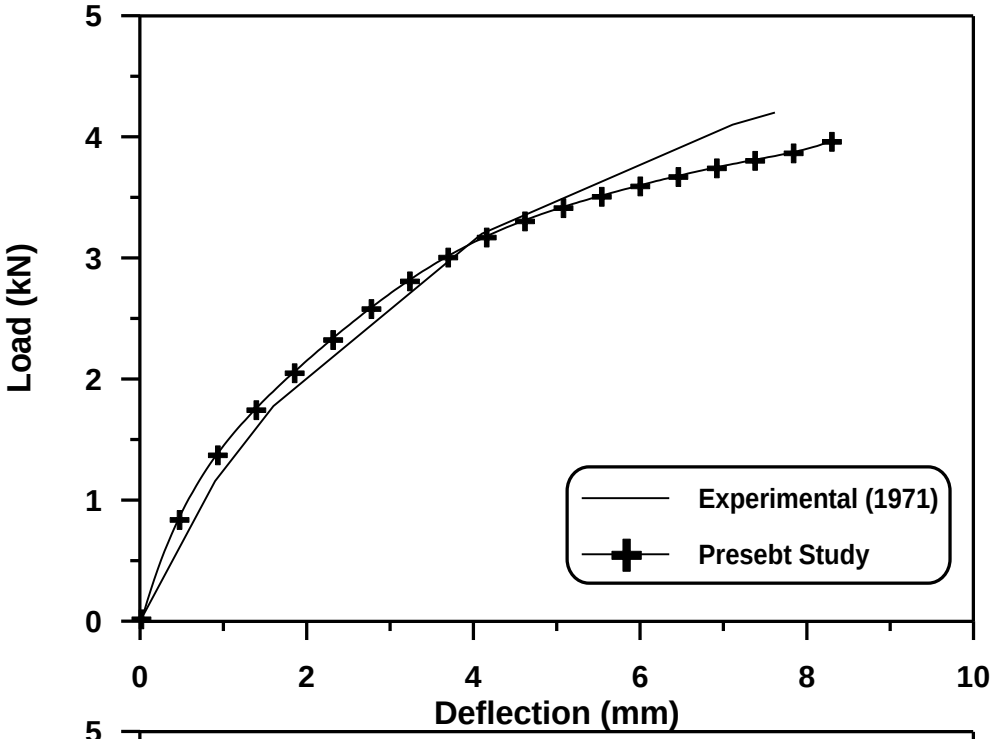

Figure (٦.٦): Load-Deflection Curves at Midspan of One –Way Simply Supported Slab

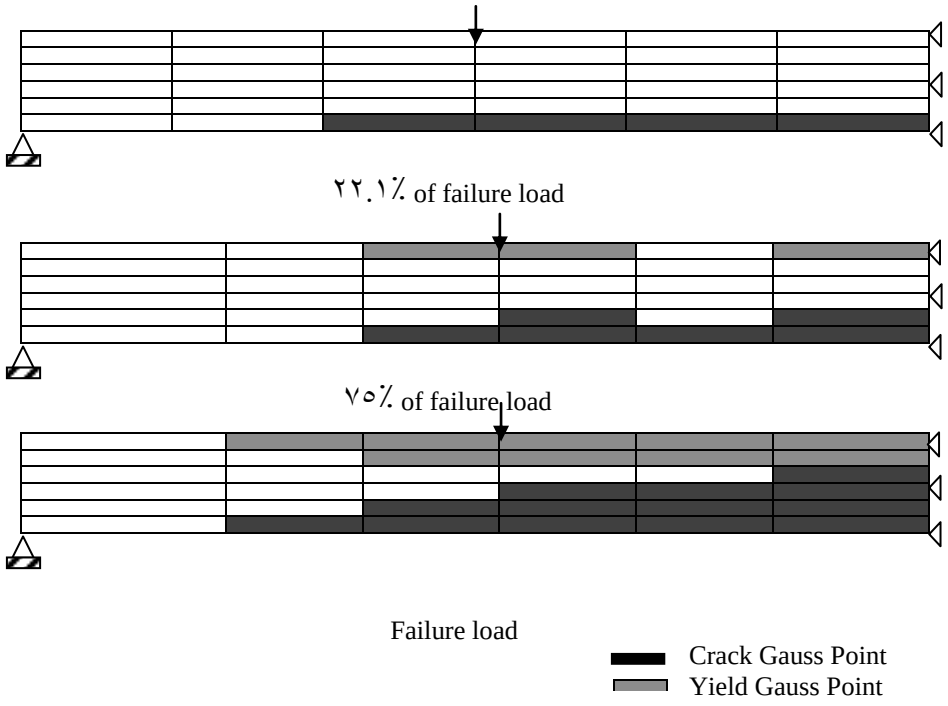

Figure (٦.٨): Crack Zone of Simply Supported One-Way Slab

٦.٤ *Corner Supported Reinforced Concrete Slab*

An isotropically reinforced concrete square slab, simply supported at four corners was tested experimentally under central point load by **McNiece et al (١٩٧١)**. Several investigators proved their theoretical work by comparing their analytical result with that of two-ways McNiece slab. Geometric details, reinforcement layout and finite element idealizations are shown in Fig. (٦.٩).

Taking the symmetry of loading and geometry, only a quarter of the slab is modeled by the finite element method. A mesh of ٨ twenty- node brick elements is used for this quarter structure [see Fig. (٦.٩.c)].

The steel reinforcement is modeled by embedded bar in two directions x and y. Number of load increments adopted in the solution is (٢٠). Material properties of concrete and steel are given in Table (٦.٣)

Fig. (٦.١٠) shows the load-deflection curve at point *A* at distance ٧٦.٢ mm from the central point. Good agreement with experimental result is obtained through most loading levels. The comparison with previous theoretical studies and the present analysis is shown in Fig. (٦.١١). From that Figure, it can be seen that the present model represented a better simulation with respect to experimental result than the other three previous models.

The crack patterns for different loading levels of bottom surface of the slab are shown in Figure (٦.١٢). Crack first appeared at ٢٥٪ of failure load, in the region under the concentrated point load at bottom face and soon spread out horizontally in fan shape along the x and y- axes. Spreading cracks are not only in the horizontal direction but also through the thickness of slab resulting in neutral axis shifting upwards with increasing load.

At load stage of about (٩٥٪) of available experimental ultimate, the numerical model used in the present study indicates crushing in Gaussian points located in the top surface of the central point of slab. The crushing occurred when the compressive strain of the Gaussian points exceeded the ultimate strain value, then its stiffness deteriorated to zero and the finite element analysis was terminated.

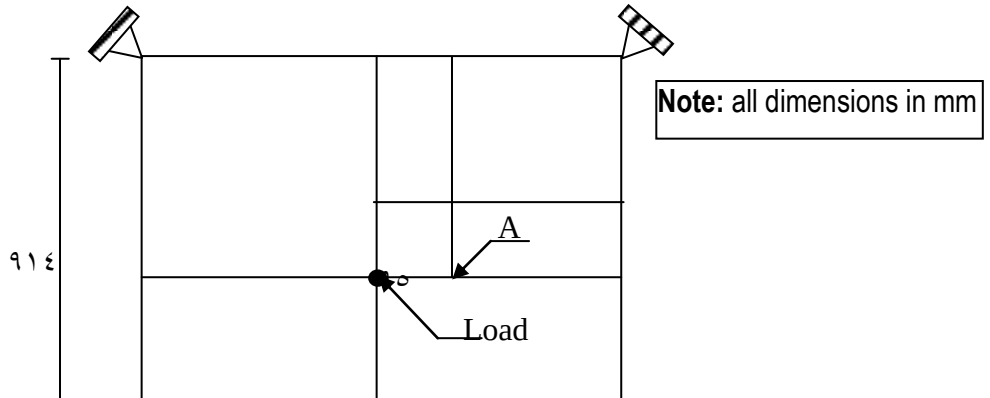

٧٦.٢

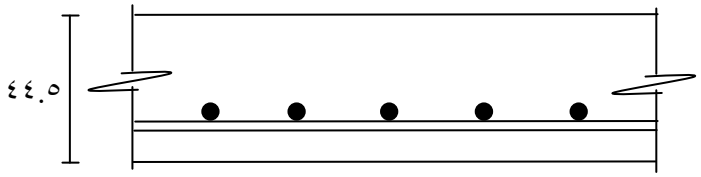

(b): Reinforcement Details

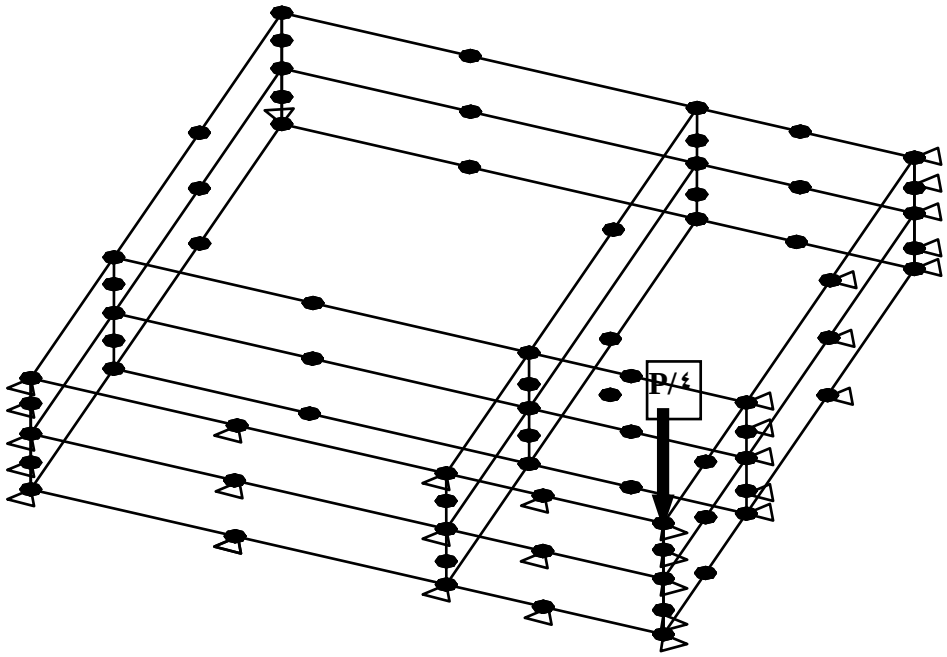

(c): Finite Element Mesh of Quarter of Corner Supported Slab

Figure (٦.٩): Corner Supported Slab

	Material properties and material parameters	Symbol	Value
concrete	Young's modulus	Ec(N/mm^{٢})	٢٨٦٣٥
	Compressive strength (cylinder test)	Fc(N/mm^{٢})	٣٧.٩٤

	Tensile strength	Ft(N/mm^{٢})	٣.٠
	Poisson's ratio	ν	٠.١٥
	Uniaxial crushing strain	εcu	٠.٠٠٣
steel	Young's modulus	Es(N/mm^{٢})	٢٠٠٠٠٠
	Yield stress	Fy(N/mm^{٢})	٣٤٥
	Hardening parameter	H	٠.٠
Tension-Stiffening parameter	Rate of decay tension stiffness	$\alpha_{١}$	٢٠.٠
	Sudden loss of tension stiffness at the instant of cracking	$\alpha_{٢}$	٠.٥
Shear retention parameter	Rate of decay of shear stiffness	$\gamma_{١}$	١٠.٠
	Sudden loss of shear stiffness at the instant of cracking	$\gamma_{٢}$	٠.٥
	Residual shear stiffness due to the dowel action	$\gamma_{٣}$	٠.١

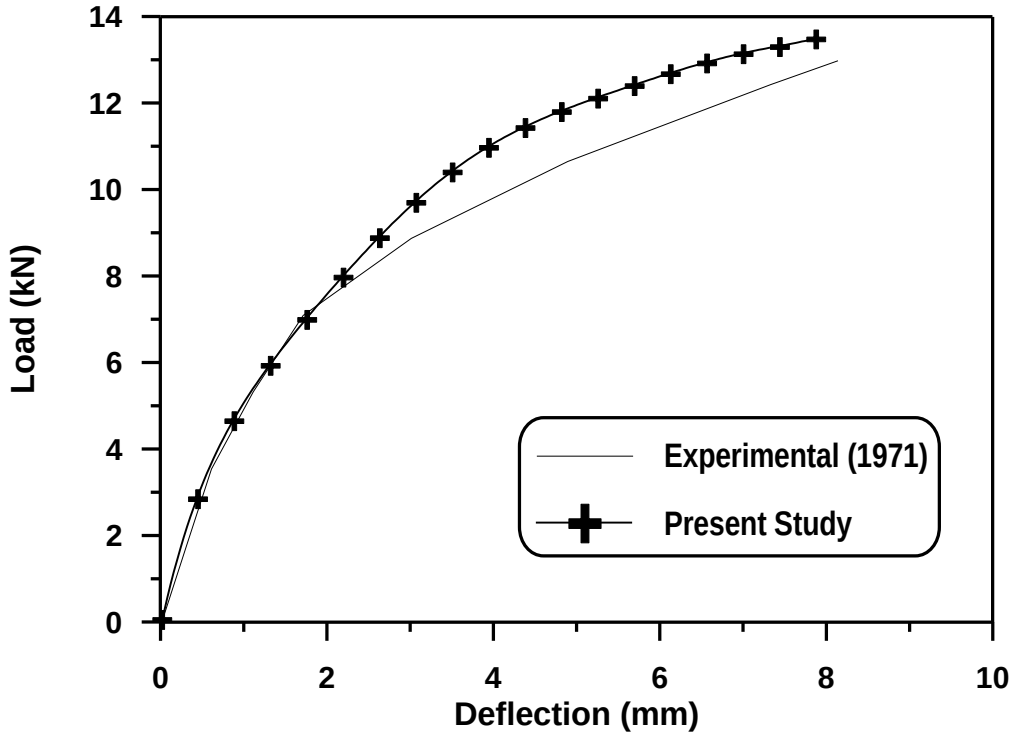

Figure (٦.١٠): Load Deflection Curve at Point A for Corner Support Slab

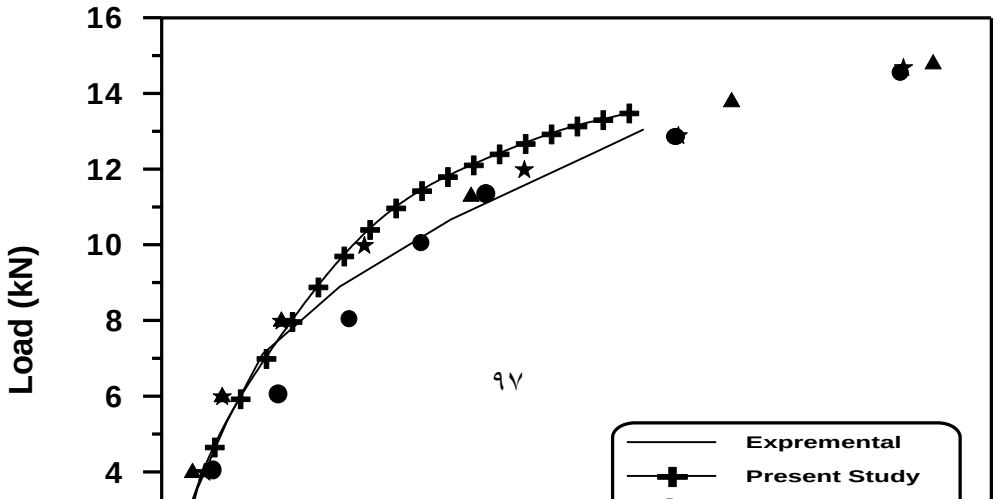

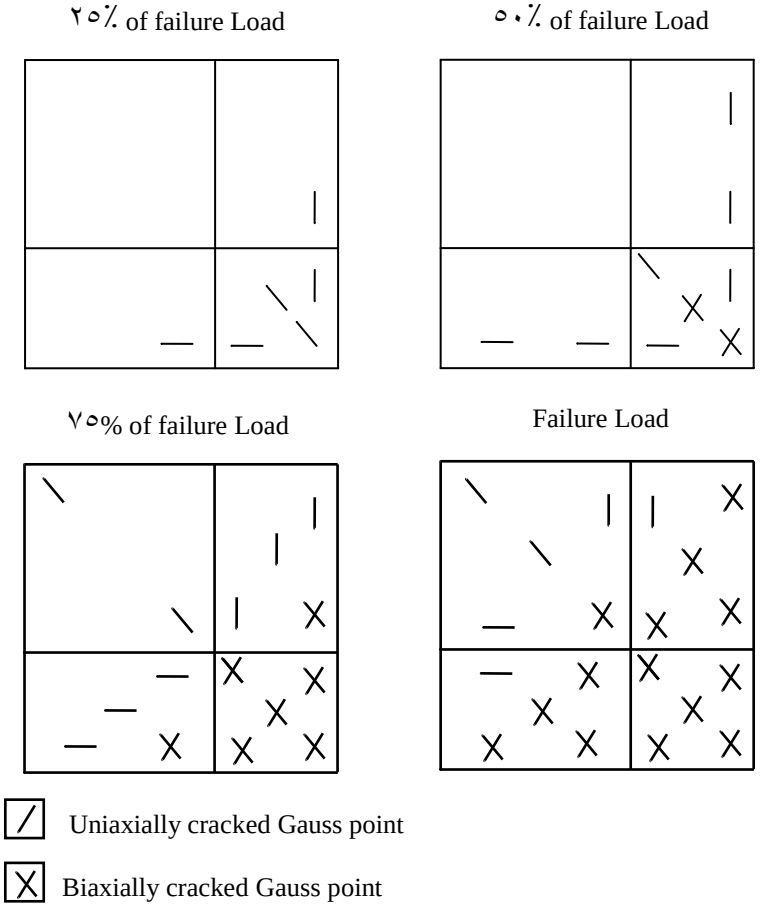

Figure (٦.١٢): Crack Patterns at bottom Surface of McNiece Slab

٦.٥ *Circular Plate Foundation*

A wire-reinforced micro-concrete circular plate foundation was studied by Husain (٢٠٠٢). The plate has a radius of (١٨٠ mm) with thickness of (١٠ mm), as

shown in Fig. (٦.١٣.a) and reinforced by seven wires in hoop direction and eight steel rods in meridional direction as shown in Fig. (٦.١٣.b).

Due to symmetry one quarter of the problem is considered. A mesh of ten elements of twenty-node brick elements is used to model the circular plate as shown in Fig. (٦.١٣.c). Material properties are shown in Table (٤). Soil is represented by polynomial model.

Fig. (٦.١٤) shows the load-deflection curve for this plate compares with previous study. It can be noticed that the polynomial model gives good agreement with that study.

Fig. (٦.١٥) shows the crack pattern for the circular plate at the failure load

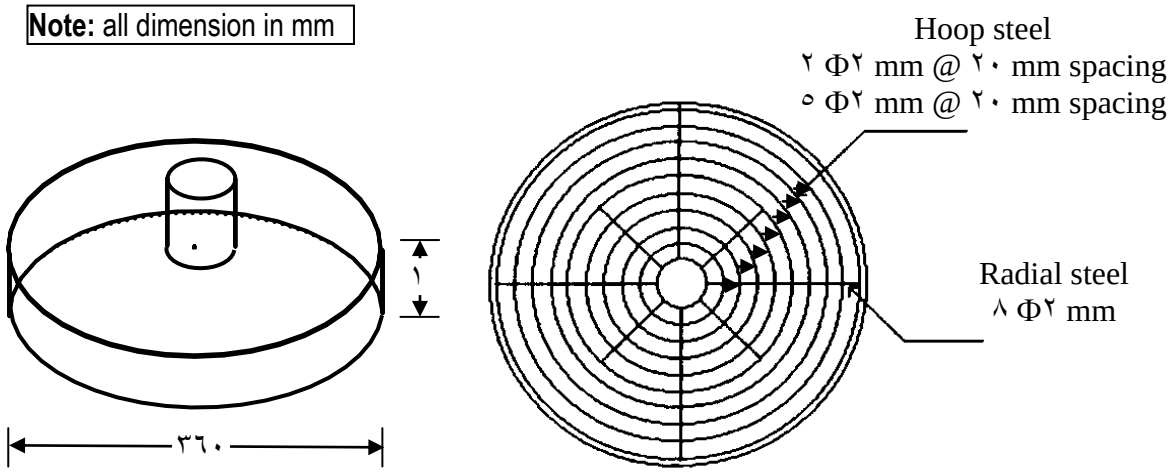

(a): circular Plate Foundation **(b):**Reinforcement detail for circular plate foundation

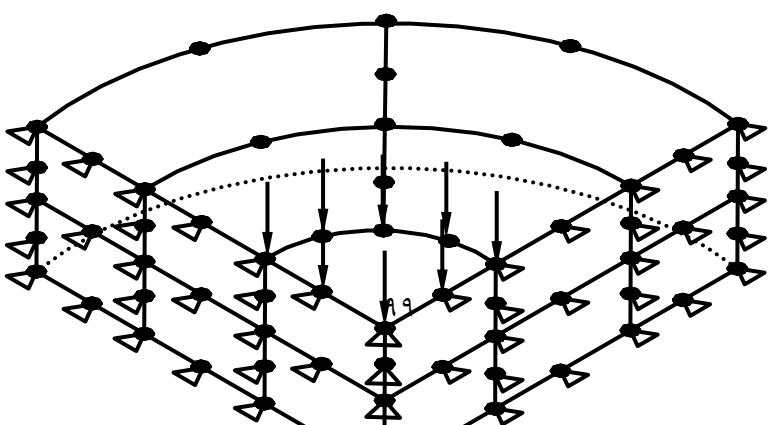

Table (٦.٤): Material Properties and Additional Parameters of circular plate Foundation.

	Material properties and material parameters	Symbol	Value
Concrete	Young's modulus	E_c (N/mm^2)	٣٠٠٠٠
	Compressive strength	f'_c (N/mm^2)	٤٤
	Tensile strength	f_t (N/mm^2)	٤.١٢
	Poisson's ratio	ν_c	٠.١٥
	Uniaxial crushing strain	ε_{cu}	٠.٠٠٣
Steel	Young's modulus	E_s (N/mm^2)	٢٠٠٠٠٠
	Yield stress	f_y (N/mm^2)	٣٠٩
	Hardening parameter	H'	٠
Tension – stiffening parameters	Rate of stress release	α_1	٢٠
	Sudden loss of stress at the instant of cracking	α_2	٠.٥
Shear retention parameters	Rate of decay of tension stiffness	γ_1	١٠
	Sudden loss of tension stiffness at the instant of cracking	γ_2	٠.٥
	Residual shear stiffness due to the dowel action	γ_3	٠.١

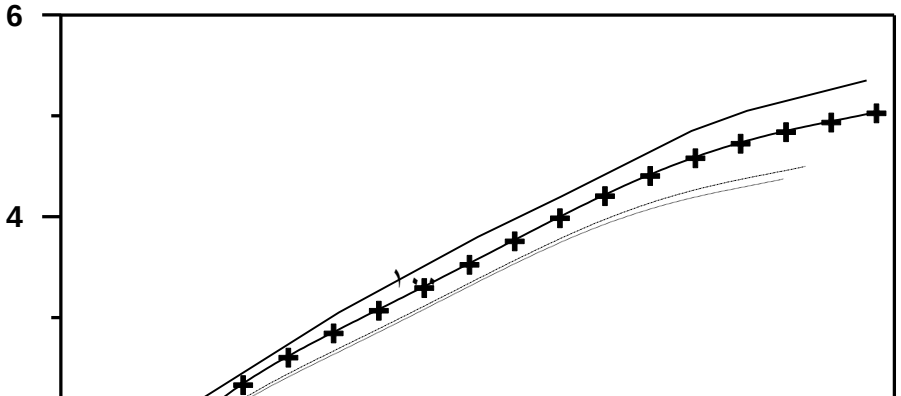

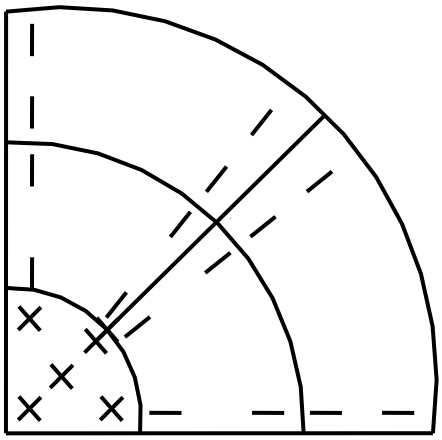

Figure (٦.١٥): Crack Zone for Circular Plate for Bottom face Foundation at Failure Load

٦.٦ *Thick Plate on Elastic Foundation*

Isotropically reinforced concrete square plate foundation of (٩١٤ mm) side length with thickness (h=٢٠٠) mm as shown in Fig. (٦.١٦.a) is considered to study the behavior of thick plate foundation. Due to symmetry of loading and geometry, one quarter of this plate is analyzed. Steel reinforcement is

represented by embedded bar in x and y direction as shown in Fig. (٦.١٦.b) with perfect bound between steel and concrete.

Material properties for concrete and steel are shown in Table (٦.٥). For Winkler model, the value of normal subgrade reaction is (٣٠٠٠٠) kN/m^{٣}, for Coulomb model the value of horizontal subgrade reaction (٣٠٠٠٠) kN/m^{٣} and the angle of friction is ($\delta_x = \delta_y = ٢٠^{o}$), for Kondner model the value of ***a*** (٣٨٤.٣٤ mm^{٣}/kN) and ***b*** (٠.١٧٦ mm^{٢}/kN), for Polynomial model the value of normal subgrade reaction is dependent on the load test for the soil as shown in Fig.(٦.١٧) to Fig. (٦.٢٠) for different types of soil.

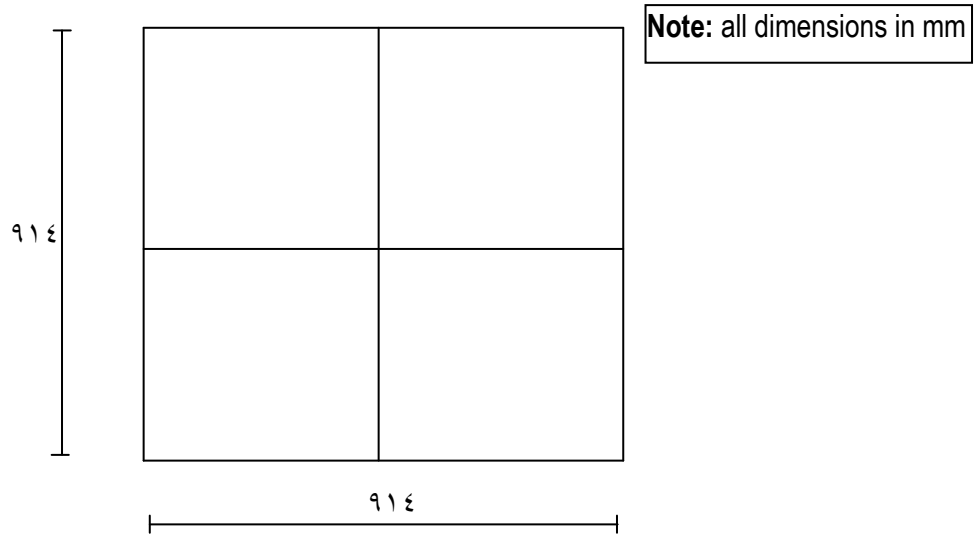

(a): Geometrical Details

(b): Reinforcement Details

Figure (٦.١٦): Thick plate foundation

Table (٦.٥): Material Properties and Additional Parameters of Thick Plate Foundation.

	Material properties and material parameters	Symbol	Value
Concrete	Young's modulus	E_c (N/mm^{٢})	٣٠٠٠٠
	Compressive strength	f'_c (N/mm^{٢})	٣٠
	Tensile strength	f_t (N/mm^{٢})	٣.٠

	Poisson's ratio	ν_c	٠.١٥
	Uniaxial crushing strain	ε_{cu}	٠.٠٠٣٥
Steel	Young's modulus	E_s (N/mm^2)	٢٠٠٠٠٠
	Yield stress	f_y (N/mm^2)	٤٠٠
	Hardening parameter	H′	٠
Tension – stiffening parameters	Rate of stress release	α_1	٢٠
	Sudden loss of stress at the instant of cracking	α_2	٠.٥
Shear retention parameters	Rate of decay of tension stiffness	γ_1	١٠
	Sudden loss of tension stiffness at the instant of cracking	γ_2	٠.٥
	Residual shear stiffness due to the dowel action	γ_3	٠.١

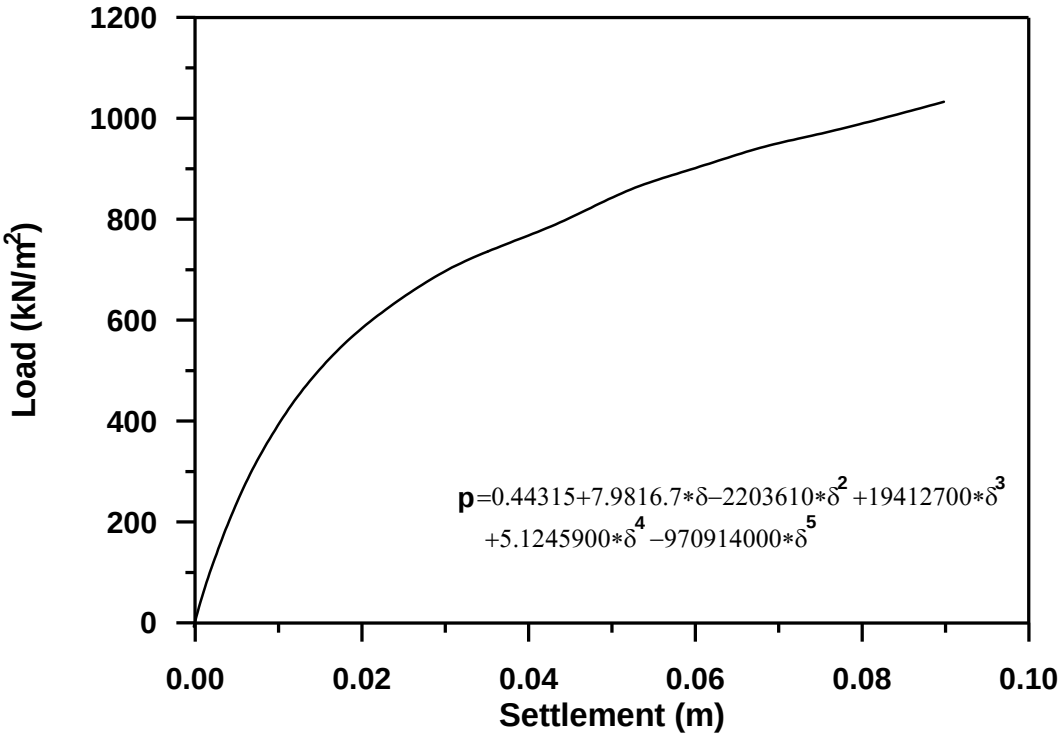

Figure (٦.١٧): Load-Settlement Curve of Soil [Dense Sand (٣٥)]

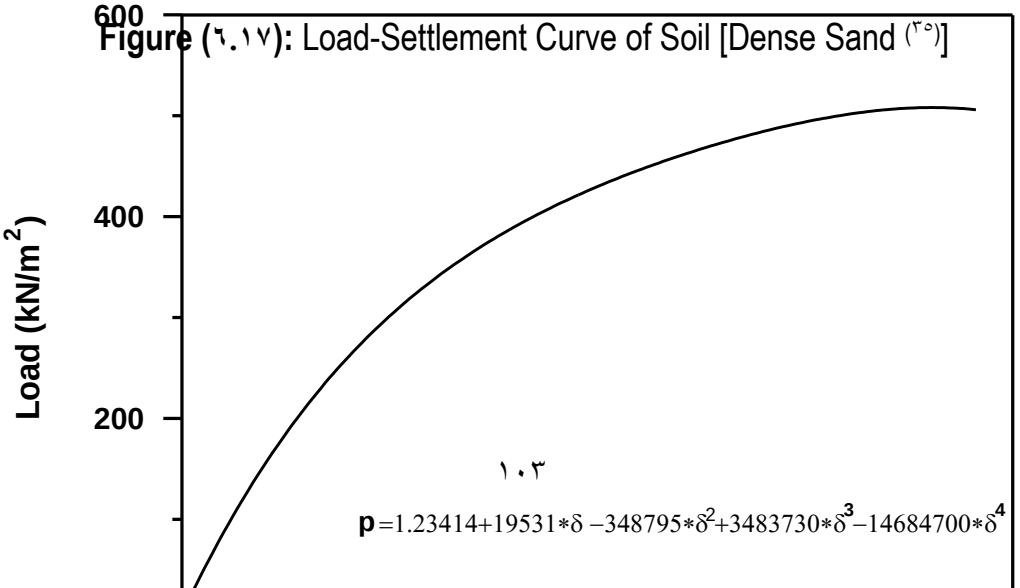

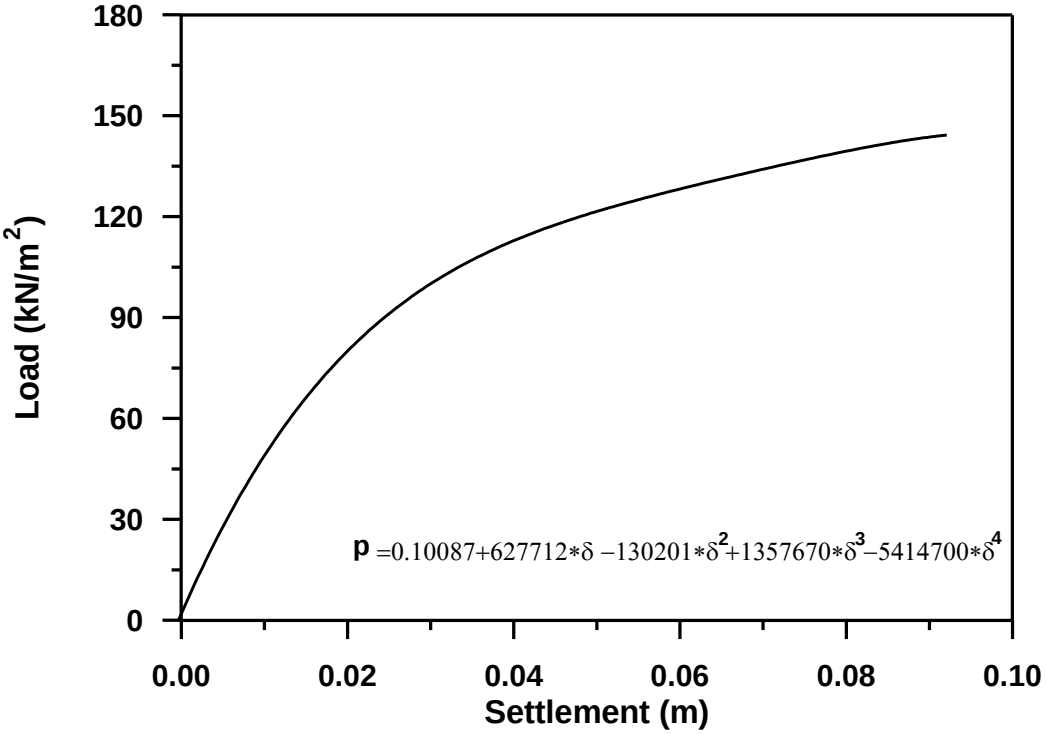

Figure (٦.١٩): Load-Settlement Curve of Soil
[Loose Sand (٣٥)]

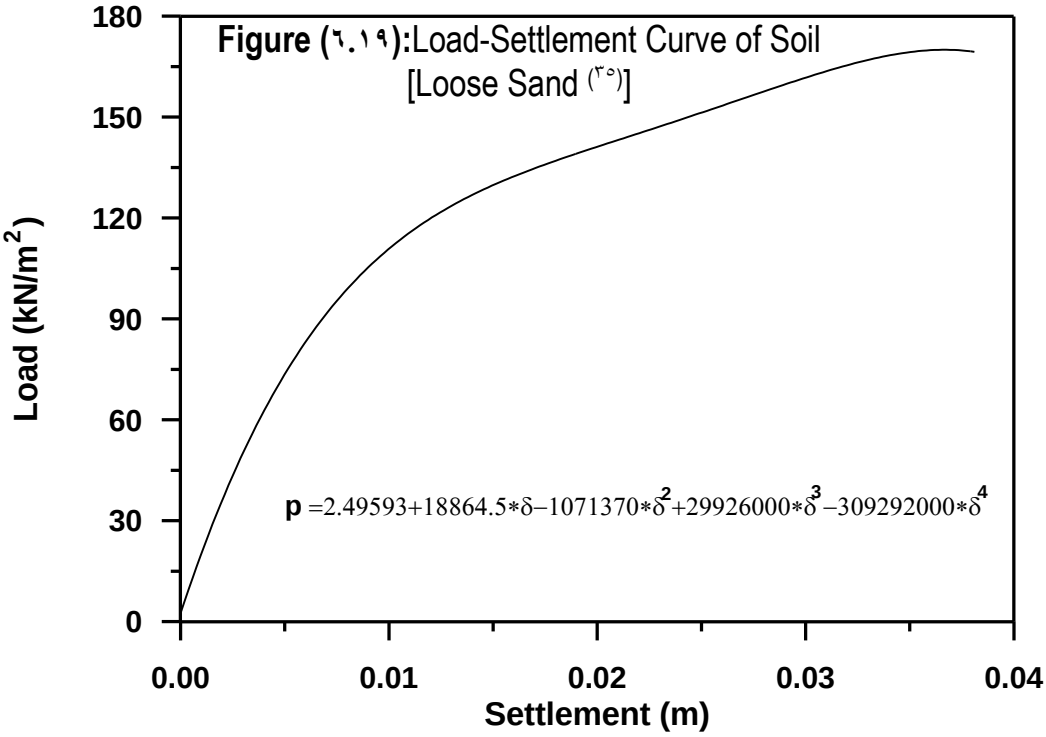

Figure (٦.٢٠): Load-Settlement Curve of Soil
[Soft Clay (١٣)]

This study takes into account different types of boundary conditions (simply supported, fixed, and free edge thick plate foundation), different types of loading (distributed and concentrated loads), different types of models for soil, and different types of soil basing on many effects:

١. Effect of boundary condition.
٢. Effect of stiffness of plate on the ultimate load and central deflection.
٣. Effect of reinforcement ratio.
٤. Effect of type of loading.
٥. Effect of type of soil.
٦. Effect of elastic foundation on the plate behavior.

٦.٦.١ *Effect of Boundary Condition*

To show the effect of boundary condition the load-deflection curve and the deflection profile for simply supported, fixed supported, and free-edge thick plate on elastic foundation are plotted for different types of models for soil.

Fig. (٦.٢١) shows the load deflection curves for simply supported thick plate foundation. Fig (٦.٢٢) shows the deflection profile for simply supported thick plate foundation. Winkler, Coloumb, and Kondner models were used to represent the foundation.

Fig. (٦.٢٣) and Fig. (٦.٢٤) show the same sequent of previous figures, but for foundation represented by a polynomial model.

Fig. (٦.٢٥) to Fig. (٦.٢٨) show the same sequent of previous figures, but for fixed supported thick plate foundation.

Fig. (٦.٢٩) to Fig. (٦.٣٢) show the same sequent of previous figures, but for free-edge thick plate foundation.

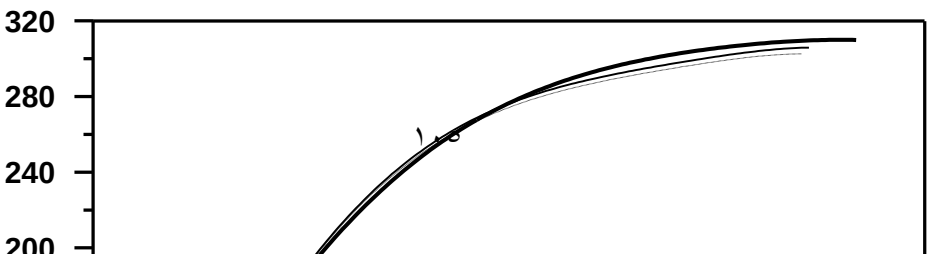

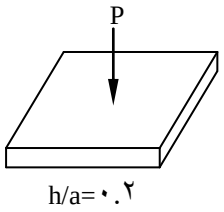

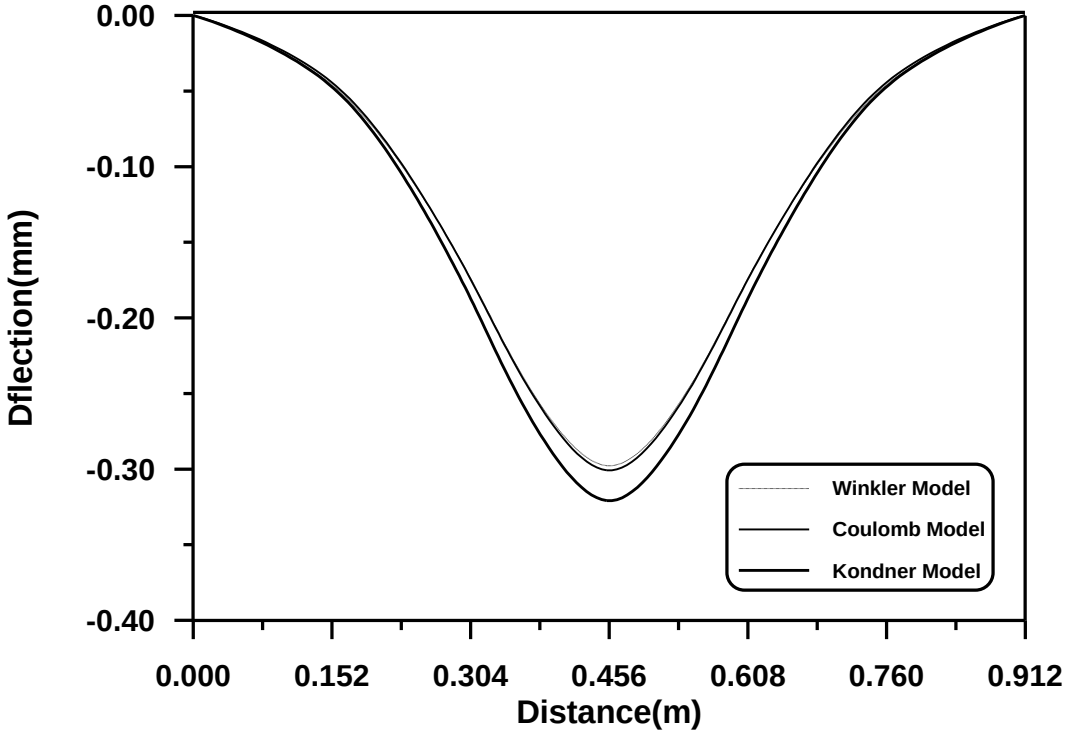

Figure (٦.٢٢): Deflection Profile for Simply Supported Thick Plate Foundation

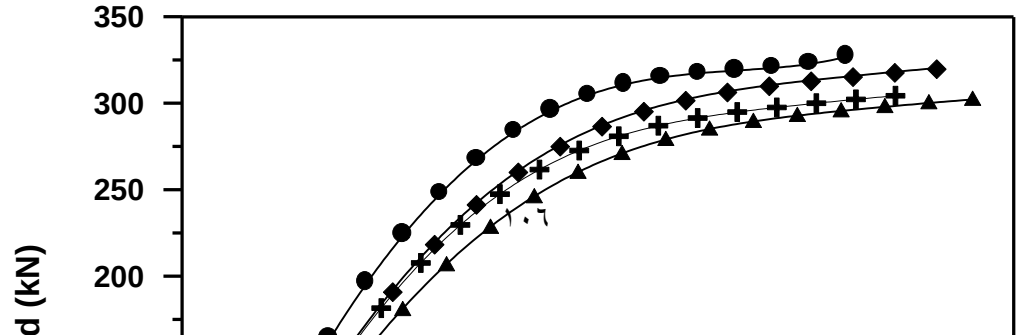

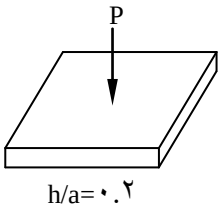

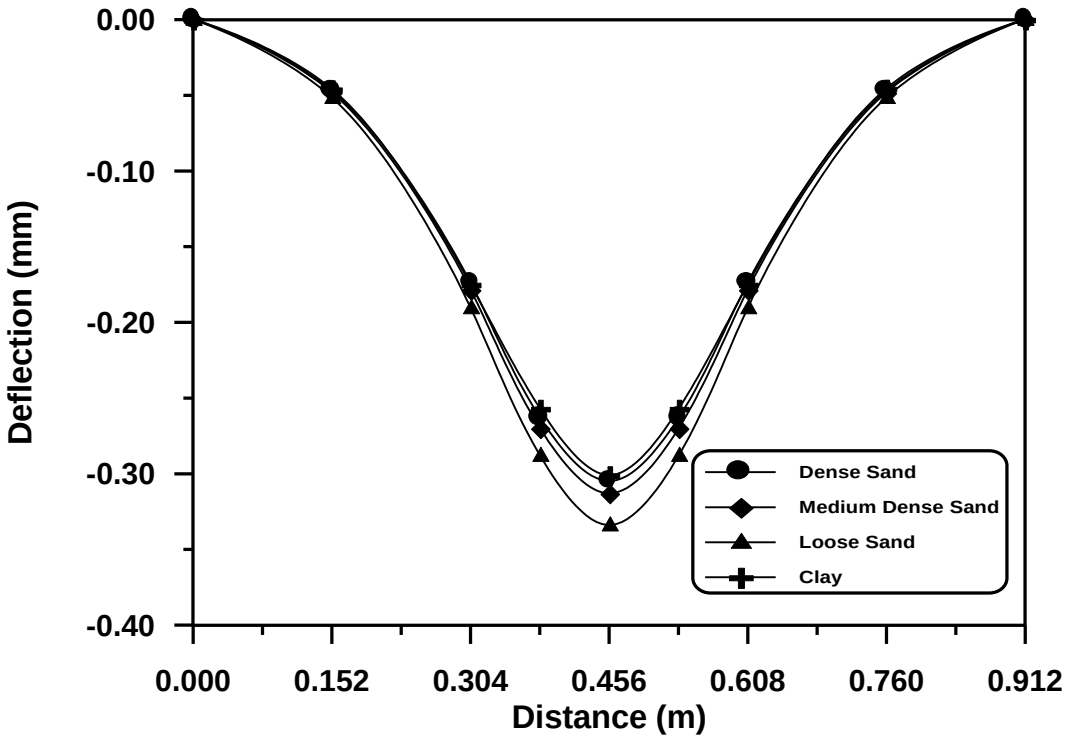

Figure (٦.٢٤): Deflection Profile for Simply Supported Thick Plate Foundation with Polynomial Model

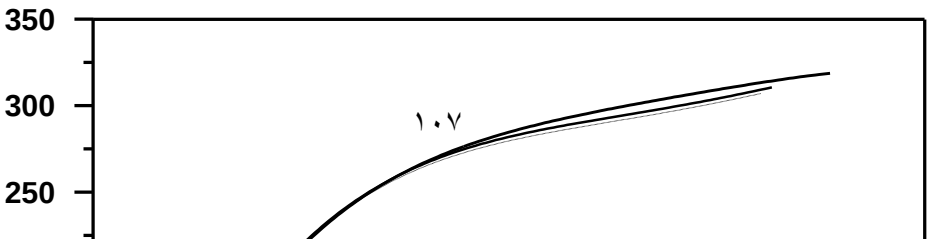

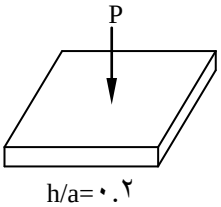

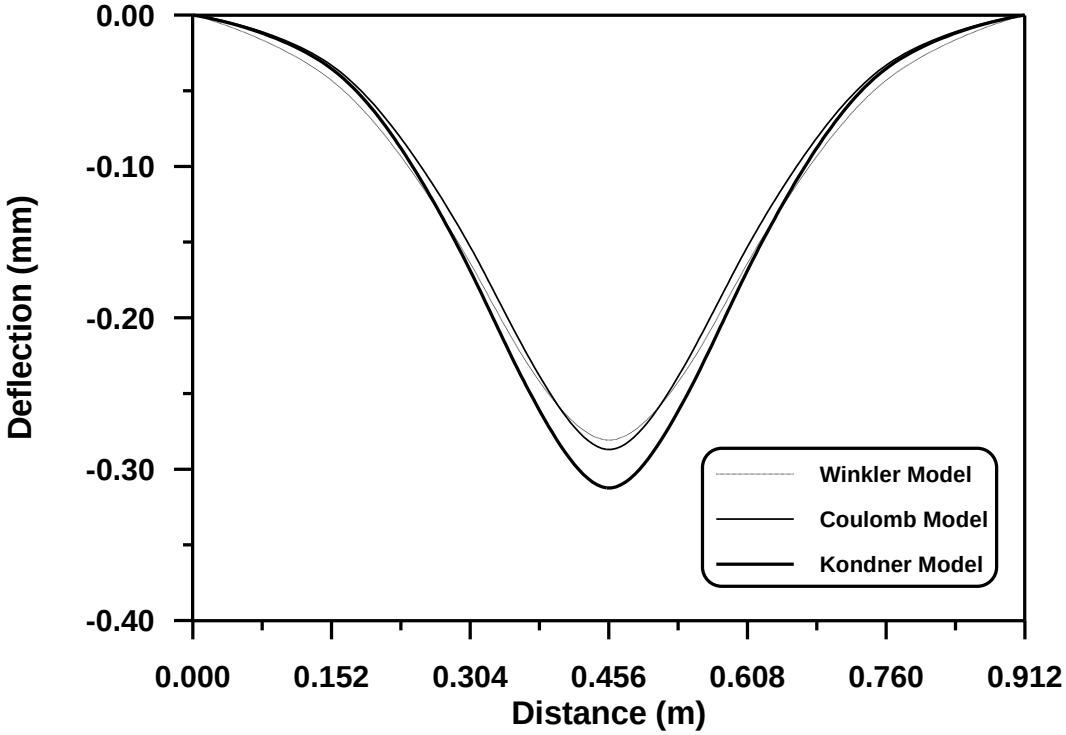

Figure (٦.٢٦): Deflection Profile for Fixed Supported Thick Plate Foundation

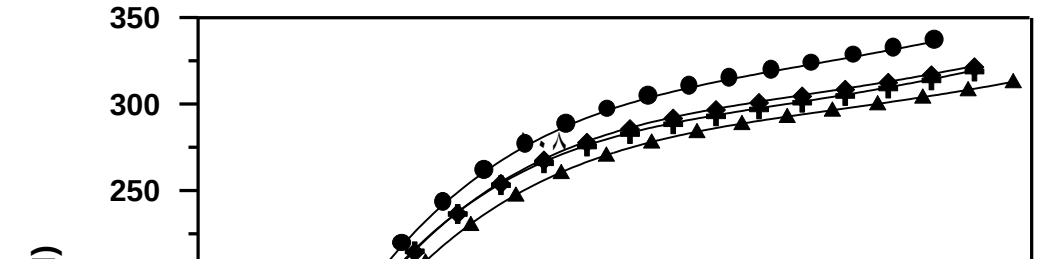

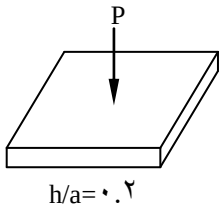

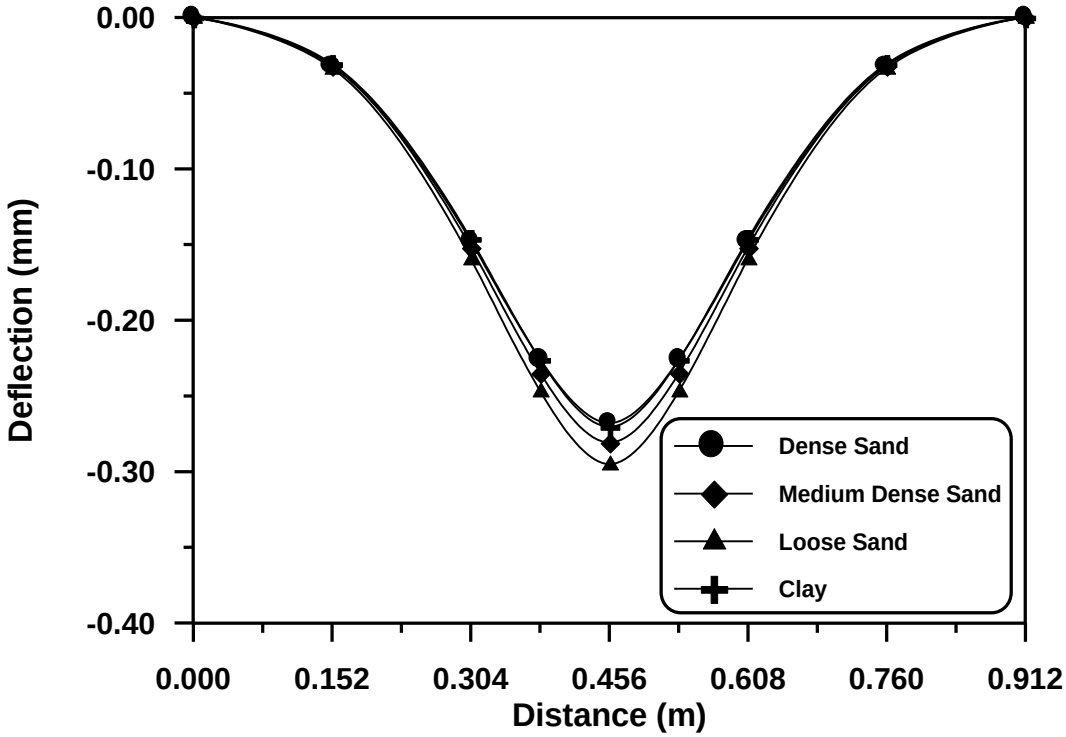

Figure (٦.٢٨): Deflection Profile for Fixed Supported Thick Plate Foundation with Polynomial Model

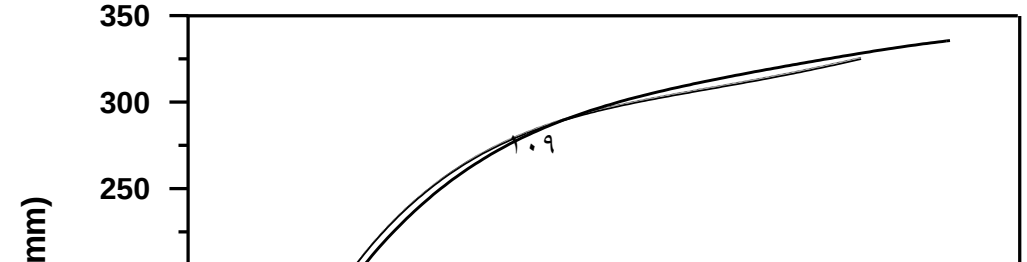

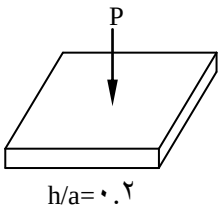

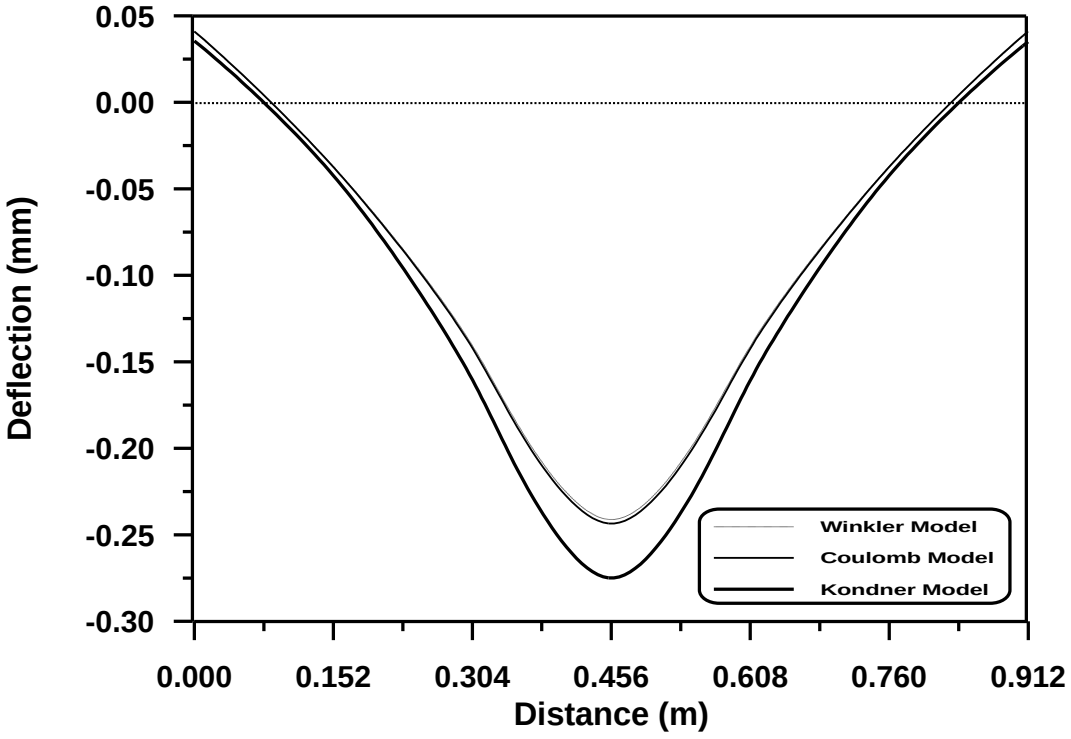

Figure (٦.٣٠): Deflection Profile for Free Edge Thick Plate Foundation with Polynomial Model

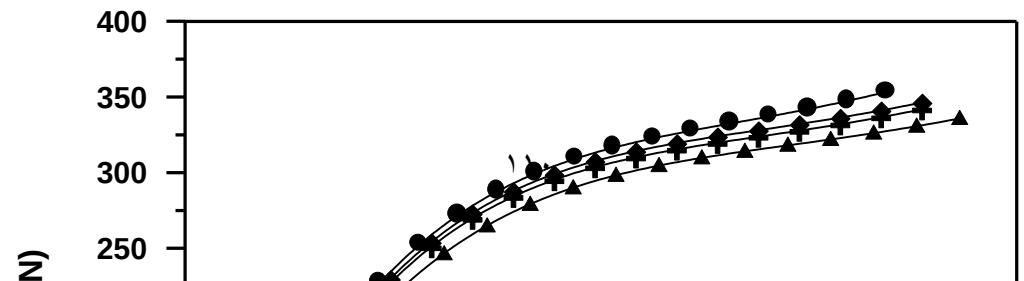

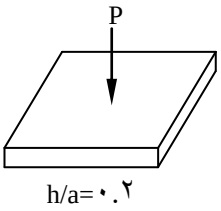

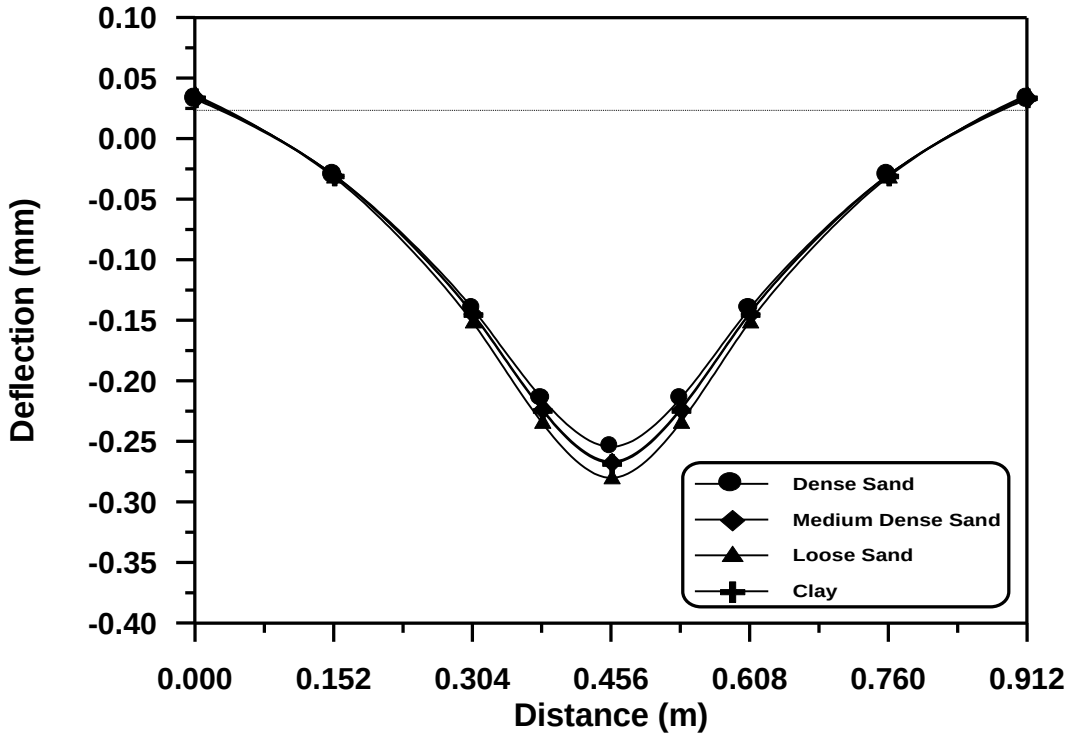

Figure (٦.٣٢): Deflection Profile for Free Edge Thick Plate Foundation with Polynomial Model

From these figures it can be noticed that:

١. For Winkler model, the load-deflection curve shows that the ultimate load that causes failure for fixed supported thick plate foundation is greater than that which causes failure for simply supported thick foundation by about (٢٪) and the ultimate load for the free-edge plate is greater than of simply supported plate by about (٧٪)

٢. For Winkler model, the deflection for the simply supported thick plate foundation is greater than that for the fixed supported plate by about (٦٪) and by about (١٩٪) for the free-edge plate.

٣. The load-deflection curve and the deflection profile for the thick plate with Winkler and Coulomb models for different boundary conditions show that there is no significant difference between their results.

٤. The ultimate loads for thick plate foundation with polynomial and Kondner models are greater than the ultimate load for Winkler and Coulomb models for all boundary conditions.

٥. The deflection for thick plate foundation with polynomial and Kondner models are greater than the deflection for Winkler and Coulomb models for all boundary conditions.

٦.٦.٢ *Effect of Stiffness of Thick Plate on Ultimate Load and Central Deflection*

A simply supported thick plate with concentrated load is considered. All information shown in Fig. (٦.١٦). Fig. (٦.٣٣) shows the relation between thickness to span ratio and the ultimate load that causes failure for this thick plate. Fig. (٦.٣٤) shows the effect of increasing the stiffness (thickness) on the central deflection of plates, foundation is represented by Winkler, Coulomb, and Kondner models. Fig. (٦.٣٥) shows the same previous figure but for foundation represented by a polynomial model for dense sand, medium dense sand, loose sand, and clay soils.

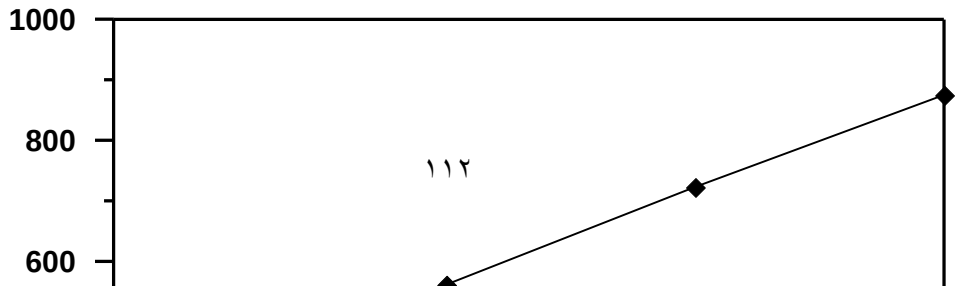

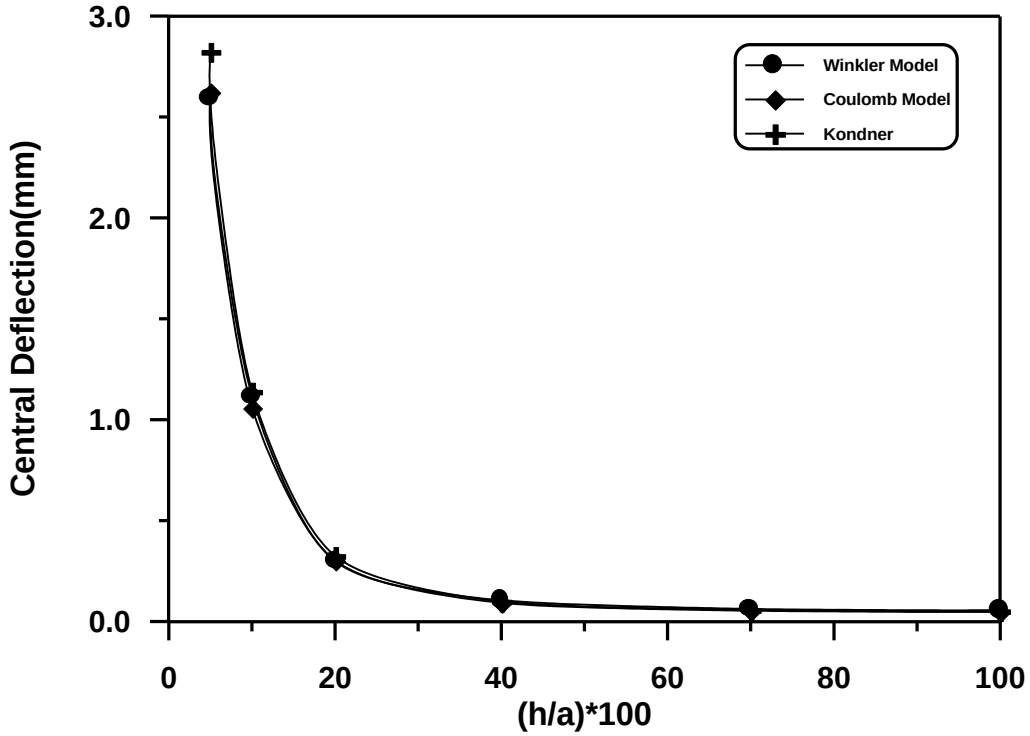

Figure (٦.٣٤): Central Deflection for Thick Plate with Different Thickness

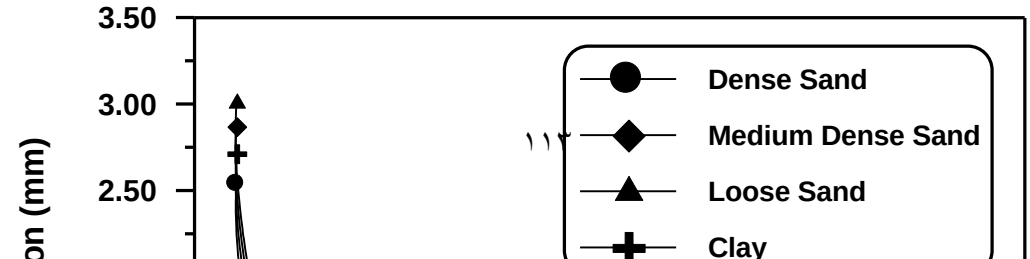

From these figures it can be noticed that:

١. For thick plate with Winkler model under concentrated load the ultimate load is increased with increasing the thickness of plate in nonlinear form.

٢. The central deflection is decreased with increasing the thickness of thick plate for all types of foundation models, the rate of decreasing in central deflection is decreased especially after the thickness to span ratio exceeding ٢٠ %

٦.٦.٣ *Effect of reinforcement ratio*

To investigate the effect of reinforcement ratio, a thick plate with Winkler and different boundary condition is considered. Fig. (٦.٣٦) shows the load-deflection curve for a simply supported thick plate for different reinforcement ratio (٠.٨, ٠.٨١١٢, ٠.٨٢٢٤, ٠.٨٤٤٨ %). Fig. (٦.٣٧) is the same as the previous figure, but for a

fixed supported thick plate. Fig. (٦.٣٨) is the same as the previous figure, but for free-edge thick plate.

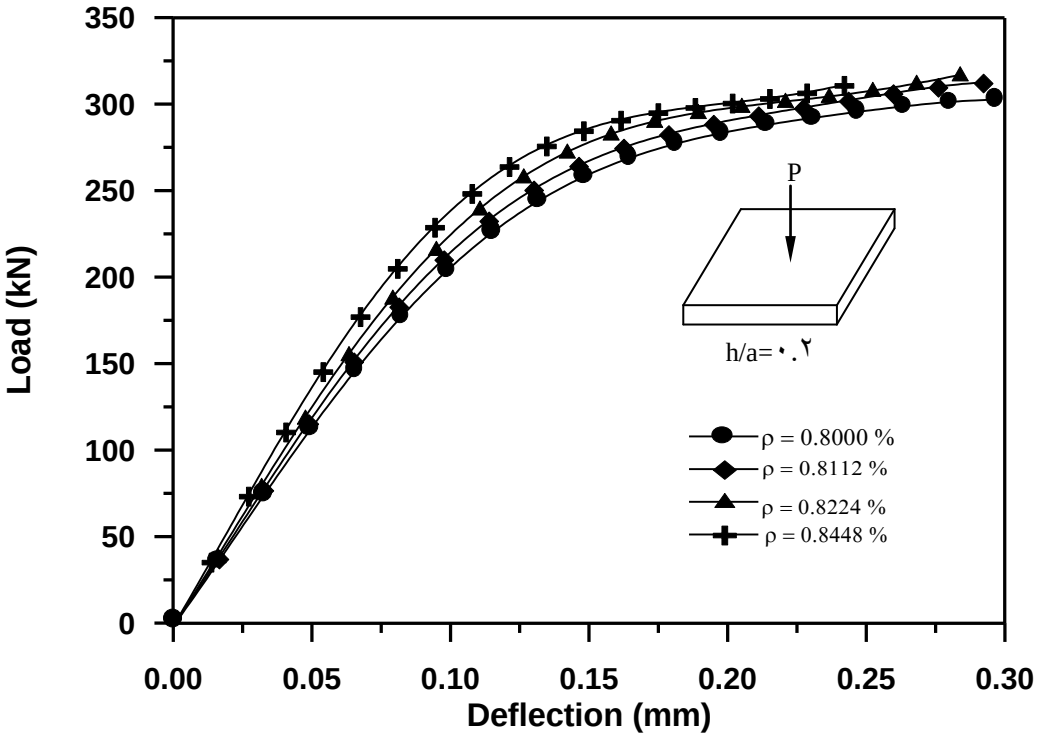

Figure (٦.٣٦): Load-Deflection Curve for Simply Supported Thick Plate with Different Reinforcement Ratio

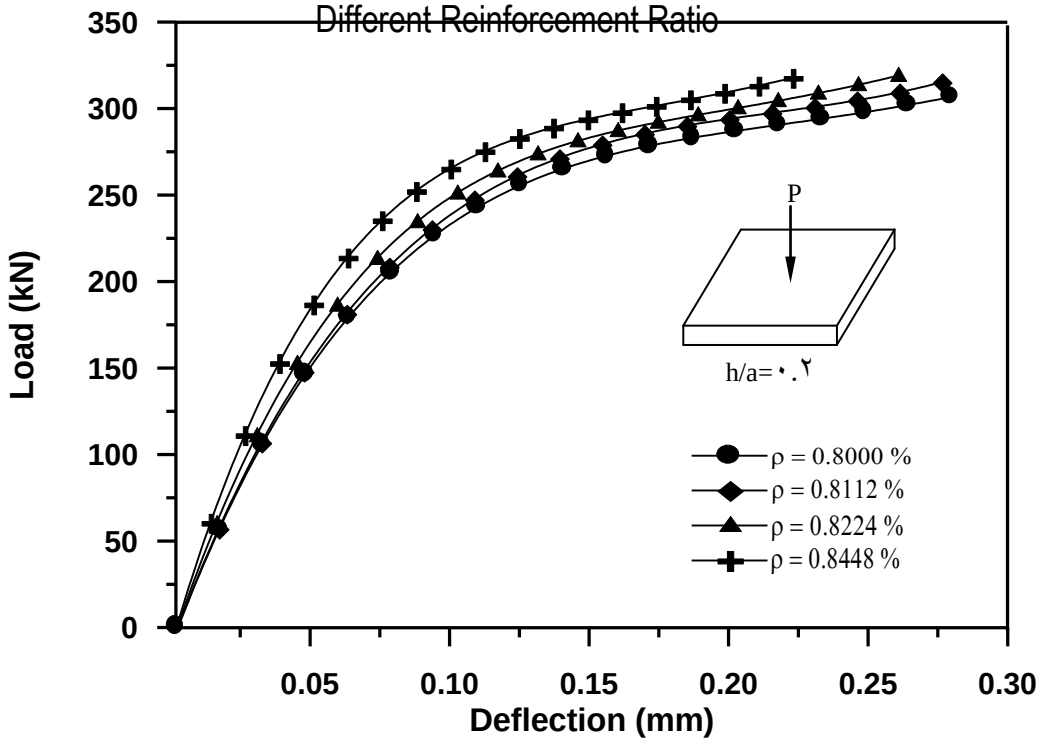

Figure (٦.٣٧): Load-Deflection Curve for Fixed Supported Thick Plate with Different Reinforcement ratio

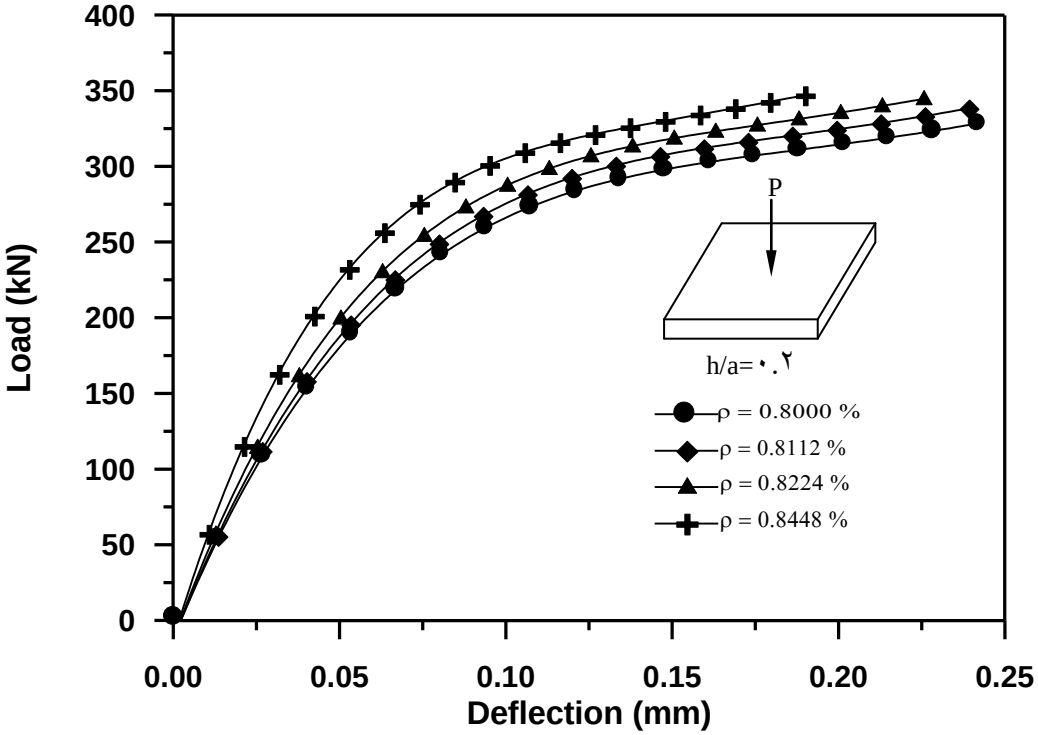

Figure (٦.٣٨): Load-Deflection Curve for Free Edges Thick Plate with Different Reinforcement Ratio

From these figures, it can be noticed that the ultimate load increases when the reinforcement ratio increases while the central deflection is inversely proportional to the reinforcement ratio.

٦.٦.٤ *Effect of Type of Loading*

To show the effect of type of loading, a simply supported thick plate and free-edge thick plate on elastic foundation with polynomial model is considered. Fig.(٦.٣٩) and Fig. (٦.٤٠) show the load-deflection curve for the thick plate with concentrated and distributed load respectively. Fig (٦.٤١) shows the deflection profile for the thick plate with concentrated and distributed load. Fig. (٦.٤٢) shows the central deflection variation with thickness to span ratio for the concentrated and distributed load. Fig. (٦.٤٣) to Fig. (٦.٤٦) show the same sequent of the previous figures, but for the free-edge thick plate foundation.

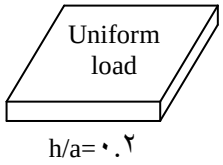

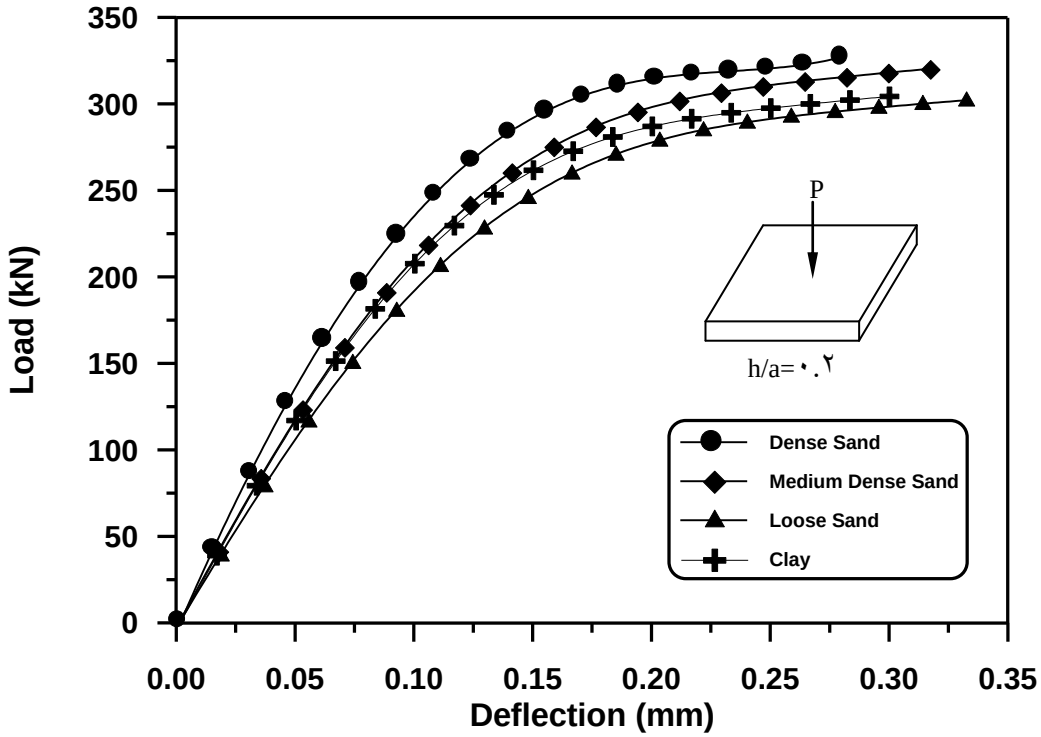

Figure (٦.٤٠): Load-Deflection Curve for Simply Supported Thick Plate with Concentrated Load

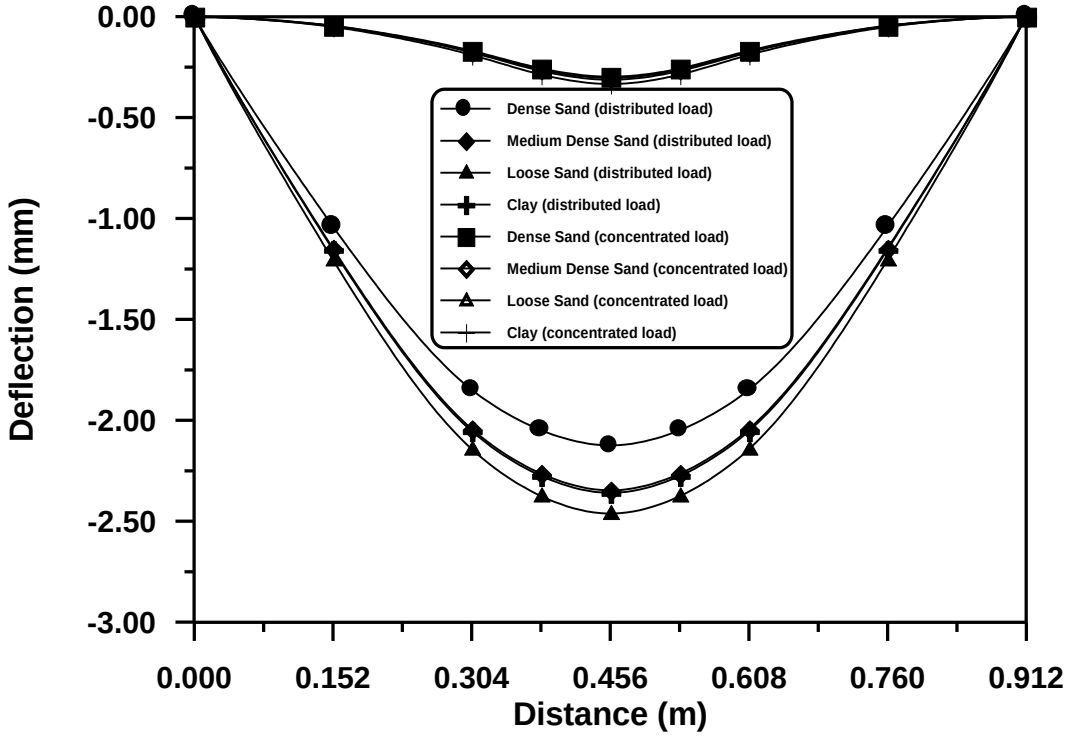

Figure (٦.٤١): Deflection Profile for Simply Supported Plate under Distributed and Concentrated Load

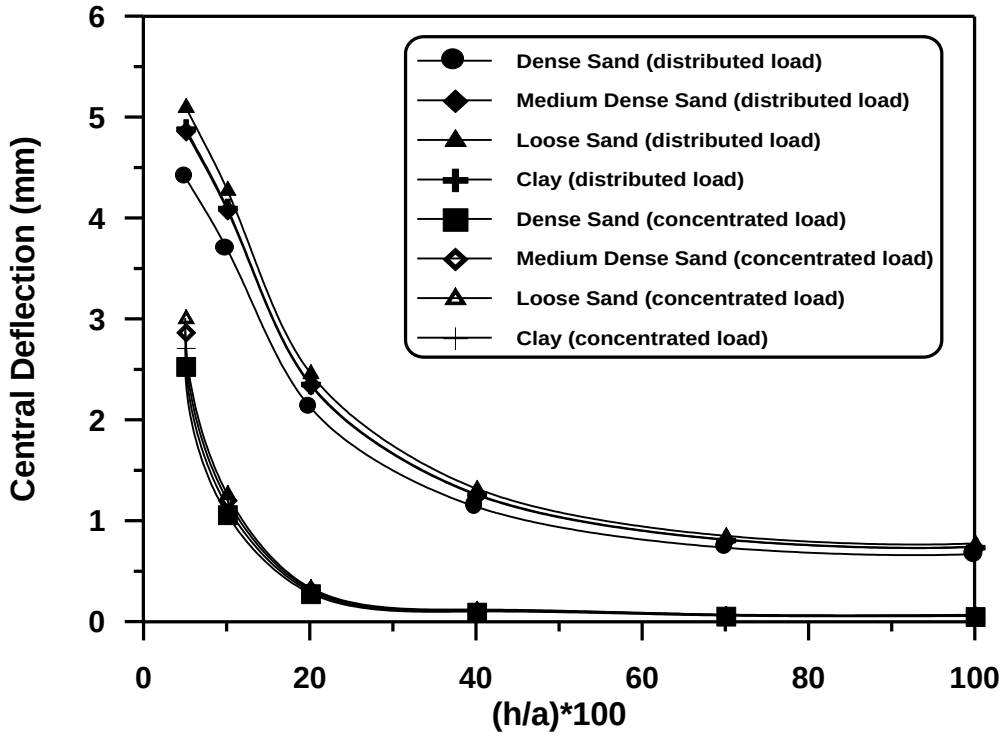

Figure (٦.٤٢): Central Deflection for Simply Supported Thick Plate with Different Thickness for Distributed and Concentrated Load

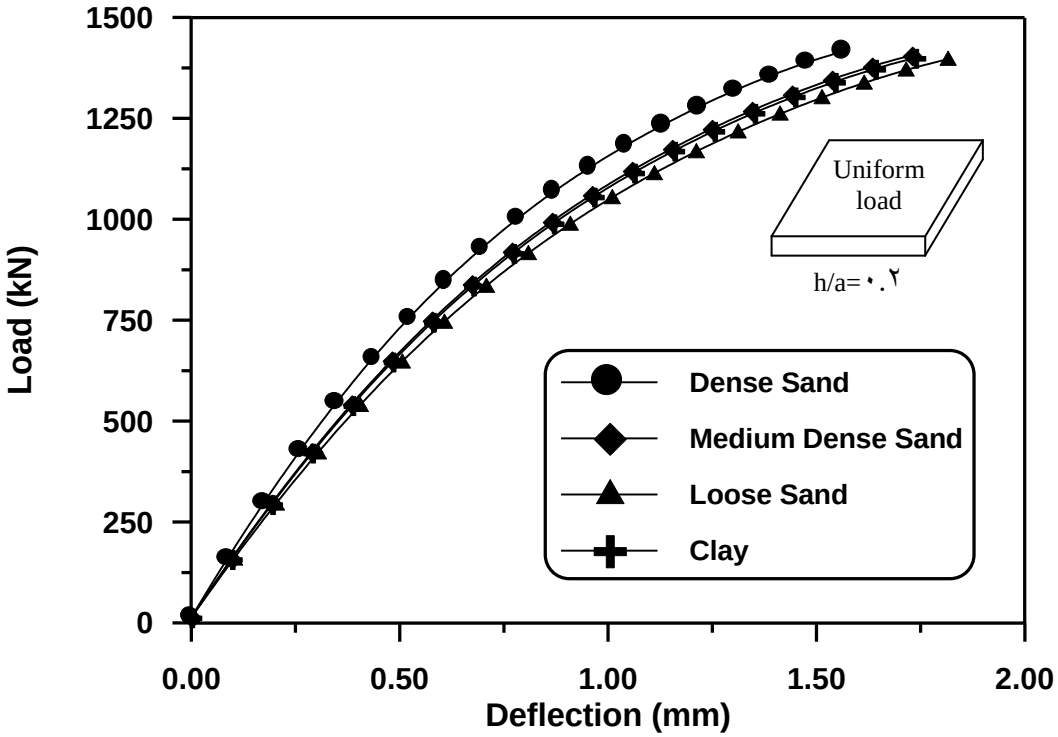

Figure (٦.٤٣): Load-Deflection Curve for Free-Edge Thick Plate with Distributed Load

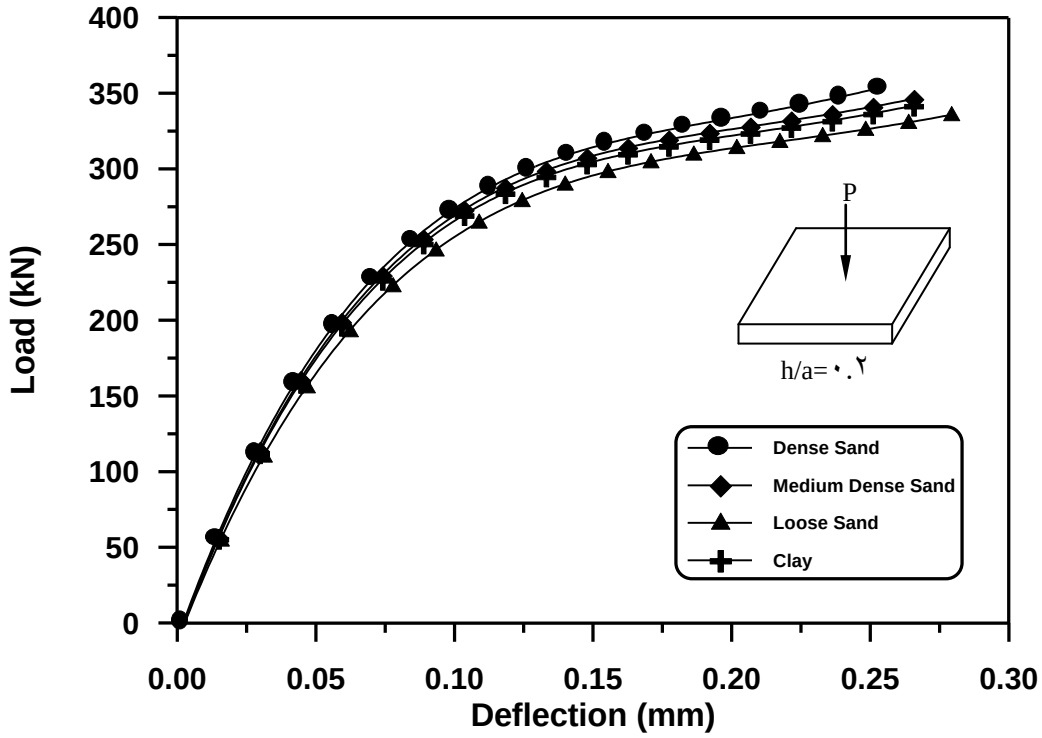

Figure (٦.٤٤): Load-Deflection Curve for Free-Edge Thick Plate with Concentrated Load

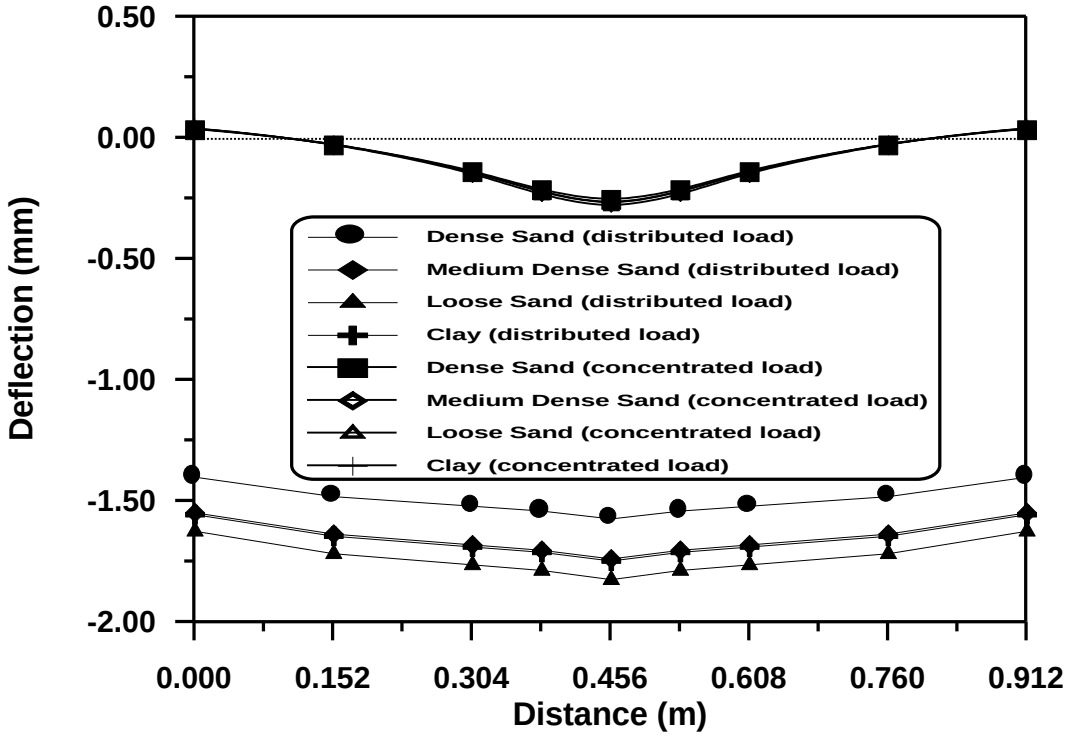

Figure (٦.٤٥): Deflection Profile for Free-Edge Thick Plate under Distributed and Concentrated Load

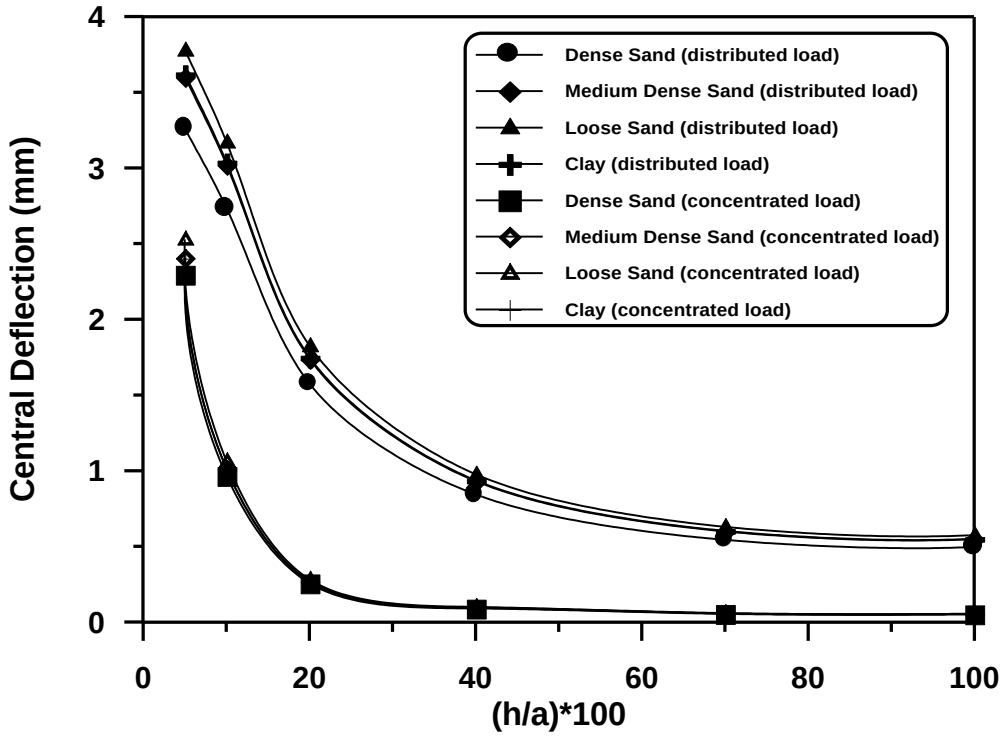

Figure (٦.٤٦): Central Deflection for Free-Edge Thick Plate with Different Thickness for Distributed and Concentrated Load

From these figures it can be noticed that:

١. The magnitude of ultimate load for thick plate under distributed load is greater than the ultimate load for concentrated load by about (٤) times. The deflection for this plate under distributed load is greater than the deflection for this plate under concentrated load by about (٧) times. These high differences in ultimate load and central deflection between thick plate under distributed load and thick plate under concentrated load are due to the effect of shear and normal stresses which are more significant in case of concentrated load at the center of plate.

٢. The rate of decreasing in central deflection for thick plate with distributed load is decreased after the thickness to span ratio exceeding ٤٠ % while for thick plate under concentrated load is after ٢٠ %.

٦.٦.٥ *Effect of Type of Soil*

A plate with simply supported and subjected to distributed load first analyzed without foundation and the results are compare with the available experimental and analytical results and then the analysis is repeated with foundation considered to study the effect of type of soil by how the deflection profile and the soil pressure change for different types of soil.

A simply supported slab under uniformly distributed load was tested by Duncan John (١٩٧٩). The test specimen has (١٨٢٨*١٨٢٨) mm with (٥٠.٨) mm thickness. The geometry and details are shown in Fig. (٦.٤٧).

The material properties of the tested slab are summarized in Table (٦). Due to symmetry of the slab, one quarter of the slab has been considered in the finite element analysis. The steel reinforcement was represented by embedded bar

through the element of concrete with perfect bond between steel and concrete as shown in Fig. (٦.٤٧.b). Eighteen ٢٠-node brick element are used to represent the concrete, as shown in Fig. (٦.٤٧.c).

The load-deflection curve is shown in Fig. (٦.٤٨). Fig. (٦.٤٩) shows the comparison with the previous study. Fig. (٦.٥٠) shows the deflection profile along the centerline of the plate with different types of soil (dense, medium dense, loose sand, and clay soils).It can be seen that the deflection of the soil increases when the density of soil decreases. Fig. (٦.٥١) shows the soil pressure under the plate, it can be seen that the pressure for dense soil is greater than the pressure for medium dense sand, and this pressure is greater than the pressure for loose sand and the pressure for clay soil is approximately the same as for loose sand.

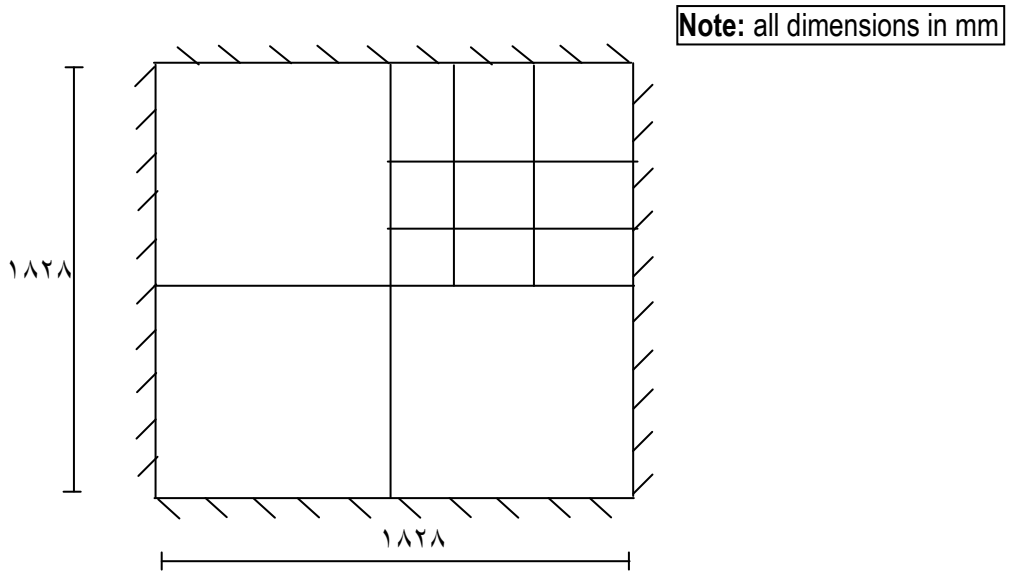

(a): Geometrical Details

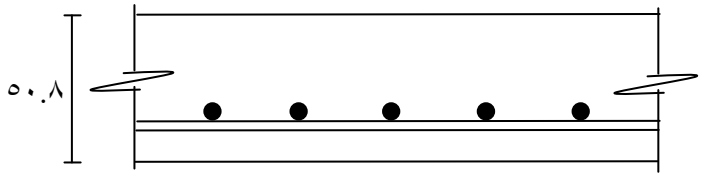

(b): Reinforcement Details

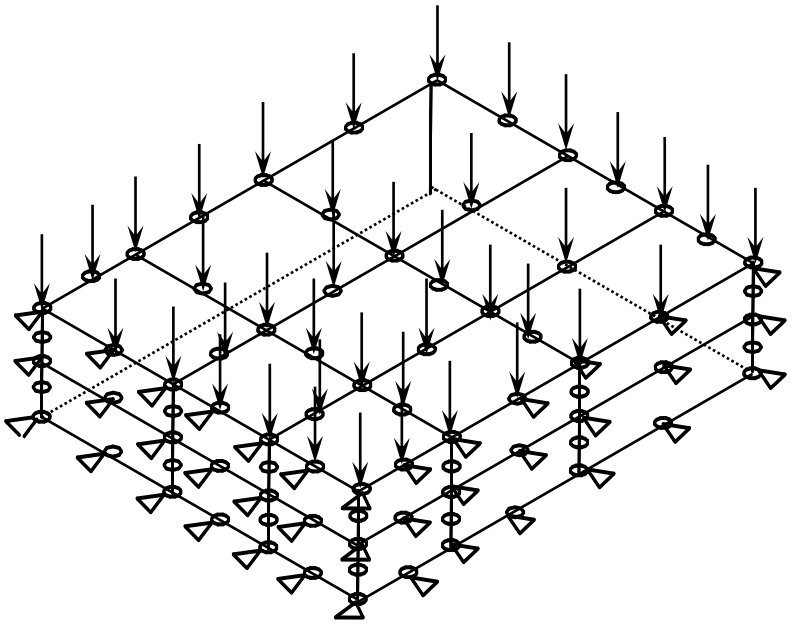

(c): Finite Element Mesh of Quarter of Two-Way Slab

Figure (٦.٤٧): Two Way Reinforced Concrete Slab of Duncan and John

	Material properties and material parameters	Symbol	Value
concrete	Young's modulus	Ec(N/mm^{٢})	٢٥٠٠٠
	Compressive strength (cylinder test)	Fc(N/mm^{٢})	٢٨
	Tensile strength	Ft(N/mm^{٢})	٢.٤
	Poisson's ratio	ν	٠.١٥
	Uniaxial crushing strain	εcu	٠.٠٠٣
steel	Young's modulus	Es(N/mm^{٢})	٢٠٠٠٠٠
	Yield stress	Fy(N/mm^{٢})	٣٧٦
	Hardening parameter	H	٠.٠
Tension-Stiffening parameter	Rate of decay tension stiffness	$\alpha_{١}$	٢٠.٠
	Sudden loss of tension stiffness at the instant of crack	$\alpha_{٢}$	٠.٥
Shear retention parameter	Rate of decay of shear stiffness	$\gamma_{١}$	١٠.٠
	Sudden loss of shear stiffness at the instant of cracking	$\gamma_{٢}$	٠.٥

	Residual shear stiffness due to the dowel action	٣٧	٠.١

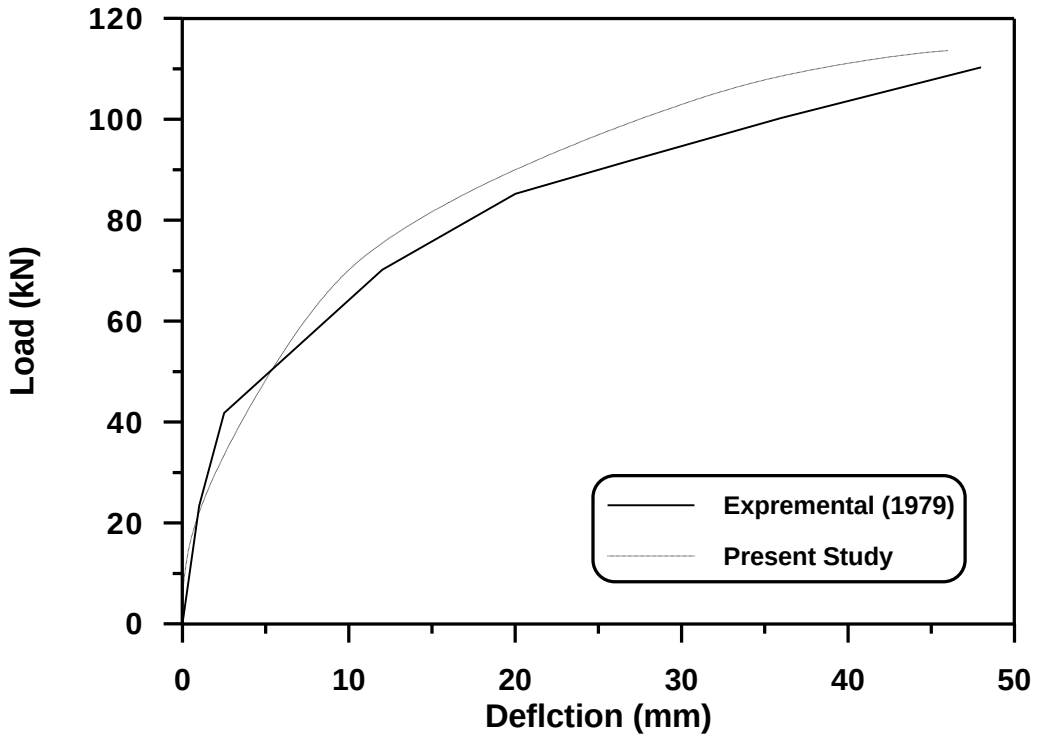

Figure (٦.٤٨): Load Deflection curve for Two Way Slab tested by Duncan and John (١٩٧٩)

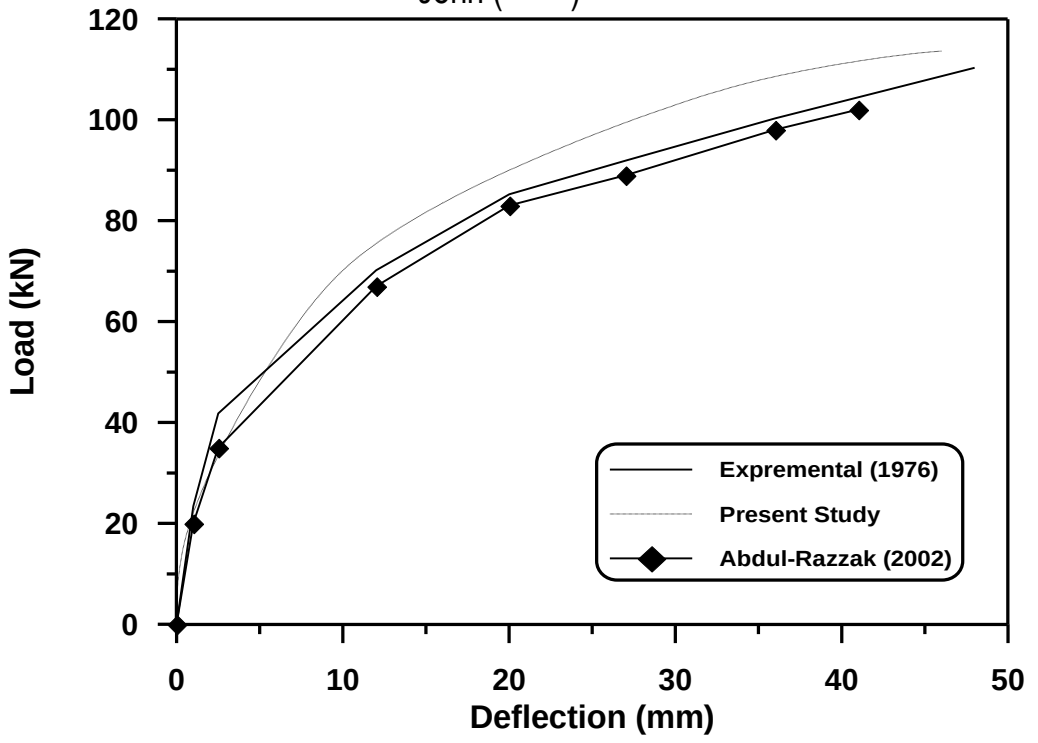

Figure (٦.٤٩): Load-Deflection curve for Two-Way Slab tested by Duncan and John (١٩٧٩)(comparison with previous study)

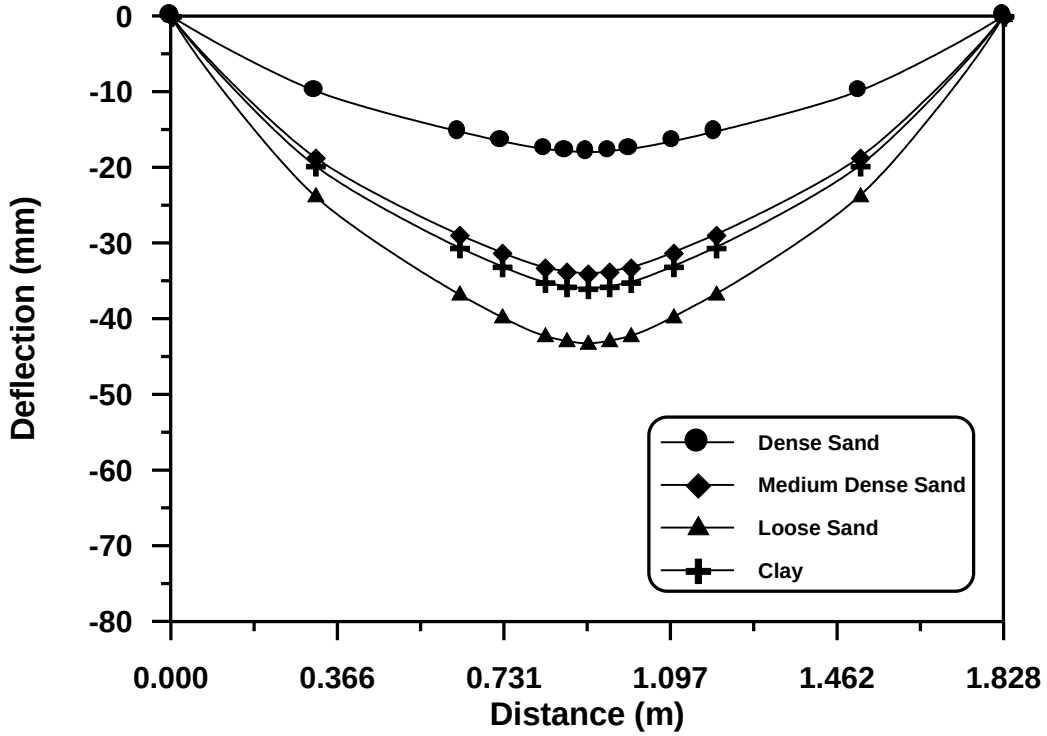

Figure (٦.٥٠): Deflection Profile for Plate Foundation

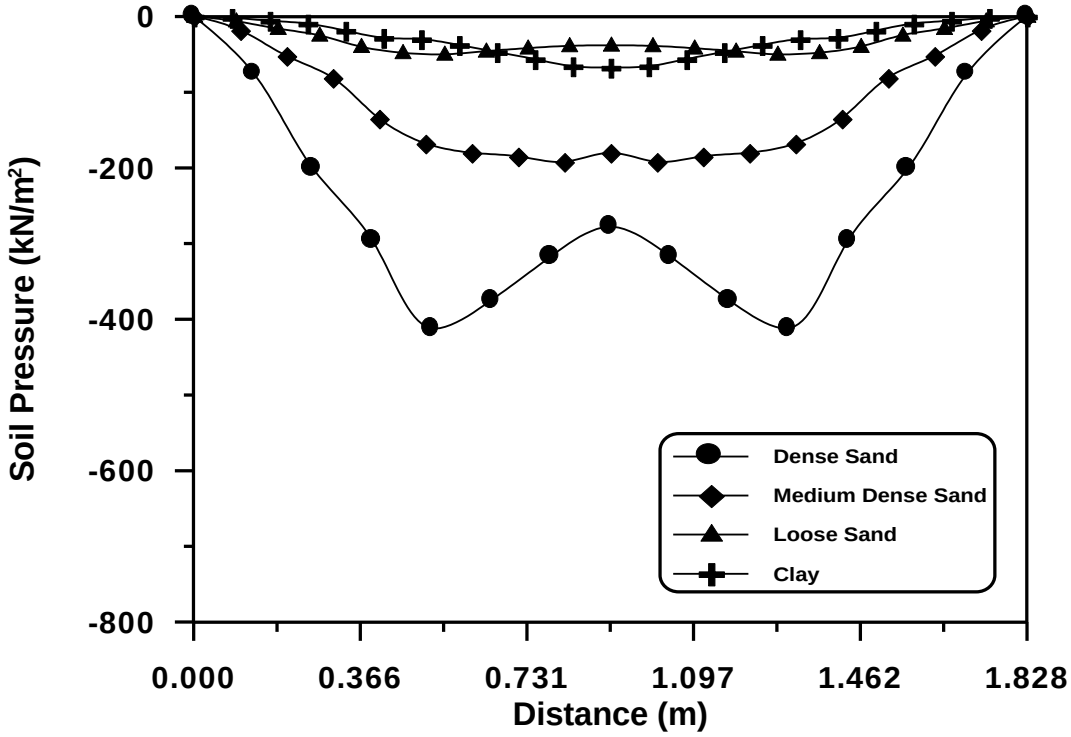

Figure (٦.٥١): Soil Pressure under Plate for Different Type of Soil

٦.٦.٦ *Effect of Elastic Foundation Modulus on Plate Behavior*

To study the effect of variation in modulus of vertical subgrade reaction on the percentage of difference in central deflection between thick plate foundation and thick plate without foundation, a simply supported thick plate with polynomial model under concentrated load is considered.

$$\%\text{DICD} = \frac{\text{Wc}_1 - \text{Wc}_2}{\text{Wc}_2} \times 100$$

where %DICD is the difference in central deflection between thick plate foundation and thick plate without foundation, Wc_1 is the central deflection for thick plate without foundation, Wc_2 is the central deflection for thick plate with foundation. All other information is shown in Fig. (٦.١٦).

Fig. (٦.٥٢) shows the variation in % DICD with the normal subgrade reaction

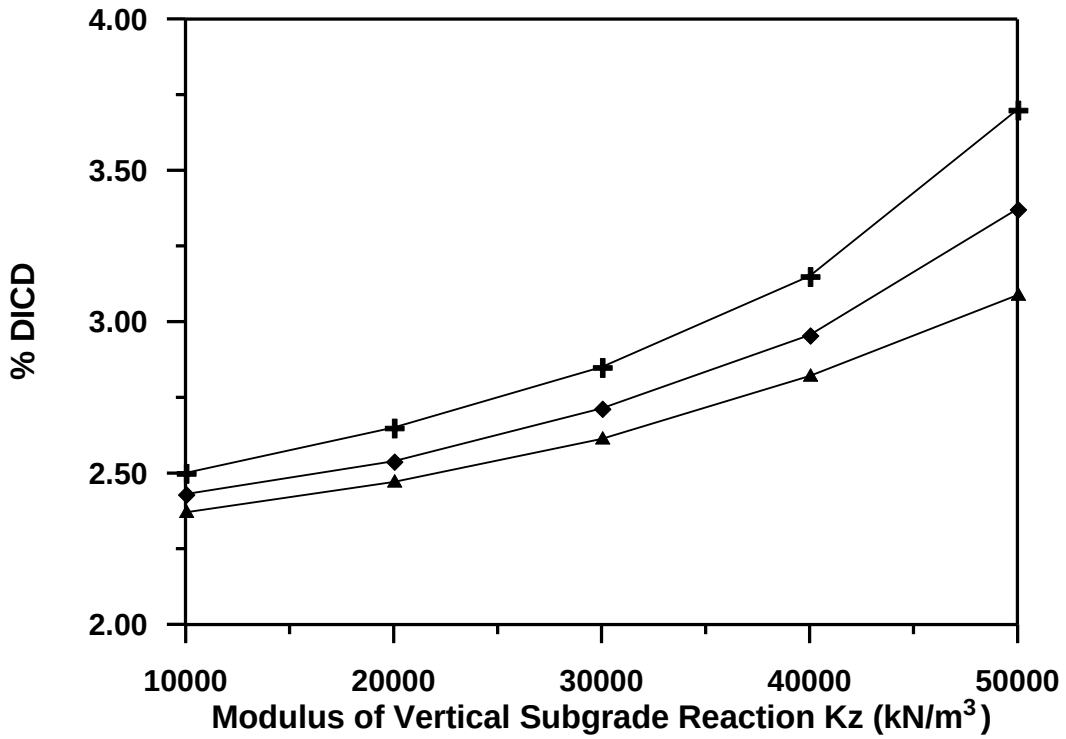

Figure (٦.٥٢): The Effect of Variation of Vertical Subgrade Reaction on the %DICD for Different Thickness

From this, it can be noticed that when the modulus of vertical subgrade reaction increases a small increase in %DICD will occur due to the decreasing of the deflection with increasing the modulus of vertical subgrade reaction, and at large thickness the effect of elastic foundation will diminish as mentioned previously.

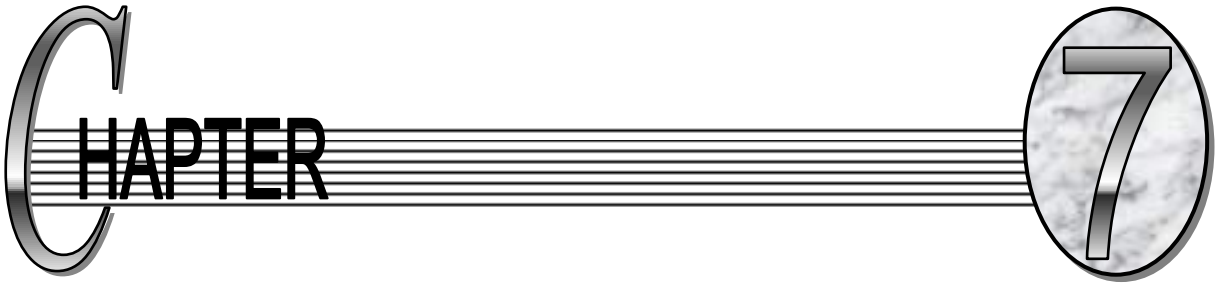

CONCLUSIONS AND RECOMMENDATIONS

٧.١ *Conclusions*

١. The results obtain from the present finite element analysis show that the computational model adopted in this study is suitable for prediction of load deflection behavior of the reinforced concrete plate and plate foundation under static loading. The comparison between the present numerical and the available experimental and analytical results has shown good agreement. The percent of difference is not more than (٥.٨٨ %) in prediction ultimate loads and (٧.٧٨ %) in deflection.

٢. In the problem of thick plate on elastic foundation, various models can be suggested to represent both compressional and frictional resistance. The normal component can be represented by Winkler, Kondner, Polnomial models while the horizontal component can be represented by Winkler and Coulomb models.

٣. The ultimate load that causes the failure for thick plate foundation with fixed edges is greater than the ultimate load for simply supported and the ultimate load for free edges is greater than for fixed support, for all type of soil models.

٤. The deflection for simply supported thick plate is greater than the deflection for fixed support and that is greater than for free-edge plate, for all types of soil models.

٥. The ultimate load for thick plate with all types of boundary condition and under the loading considered is increased with increasing the thickness of the plate, while the deflection is inversely proportional to the thickness of plate, for all types of soil models.

٦. The ultimate load for thick plate is increased with increasing the reinforcement ratio, and the deflection is inversely proportional to the reinforcement ratio.

٧. The deflection for thick plate under distributed load and for all types of soil models is greater than the deflection for same plate under concentrated load at failure.

٨. The effect of elastic foundation (normal compressional reaction) on the thick plate is small in case of high stiffnesses (large thickness).

٩. The polynomial model proposed in this study is efficient in estimating the non-linear behavior of soil and can easily be implemented a computer - based structural analysis.

١٠. The deflection increased with decreasing the density of soil, while the pressure under the plate is increased with increasing the density of soil.

٧.٢ Recommendations

The following topics are suggested as an extension for the present work:

١. Investigating the behavior of thick plate on elastic foundation experimentally.

٢. Analysis the soil by using twenty-node brick element and the interface element between the thick plate and the soil.

٣. The dynamic behavior of thick plate foundations needs to be investigated. This due to the fact that structural foundations may be exposed to dynamic effects such as earthquake and blast loading.

٤. Time dependent effect of creep and shrinkage of concrete in thick plates used as foundations need to be incorporated in the proposed method of analysis.

٥. Bond slip model needs to be incorporated in the proposed method of analysis.

٦. Optimum design studies of thick plate foundation need to be carried out. This is because labors and materials used for these plates are very important in reducing their cost.

الخلاصة

هذا البحث يتناول تحليل الصفائح السميكة المصنوعة من الكونكريت المسلح والمستندة على التربة باستعمال طريقة العناصر المحددة. تم اخذ اللاخطيه لتصرف المادة بنظر الاعتبار للأساس الكونكريتي. عنصر طابوقي ذي عشرين عقده وستين درجه حرية تم توظيفه لتمثيل الأساس الكونكريتي. تمت صياغة مصفوفة الصلاده بالاعتماد على تضمين كافة أنواع الاجهادات والانفعالات. قضبان حديد التسليح مثلت كعناصر محوريه مطمورة ضمن العناصر الطابوقيه الكونكريتيه مع ترابط تام بينهما .

التربة قد مثلت باستعمال مقاومات ضغط واحتكاك ,مركبة الضغط مثلت باستعمال موديلات (Winkler, Kondner and Polynomial) بينما المركبات الاحتكاكية مثلت باستعمال موديلين (Winkler and Coulomb)و موديل (Polynomial) اظهر توافق جيد مع دراسه سابقه.

المقارنة بين نتائج العناصر المحددة والنتائج النظرية والعمليه المتوفره للصفائح والصفائح المستندة على التربة أظهرت توافقا جيدا.النسبة المئوية لم تتجاوز(% ٥.٨٨) للحمل الأقصى و (%٧.٨٨) للهبوط .

نظمت دراسة نظريه لاختبار تأثير بعض المتغيرات مثل (الظروف المحيطة ,تغير القوة ,نسبة حديد التسليح , نوع الحمل ,نوع التربة و معامل الأساس المرن) على تصرف الصفائح . وقد تم التوصل إلى إن الحمل الأقصى للصفائح السميكة الحرة على التربة يكون اكبر منه للصفائح المسندة إسناد بسيط والصفائح المثبتة النهايات , الحمل الأقصى يزداد بزياد نسبة حديد التسليح , الهطول للصفائح السميكة تحت تأثير الأحمال الموزعة بانتظام اكبر من الهطول لنفس الصفائح تحت تأثير الحمل المركز عند الفشل , الهطول يزداد مع نقصان كثافة التربة وضغط التربة تحت الصفائح يزداد مع زيادة كثافة التربة.

REFERENCES

١- Abdul-Razzak, A.A., (٢٠٠٢), "***The Infleuece of Tension Stffening models on The Geometric and Material Nonlinear Analysis of Reinforced Concrete Slab***", Engineering and Technology Baghdad, Vol. ٢١, No. ١٠, pp. ٧١٦-٧٣٥

٢- Al-Azzawi, A., (١٩٩٥), "***Thick Circular Plate on Elastic Foundation***", M.Sc. Thesis, Saddam University (Now Al-Nahrain University), Baghdad, Iraq

٣- Al-Azzawi, A.A., (٢٠٠٠), "***Finite Element Analysis of Thin and Thick Reinforced Concrete Shell Foundation***", Ph.D. Thesis, Baghdad University, Baghdad, Iraq.

٤- Al-Imam, R.F., (١٩٩٢), "***Nonlinear Finite Element Analysis of Reinforced Concrete Slab-Beam Systems***", M.Sc. Thesis, University of Baghdad, Baghdad, Iraq.

٥- Al-Jubori, A.A., (١٩٩٢), "***Deep Beams and Thick Plate under generalized Loadings***", M.Sc. Thesis, Saddam University (Now Al-Nahrain University), Baghdad, Iraq.

٦- Al-Mahdi, A.R.N., (١٩٩٤), "***Thick Orthotropic Rectangular Plate on Elastic Foundations***", M.Sc. Thesis, Saddam University (Now Al-Nahrain University), Baghdad, Iraq.

٧- Al-Naimi, H.A., (١٩٩٦), "***٣-Dimensional Dynamic and Static Time Dependent Finite Element Analysis of Reinforced Concrete Members***", Ph.D Thesis, University of Baghdad, Baghdad, Iraq.

٨- Al-Rubai, Q.K, (٢٠٠١), "***Large Displacement Elastic Staibility Analysis of Plane Structure under Static Loads and Resting on Nonlinear Winkler Foundation***", M.Sc. Thesis, University of Technology, Baghdad, Iraq

٩- Al-Shaarabaf, I.A.S, (١٩٩٠), "***Three-Dimensional Nonlinear Finite Element Analysis of Reinforced Concrete Beams in Torsion***", Ph.D. Thesis, University of Brandford, England.

١٠- Al-Shaarabaf, I.A.S., and Mohammed, A.Z., (١٩٩٩), "***Nonlinear Analysis of Reinforced Concrete Cylindrical Shell Using Two and Three-Dimentional Finite Element Methods***", Engineering and Technology (Baghdad), Vol. ٢١, No. ٨, pp. ١-١٠

١١- ASCE Committee on Concrete and Masonary Structures, (١٩٨١), "***A state of the Art Report on the Finite Element Analysis of Reinforced Concrete Structures***", ASCE, Special Publication (as cited by Al-Shaarabaf (١٩٩٠)).

١٢- Bathe, K.J.,Ramaswamy, S., (١٩٧٩), "***On Three-Dimensinal Nonlinear Analysis of Concrete Structures***" Nuclear Engineering and Design, Vol. ٥٢, pp. ٣٨٥-٤٠٩.

١٣- Bowels, J.E., (١٩٩٦),"***Foundation Analysis and Design***", McGraw-Hill International Edition, ٥th Edition.

١٤- Cervenka, V., (١٩٨٥), "***Constitutive Model for Cracked Reinforced Concrete***" ACI Journal, November-December, pp. ٨٧٧-٨٨٢.

١٥- Cervera, M., Hinton, E., and Hassan, O., (١٩٨٧), "***Nonlinear Analysis of Reinforced Concrete Plate and Shell Structures Using ٢٠-Noded Isoparametric Brick Elements***", Computers and Structures, Vol. ٢٥, No. ٦, pp. ٨٤٥-٨٦٩.

١٦- Chen, W.F., (١٩٨٢), "***Plasticity in Reinforced Concrete***", McGraw-Hill, Inc., New York

١٧- Cheung, Y.K., and Nag, D.K., (١٩٦٨), "***Plates and Beams on Elastic Foundations Linear and Nonlinear behavior***", Geotechnique, Vol. ١٨, pp. ٢٥٠-٢٦٠

١٨- Cook, R.D., (١٩٧٤), "***Concept and Application of Finite Element Analysis***", John Wilely and Sons, Inc., New York.

١٩- Crisfield, M.A., (١٩٨٢), **"*Local Instabilities in the Nonlinear Analysis of Reinforced Concrete Beams and Slabs*"** Proccedings of Institute of Civil Engineers (U.k.), Vol. ٧٣, Part ٢, March , pp. ١٣٥-١٤٥.

٢٠- Damjanic, F., and Owen, D.R.J., (١٩٨٤), **"*Practical Considerations for Modeling of Post-Cracking Concrete Behavior for Finite Element Analysis of Reinforced Concrete Structures*"**, Proc. Int. Conf. Comp. Aided and Design, Placed and Publishers, pp. ٦٩٣-٧٠٦

٢١- Duncan, W., and John, (١٩٧٩), "***Further Studies on Constant Stiffness Method of Nonlinear Analysis of Concrete Structures***", Procceding of the Institute of Civil Engineers (U.k.), Part ٢, Vol. ٧٦, June, pp. ٩٥١-٩٦٩

٢٢- Fan, J., and Ye, J., (١٩٩٠), " ***A Series Solution of The Exact Equation for Thick Orthotropic Plates***", International Journal of Solids and Structures, Vol. ٢٦, No. ٧, pp. ٧٧٣-٧٧٨.

٢٣- Frederick, D., (١٩٥٦), "***On Some Problems in Bending of Thick Circular Plate on Elastic Foundation***", ASME (Trans.) Journal of Applied Mechanics, Vol. ٢٣, pp. ١٩٥-٢٠٠

٢٤- Gilber, R.I., and Waner, R.E., (١٩٧٥), "***Tension Stiffening in Reinforced Concrete Slab***", Journal of Structure Divison, ASCE, Vol. ١٠١, No. ST٣, pp. ١٨٨٥-١٩٠٠, March

٢٥- Hand, F.R, and Schnobrich W.C., (١٩٧٣), "***Nonlinear Layer Analysis of Reinforced Concrete Plates and Shells***", Journal of Structure Division, ASCE, Vol. ٩٩, No. ST٧, July, pp. ١٤٩١-١٥٠٥.

٢٦- Henry, F.D.C., (١٩٨٦), "***The Design and Construction of Engineering Foundations***", Chapman and Hall Publication Company, London.(as cited by Naser)

٢٧- Hinton, E., Rassoque, A., Zienkiewicz, O.C., and Davies, J.D., (١٩٧٥),"***A Simple Finite Element Solution for Plates of***

Homogeneous, Sandwich and Cellular Construction"' Proccedings of Institute of Civil Engineers (U.k.), Vol. ٥٩, part ٢, March, pp. ٤٣-٦٥.

٢٨- Hu, H., and Schnobrich, W.C, (١٩٩٠), " ***Nonlinear Analysis of Cracked Reinforced Concrete***", Journal of ACI, Vol. ٨٧, No.٢, March April, pp. ١٩٩-٢٠٧.

٢٩- Husain, A.H., (٢٠٠٢), "***Static Analysis of Concrete Shell Foundation by Finite Elements***", M.Sc. Thesis, Kufa University, Kufa, Iraq

٣٠- Husain, H.M., Al-Jubori, A.A., and Al-Hamed, A.M.S.,(١٩٩٩), "***Numerical Solution of Thick Plate under General Loading*** ", Engineering and Technology (Badhdad), Vol. ١٨, No. ١, pp. ١-١٧

٣١- Irons, B.M., (١٩٧١),"***Quadrature Rules for Brick Based Finite Elements***", International Journal of Numerical Methods in Engineering, Vol. ٣, pp. ٢٩٣-٢٩٤

٣٢- Jofriet, J.C, and McNeice, M., (١٩٧١), "***Finite Element Analysis by Reinforced Concrete Slabs***", Journal of Structural Division Proceedings, ACI, Vol. ٩٧, March, No. ST٣, pp. ٧٨٥-٨٠٦

٣٣- Kerr,A.D, (١٩٦٤), " ***Elastic and Viscoelastic Foundation Models***"' Journal of Applied Mech., Trans. ASME, Vol. ٣١, Series E., No. ٣.

٣٤- Kondner, R.L., (١٩٦٣), "***Hyperbolic Stress- Strain Response: Cohesive Soils***", Journal of Soil Mechanics and Foundations Division, ASCE, Vol. ٨٩, No. SM١, February, pp. ١١٥-١٤٣

٣٥- Kupfer, H.b., and Gerstle K.H, (١٩٧٣), "***Behaviur of Concrete under Biaxial Stresses***", Journal of Engineering Mechanics Division, ASCE, vol. ٩٩, no.EM٤, August, pp.٨٥٣-٨٦٦

٣٦- Lambe, T.W. and Whitman, R.V., (١٩٨٤), "***Soil Mechanics, SI Version***", ٢nd Edition Wiley Eastren Limited

٣٧- Lee, S.W., and Wong, S.G., (١٩٨٢), "***Mixed Formulation Finite Element for Mindlin Theory of Plate Bending***", International Journal

of Numerical Method in Engineering, Vol. ١٨, No.٩, September, pp. ١٢٩٧-١٣١٠.

٣٨- Mehta, R.P., (١٩٨٦), "***Concrete Structures: Purposes and Materials***", Prentice-Hil, Inc., New Jersey.

٣٩- Mindlin, R.D., (١٩٥١), "***Infleunce of Rotatory Inertia and Shear on Flexure Motion of Isotropic , Elastic Plate***"' Journal of Applied Mechanics, Vol. ١٨, No. ١, March, pp. ٣١-٣٨.(as cited by Naser)

٤٠- Moaveni, S., (١٩٩٩), "***Finite Element Analysis Theory and Application with ANSYS***" Prentice-Hall, Inc., New Jersey.

٤١- Naser, N.B., (١٩٩١), "***A Finite Difference Analysis of Thick Plate with Various Boundary Condition***", M.Sc. Thesis University of Mosul, Mosul, Iraq.

٤٢- Phillips,D.V., and Zienkiewcz, O.C., (١٩٧٦), "***Finite Element Nonlinear Analysis of Concrete Structures***", Proccedings of the Institute of Civil Engineers (U.k.), Vol. ٦١, part ٢, pp. ٥٩-٨٨.

٤٣- Pryor, C.W., Barker, R.M., and fraderick, D., (١٩٧٠), " ***Finite Element Bending Analysis of Reissner Plates***", Journal of Engineering Mechanics Division, ASCE, Vol.٩٦, No.EM٦, December, pp. ٩٦٧-٩٨٣.

٤٤- Ramarkrishan, V., and Anathanarayana, Y., (١٩٦٨),"**Ultimate Strength of Deep Beams in Shear**", Journal of ACI, Vol. ٦٥,pp. ٨٧-٩٨

٤٥- Reddy, J.N., (١٩٨٤), "***A Refined Nonlinear Analysis of Plates with Tranverse Shear Deformation***", International Journal of Solids and Structures, Vol. ٢٠, No. ٩/١٠, pp. ٨٨١-٨٩٦.

٤٦- Reddy, J.N., (١٩٨٦), "***A Refined Shear Deformation Theory for Analysis of Laminated Plates***", NASA (U.S.A) Contract Report ٣٩٥٥, January, ٣٣ page.

٤٧- Reissner, E., (١٩٤٥), " ***The Effect of Transverse Shear Deformation on the Bending of Elastic Plates***", Journal of Applied Mechanics, vol. ١٢, pp.A٦٩-A٧٧.(as cited by Naser)

٤٨- Salerno, V.L, and Goldbreg, M.A., (١٩٦٠), "***Effect of Shear Deformation on the Bending of Rectangular Plates***", Journal of Applied Mechanic, Transaction of ASME, Vol. ٢٧, No. ١, march, PP. ٥٤-٥٨.

٤٩- Shlash, Q.T., (١٩٧٤), "***Soil-Structure Interaction by Finite elemnt Method***", M.Sc. Thesis, Bagdad University, Baghdad, Iraq.

٥٠- Speare, P.R.S, and kemp, K.O., (١٩٧٦), "***Shear Deformation in Elastic Homogenous and Sandwich Plates***", Proceedings Instn. Civil Engineers, Vol.٦١, part ٢, December, pp. ٦٩٧-٧١٠.

٥١- Srinivas, S., and Rao, A.K., (١٩٧٣), "***Flexure of Thick Rectangular Plates***" Journal of Applied Mechanics, March, PP. ٢٩٨-٣٠١.

٥٢- Srinivas, S., Rao, A.K., and Rao, C.V.J, (١٩٦٩), ***" Flexure of Simply Supported Thick Homogeneous and Laminated Rectangular Plate***" ZAMM (Germany), Vol. ٤٩, No. ٨, Augest, pp. ٤٤٩-٤٥٨.(as cited by Srinivas(١٩٧٣))

٥٣- Svec,O.j., (١٩٧٦), "***Thick Plate On Elastic Foundations By Finite Elements***", Journal of the Engineering Mechanic Division, Vol. ١٠٢, No. EM٣, June, pp. ٤٦١-٤٧٧.

٥٤- Timoshenko, S. and Woinowsky-Krieger,S., (١٩٥٩), "***Theory of Plates and Shells***", McGraw-Hill

٥٥- Timoshenko, S., (١٩٢١), "***On the Correction for Shear of Diffrential Equation for Transverse Vibration of Prismatic Bars***", The Philosophical Magazine (London), Ser. ٦, Vol. ٤١, May, pp.٧٤٤-٧٤٦ (as cited by Al-Mahdi).

٥٦- Voyiadjis, G.Z., and Katten, P.I., (١٩٨٦), "***Thick Rectangular Plate on an Elastic Foundation***", Journal of Engineering Mechanics, Vol. ١١٢, No. ١١, November, pp. ١٢١٨-١٢٤٠

٥٧- Wanchoo, M.K., and May, G.W., (١٩٧٥), "***Cracking Analysis of Reinforced Concrete Plates***", Journal of Structure Division, Vol.١٠١, No.ST١, January, pp. ٢٠١-٢١٥

٥٨- Zeinkiewcz, O.C., (١٩٧٧), "***The Finite Element Method***" ٣rd Edition, McGraw-Hill Book Company, New York.